Cal Poly Pomona

RED HORIZON
CAL POLY POMONA

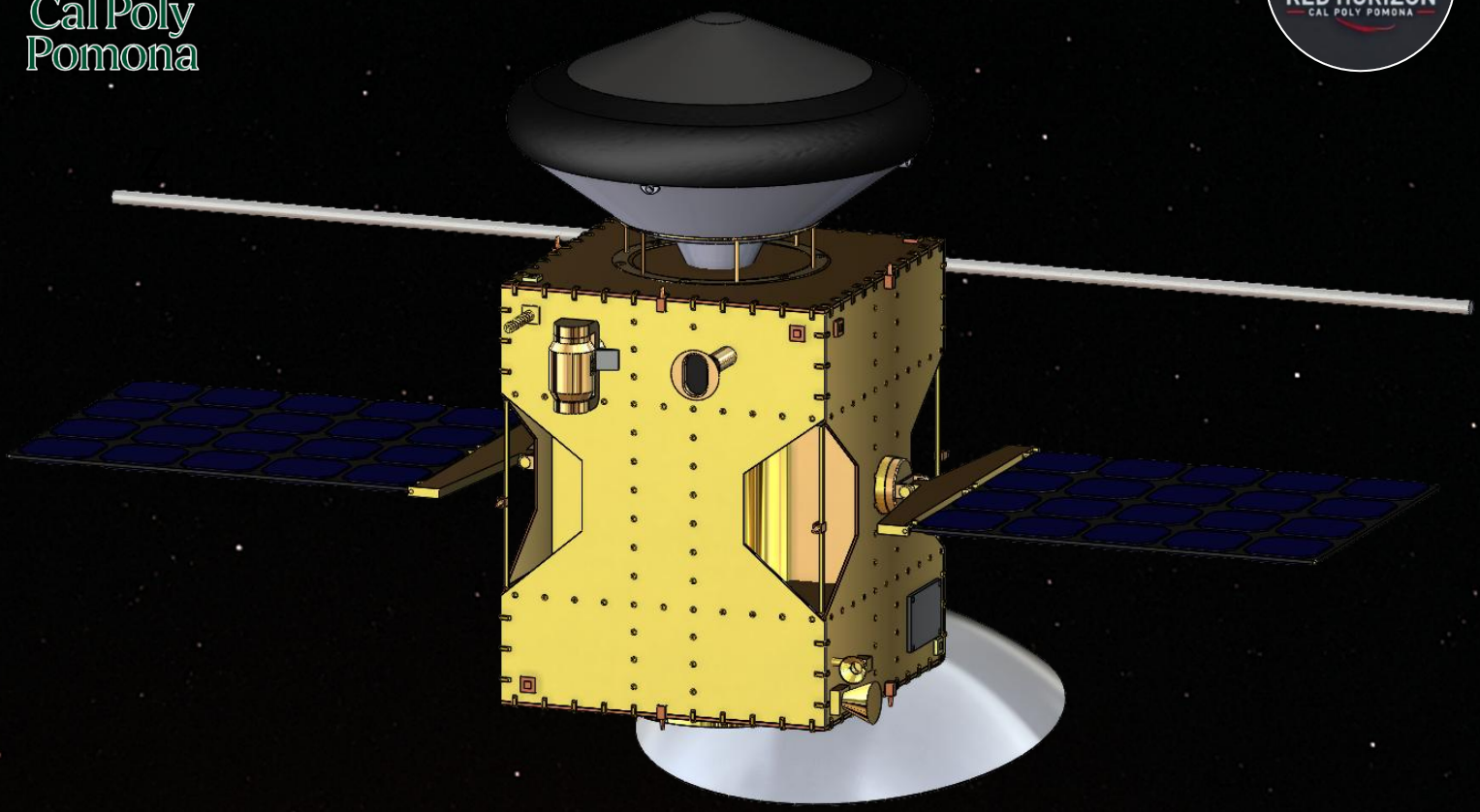

2024-2025 AIAA Space Design Competition

Mars Exploration Surveyors to Enable Human Exploration

Proposal for a Mars Orbiter with Atmospheric Balloon Vehicle

Duo by Red Horizon

AIAA

Red Horizon

Randy Vazquez

Project Manager
AIAA #1788069

Ethan Cascio

Deputy Project Manager
AIAA #1799088

Jay Tomlinson

Telecomm Engineer
AIAA #1799283

Christopher Camara

Structural Engineer
AIAA #1799101

Lucas McGarity

Trajectory Engineer
AIAA #1746717

Brian Reyna Mota

Balloon Design Engineer
AIAA # 1811185

Elmer Portillo

Mission Design Engineer
AIAA # 1494697

Hakop Sinanian

C&DS Engineer
AIAA #1799341

Dr. Navid Nakhjiri

Faculty Advisor
AIAA # 307328

Table of Contents

TABLE OF CONTENTS III
LIST OF FIGURES IV
LIST OF TABLES V
EXECUTIVE SUMMARY 7
1.0 INTRODUCTION 12
2.0 REQUIREMENTS DEFINITION 13
3.0 DESIGN APPROACHES 14
3.1 Design Reviews 14
3.2 Architecture Down Selection 15
4.0 MISSION DESIGN 18
4.1 Launch Date Selection 18
4.2 Martian Trajectory Design 18
4.3 Concept of Operations 20
5.0 SCIENCE INSTRUMENTS 25
5.1 Science Traceability Matrix 25
5.2 Science Instrument Selection 27
6.0 SUBSYSTEM DESIGN - BRONCO 30
6.1 Telecommunications 30
6.2 Command and Data Handling 32
6.3 Propulsion 36
6.4 Attitude Control System 42
6.5 Structures 46
6.6 Thermal 53
6.7 Power 60
7.0 SUBSYSTEM DESIGN - BRONCITO 63
7.1 Entry Vehicle Design Summary 63
7.2 Entry Vehicle Sizing 63
7.3 Lifting Gas & Tank Sizing 67
7.4 Balloon Selection and Sizing 69
7.5 Telecommunications 69
7.6 Command and Data Handling 70
7.7 Propulsion 72
7.8 Thermal 73
7.9 Broncito Power 80
7.10 Structure 81
8.0 ARCHITECTURE OVERVIEW 84
8.1 Mass & Power Breakdown 84
8.2 Launch Vehicle Selection 86
9.0 SCHEDULING & RISK MANAGEMENT 88
9.1 Scheduling 88
9.2 Risk Management 90
10.0 COST ESTIMATION 92
APPENDIX A: COMPLIANCE MATRIX A-1
REFERENCES R-1

List of Figures

FIGURE 3.1-1: DESIGN REVIEW SCHEDULE....14
FIGURE 4.3.1-1: BRONCO CONCEPT OF OPERATIONS....22
FIGURE 4.3.2-1: BRONCITO CONCEPT OF OPERATIONS....24
FIGURE 6.3.6-1: PROPULSION SCHEMATIC....40
FIGURE 6.4.2-1: ADCS BLOCK DIAGRAM....45
FIGURE 6.5.3-1: INTERNAL CONFIGURATION OF BRONCO....48
FIGURE 6.5.3-2: DUO SYSTEM INSIDE THE FALCON PAYLOAD FAIRING....48
FIGURE 6.5.3-3: DEPLOYED CONFIGURATION OF THE BRONCO ORBITER....49
FIGURE 6.5.5-1: CYLINDER STRUCTURE ANALYSIS....51
FIGURE 6.5.5-2: PRIMARY STRUCTURE DEFLECTIONS UNDER LAUNCH LOADS....52
FIGURE 6.5.5-3: PRIMARY STRUCTURE VIBRATION MODAL ANALYSIS....53
FIGURE 6.6.2-1: CRITICAL COMPONENT TEMPERATURE RANGES (BRONCO)....54
FIGURE 6.6.3-1: BRONCO HEAT TRANSFER DIAGRAM....55
FIGURE 6.6.4-1: BRONCO THERMAL MODEL (EXTERNALS)....57
FIGURE 6.6.4-2: BRONCO THERMAL MODEL (INTERNALS)....58
FIGURE 7.2.1-1: MARS ENTRY TRADE SPACE....63
FIGURE 7.2.1-2: FULLY SIZED ENTRY CAPSULE....65
FIGURE 7.3-1: INFLATION PROFILE....68
FIGURE 7.7-1: HEAT SHIELD THRUSTER SCHEMATIC....73
FIGURE 7.8.2-1: BRONCITO COMPONENT TEMPERATURE RANGES....74
FIGURE 7.8.3-1: LIQUID HYDROGEN TANK THERMAL NETWORK....75
FIGURE 7.8.3-2: BRONCITO HEAT TRANSFER DIAGRAM (DAY VS. NIGHT)....76
FIGURE 7.10.2-1: HEAT SHIELD SEPARATION CLAMP....82
FIGURE 7.10.2-2: BURN WIRE SEPARATION SPRING AND MOUNTED LOCATIONS....83
FIGURE 9.1-1: DUO SCHEDULING (PHASE E EXPANDED)....89

List of Tables

TABLE 2.0-1: PROGRAM AND MISSION LEVEL REQUIREMENTS 13
TABLE 3.2-1: OPERATIONAL CAPABILITIES FOM 16
TABLE 3.2-2: KEY PERFORMANCE PARAMETER FOM 16
TABLE 3.2-3: OPERATIONAL CAPABILITIES FOM 16
TABLE 4.1-1: EARTH-MARS MISSION LAUNCH OPPORTUNITIES 18
TABLE 5.1-1: DUO SCIENCE TRACEABILITY MATRIX 26
TABLE 6.1.1-1: TELECOMMUNICATION REQUIREMENTS (BRONCO) 30
TABLE 6.2.1-1: COMMAND AND DATA HANDLING REQUIREMENTS 32
TABLE 6.2.2-2: MAIN STORAGE TRADE STUDY 33
TABLE 6.3.1-1: PROPULSIONS REQUIREMENTS 36
TABLE 6.3.4-1: MAIN ENGINE TRADE STUDY 38
TABLE 6.3.6-1: PROPULSION SCHEMATIC LEGEND 41
TABLE 6.4.1-1: BRONCO'S ACS REQUIREMENTS 43
TABLE 6.4.2-1: ROTATIONAL KINEMATICS RESULTS 43
TABLE 6.4.2-2: ACS THRUSTER STUDY 44
TABLE 6.4.2-3: DISTURBANCE TORQUES 44
TABLE 6.4.2-4: REACTION WHEEL TRADE STUDY 45
TABLE 6.4.3-1: ADCS MASS AND POWER STATEMENT 46
TABLE 6.5.1-1: STRUCTURE REQUIREMENTS (BRONCO) 46
TABLE 6.6.1-1: THERMAL REQUIREMENTS (BRONCO) 53
TABLE 6.6.4-1: BRONCO PAINT/COATING SELECTION 56
TABLE 6.6.4-2: BRONCO COMPONENT HEAT FLUX SUMMARY 59
TABLE 6.7.1-1: POWER REQUIREMENTS (BRONCO) 60
TABLE 6.7.2-1: DUO BATTERY TRADE STUDY 61
TABLE 6.7.3-1: DUO SOLAR CELL TRADE STUDY 62
TABLE 6.7.4-1: BRONCO POWER PHASE PROFILE 62
TABLE 7.6.1-1: BRONCITO COMMAND AND DATA HANDLING REQUIREMENTS 70
TABLE 7.8.1-1: THERMAL REQUIREMENTS (BRONCITO) 73
TABLE 7.8.4-1: BRONCITO PAINT/COATING SELECTION 77
TABLE 7.8.4-2: BRONCITO COMPONENT STEADY-STATE TEMPERATURE (DAY) 77
TABLE 7.8.4-3: BRONCITO COMPONENT STEADY-STATE TEMPERATURE (NIGHT) 78
TABLE 7.8.4-4: BRONCITO COMPONENT HEAT FLUX SUMMARY (DAY) 78
TABLE 7.8.4-5: BRONCITO COMPONENT HEAT FLUX SUMMARY (NIGHT) 79
TABLE 7.9.1-1: POWER REQUIREMENT (BRONCITO) 80

TABLE 7.9.2-1: BRONCITO POWER PHASE PROFILE 81
TABLE 8.1-1: BRONCO MASS AND POWER STATEMENT 85
TABLE 8.1-2: BRONCITO MASS AND POWER STATEMENT 85
TABLE 8.1-3: DUO COMBINED MASS STATEMENT 86
TABLE 8.2-1: LAUNCH VEHICLE REQUIREMENTS 86
TABLE 8.2-2: LAUNCH VEHICLE TRADE STUDY 87
TABLE 9.2-1: RISK STATEMENTS AND MITIGATION STRATEGIES 91
TABLE 10.0-1: DUO NASA PCEC COST ESTIMATE (FY24, $M) 93
TABLE A-1: COMPLIANCE MATRIX A-1

Executive Summary

The 2024 – 2025 AIAA Undergraduate Team Space Design Competition Request for Proposal (RFP) challenged student AIAA members to design an integrated, comprehensive mission to send one or more exploration assets to Mars with the primary science objectives to characterize the atmospheric composition, conduct a detailed geographic survey, and/or determine the potential surface and subsurface resources on Mars. Human exploration of Mars is a long-term goal for global space exploration, and previous Mars missions have aided in the creation of this proposal response. Red Horizon, a team of 8 undergraduate students from California State Polytechnic University, Pomona, created Duo. Duo on its Mars mission will take data on the previously mentioned science objectives to support an eventual Human Mars exploration campaign.

The program and mission level requirements were derived from the AIAA RFP [1], these high-level requirements defined the approaches and constraints of the potential architecture and mission design. The main program goal derived from the AIAA RFP is that the system shall support a Human Mars exploration campaign. Science objectives require the mission to cover no less than 75% of the Martian globe in one of the following areas: atmospheric composition and density profile, geographic terrain and elevation survey, and surface and subsurface resource investigation, identification, and quantification. Key program requirements of the mission include the ability to operate into the late 2030s, completion of the primary mission data-gathering by December 31, 2033, a budget not exceeding 1.0 billion USD (FY24), and the system should include technologies demonstrated on previous programs.

Eight individual architectures were designed by students in Red Horizon's roster, including an orbiter and orbiter/rover architecture in the individual design phase. Two distinct designs were carried out up to System Design Review (SDR), where one architecture would be down-selected via a system-level trade study. Two separate design approaches, one risky and one conventional/safe, were created. Solo, the first design architecture, is a traditional design approach; it is purely an orbiter mission with remote sensing payloads. Solo's orbit around Mars is circular during its primary data-gathering phase. Then it enters a lower elliptical orbit to collect higher fidelity data of potential future human landing locations during its secondary mission phase. The second architecture, Duo, is the risky design approach with an orbiter named Bronco and a balloon vehicle named Broncito. Duo takes remote sensing data with Bronco's instruments and direct sensing data with Broncito's instruments. Both missions utilize a sun-synchronous orbit (SSO). The system-

level trade study evaluated key performance parameters, key system attributes, and operational capabilities of both architectures and the Mars Reconnaissance Orbiter (MRO) [2]. The MRO was included in the system-level trade study to act as a baseline for the candidate architectures in this type of mission. Duo exceeded all basic system needs in the trade study and was selected as Red Horizon's design in response to the AIAA RFP. The key operational capability of Duo is its time in the atmosphere; Duo has 90 days in the atmosphere, which allows instruments to take in-situ measurements of Mars' atmosphere while the MRO and Solo do not have this capability.

The primary mission phase consists of an interplanetary transfer, Mars capture, aerobraking maneuvers, systems diagnostics, and data collection. The selected launch date is December 13, 2030, providing Red Horizon 5.5 years from acquiring the proposal contract through to the launch date. Duo coasts to Mars for 286 days, a Mars Orbit Insertion (MOI) burn is performed upon arrival, and the aerobraking phase begins. Duo will perform approximately 26 precise burns to enter a sun-synchronous orbit of 700 km over 176 days. Bronco begins collecting data on April 9, 2032. A maximum coverage of ~95.57% of Mars will occur 107 days after data collection begins, concluding the primary mission phase.

The extended mission includes the deployment of Broncito to Mars to complete the Balloon mission, along with all further data collection and transmission to Earth. At the end of the primary mission phase, the Broncito balloon will separate from the Bronco orbiter via a clamp band system. Upon deployment, Broncito is encased in a Mars entry vehicle designed for controlled entry, descent, and landing. Broncito uses a combination of propulsion, aerodynamic drag, parachute deployment, and airbag cushioning to reach the surface of Mars safely. The entry velocity of the heat shield is 3,500 m/s with a flight path angle of -3°. The parachute will deploy at 11 km altitude, and Broncito will slow down to 6 m/s, where it will detach from the parachute near the ground and deploy airbags to absorb the impact. Broncito will take flight and be the first super-pressure balloon in the Martian atmosphere. The 30-meter diameter super-pressure balloon will deploy, and Broncito will rise to a 7 km altitude. Ballast drops will keep the balloon at the 6-7 km altitude range for 90 days, and hydrogen diffusion will eventually cause the balloon to drop in altitude. A cutting mechanism will separate the balloon from the structure upon touchdown at its final resting spot.

A science traceability matrix was created to track the mission's science goals, instrument requirements, and the data products of each instrument. Three science objectives are derived from the requirements: 1) Characterize the atmospheric composition and create a detailed density profile of the Martian atmosphere. 2) Conduct a detailed

geographic survey of the Martian surface, including a terrain and elevation profile. 3) Investigate, identify, and quantify the Martian surface's potential surface/subsurface resources. Bronco and Broncito will be used to complete the science objectives with unique instruments on each spacecraft. Instruments already in NASA's technology portfolio were chosen to fly on the mission.

Bronco, an orbiter with remote sensing science instruments, will exceed the 75% minimum coverage requirement in the three categories: atmospheric composition and density profile, geographic terrain and elevation survey, and surface and subsurface resource investigation, identification, and quantification. The Mars Climate Sounder (MCS) [2] will address science objective one and produce an atmospheric composition, temperature, pressure, and density profile. The Context Camera (CTX) [2] and Shallow Radar Sounder (SHARAD) [2] will address science objective two. They will produce global Martian terrain imagery and a 3D topographic map to aid in the identification of potential landing locations. Finally, the SHARAD will address the third science objective and produce surface and subsurface material maps for future manned missions.

Broncito will be an extension of the mission to aid in the science objectives by taking atmospheric measurements. Broncito will carry the Rover Environmental Monitoring System (REMS) sensors [3], which include temperature, humidity, and pressure-sensing capabilities. The REMS sensors aim to complete a high-resolution study of the atmosphere. Science objective number 1 is addressed by the REMS sensors, which will take data at different altitudes throughout the mission. Science objective number two is addressed on Broncito with the Miniature Synthetic Aperture Radar (Mini-SAR) [4] and the Mars Descent Imager (MARDI) [3]. The Mini-SAR will produce a 3D topographical map, and the MARDI will deliver high-resolution imagery of landing locations and travel paths. Broncito does not address science objective number 3.

The telecommunications subsystem ensures consistent data communication between Duo and Earth throughout all mission phases, including the primary and secondary mission phases. Bronco serves as the central command module for both spacecraft. Broncito does not communicate with Earth directly but transmits its data to Bronco for storage and transmission back to Earth. The telecommunications system uses a 3-meter parabolic antenna and has a 10-hour/day contact time with a 34 m NASA Deep Space Network (DSN) receiver for its science operations. The primary mission data can be transmitted within 216 days, while the balloon extension increases the full transmission time by

another 5 years. Emergency communication is safeguarded by dual Medium Gain (MG) horn antennas, ensuring reliable contact recovery with Earth.

The command and data handling (C&DH) systems of Bronco and Broncito are robust and reliable, and each component was chosen for its heritage and compatibility with the NASA DSN. Bronco is outfitted with 4.5 TB of storage, while Broncito is outfitted with 2.5 TB of storage for temporary staging.

Bronco employs a dual-mode tank design, combining the advantages of bipropellant propulsion for the main engine and monopropellant propulsion for the attitude control system (ACS). The selected bipropellant system, utilizing hydrazine fuel and nitrogen tetroxide oxidizer (NTO), provides superior performance with higher specific impulse and thrust ideal for critical mission operations such as MOI. A trade study led to the selection of the R-4D-15 HiPAT engine due to its optimal balance of I_{sp}, thrust, and technology readiness level (TRL). Propellant mass was calculated at 2,500 kg, factoring in trapped propellant, loading uncertainties, and outages. Spherical diaphragm tanks, using elastomer for hydrazine and Teflon for NTO, were chosen to prevent gas ingestion and allow ground testing. Pressurant tanks were sized using ideal gas law calculations with safety considerations, including a safety factor of 2 and structural reinforcements. A regulated helium pressurant system ensures consistent and stable propellant combustion conditions throughout the mission.

Due to instrument pointing requirements, the ACS for the Bronco spacecraft contains a 3-axis stabilized reaction wheel assembly. The system also includes precise attitude determination using 12 sun sensors, 2 star sensors, and 1 inertial measurement unit (IMU), with components chosen through trade studies. The ACS employs a 3-axis reaction wheel system, with disturbance torques modeled to determine the necessary momentum capacity for the wheels. A reaction wheel desaturation frequency of 2.25 days was calculated. A fourth reaction wheel is included to prevent the loss of control of a singular axis from a single-point failure. The system is managed by Bronco's central command and data-handling computer.

The thermal system was designed to keep Bronco’s operational temperature limits within a 5° margin for the entire mission. To meet this requirement, thermal paint/coatings were iteratively selected for Bronco’s external surfaces to minimize net heat flux, favoring passive thermal control systems and positive net heat flux to avoid using electric heaters. A 2.6 m^2 radiator was required to dissipate 922 W/m^2 of excess heat flux. For redundancy, critical instruments and areas were fitted with Kapton heaters.

For Broncito's balloon ascent, a 30-meter-diameter super-pressure balloon lifts the vehicle to 7 km in altitude. Hydrogen was selected as the balloon's lifting gas due to its low molecular weight and high lift capacity. The hydrogen will be kept in a liquid state at 30 MPa until inflation. A liquid state for hydrogen was chosen to reduce the size and weight of the tanks and heat shield needed. An aluminum vacuum jacket was designed to compensate for the low-temperature demands of liquid hydrogen, and 34 layers of multi-layer insulation (MLI) were used to keep the hydrogen in a fluid state until it was required for balloon inflation. Upon landing, a chemical reaction will heat the liquid hydrogen into a gaseous state, reducing balloon inflation time. A shorter inflation time reduces the exposure to winds that can damage or destroy the balloon.

Broncito's thermal control system was designed with a 5° C margin for the entire mission. Broncito will experience night and day while floating; heat loads are assumed to be radiation-dominated at 7 km altitude. To manage heat loads in the atmosphere, a 0.27 m^2 radiator was included to dissipate 165 W/m^2 of heat during the day.

The total power required for Bronco is 1150 W, and the total power needed for Broncito is 287 W. Bronco's solar array area is 14.39 m^2. The solar array supported a 15% degradation for the whole mission duration. Broncito's solar array area is 5.2 m^2, but it is not sized for degradation because of its short lifespan. Trade studies determined that Bronco and Broncito would use the same solar and lithium-ion cells.

A launch mass of 4690 kg was obtained for Duo. Based on a trade study, the selected launch vehicle was the Falcon Heavy reusable due to its lifting capabilities, low cost, and reliability. The Falcon Heavy Reusable's 6g axial and 2g lateral loads produce the most significant structural loads [5]. The structure is composed of sandwich composite carbon fiber with aluminum honeycomb; the maximum deformation on the primary load path cylinder is a manageable 2.77 mm in load simulations. The natural frequency requirement of the launch vehicle is 50 Hz, and our analysis showed a natural frequency of ~100 Hz which provides an adequate safety margin.

NASA's Project Cost Estimating Capability (PCEC) [6] tool allowed Red Horizon to perform a thorough cost analysis by inputting all calculated weights and scheduling of the mission. The cost estimate includes all development and operational costs from architecture feasibility until the end of the primary mission phase. The cost to meet the program requirements was determined to be $874 (FY24, $M). The margin we have with our budget for this scenario is $125 (FY24, $M). While the RFP explicitly states that the budget is limited to the primary mission phase, extending the primary mission phase to December 31, 2033, still leaves the program with over $100 (FY24, $M) margin.

1.0 Introduction

Human Mars exploration has been a long-term goal for global space exploration objectives. It is crucial to investigate and collect data for future Mars mission planners to understand the potential mission challenges and constraints to achieve science and exploration goals. We acknowledge the Mars Global Surveyor [7], MRO [2], and numerous rovers and landers that have contributed to the extensive knowledge base of our neighboring planet, which provided valuable data to support this proposal.

As the AIAA RFP [1] states: “To support an eventual Human Mars exploration campaign, specific data to characterize Mars’ atmosphere, geography, and potential physical makeups are all critical to enable detailed mission planning and accurate architecting to maximize the potential to achieve exploration objectives”, the quoted statement highlights the goals of the program. The main program goal is to support an eventual Human Mars exploration campaign by providing future mission planners with atmospheric, geographic, and physical makeup data. The data provided by the program’s goals assists mission planners in the following: 1) Entry, descent, and landing, 2) Ability to pinpoint potential landing locations and travel paths, and 3) Support human activities with surface and subsurface resources. By meeting data collection objectives in this proposal, future Mars missions will be able to meet global space exploration objectives.

2.0 Requirements Definition

The program and mission level requirements were derived from design requirements and constraints stated in the AIAA RFP [1] and are shown in Table 2.0-1 below. These high-level requirements define the system's design constraints and establish the mission success criteria.

Table 2.0-1: Program and Mission Level Requirements

RFP. Ref.	Req. #	Req. Type	Requirement Description
4.2	0.0-1	Program	The system shall support a human Mars exploration campaign.
4.4 - 4.7	0.0-2	Mission	The mission shall cover no less than 75% of the Mars globe in at least one of the following areas: a) Atmospheric composition and density profile b) Geographic terrain and elevation survey c) Surface and subsurface resource investigation, identification, and quantification.
4.8	0.0-3	Program	The system should use technologies already demonstrated on previous programs or currently in the NASA technology development portfolio.
4.8	0.0-4	Mission	The system should utilize technologies with a Technology Readiness Level of no less than 7.
4.12	0.0-5	Program	The mission shall not exceed a total cost of $1.0 Billion USD (FY24), including development, hardware, launch, and operations through the primary mission phase.
4.13	0.0-6	Mission	The system should complete deployment and primary data-gathering activities no later than December 31, 2033.
4.13	0.0-7	Mission	The system shall be designed to operate into the late 2030s.

Requirements for each subsystem are shown within their respective sections. A compliance matrix for all program and mission can be found in Appendix A.

3.0 Design Approaches

Section 3.0 discusses the design reviews as well as the down selection process that Red Horizon performed. Architecture down selection was a crucial process that resulted in the selection of the optimal system to meet the program requirements and satisfy stakeholder expectations.

3.1 Design Reviews

Eight architectures were designed, two were taken into the SDR Level, and one continued into the Preliminary Design Review (PDR). Each team member was responsible for one architecture design in a blackout period designed to increase the originality of each architecture. In the team design phase, 2 designs were selected, and one architecture was eventually selected at the SDR. An orbiter/rover, as well as a conventional orbiter design, were considered in the individual design phase of our class, and a conventional orbiter and a orbiter/balloon design were considered into the team design phase. A schedule with the design reviews that were completed is seen on Figure 3.1-1. The reviews completed are the project management plan, systems requirements review, oral progress review (OPR), SDR, and PDR.

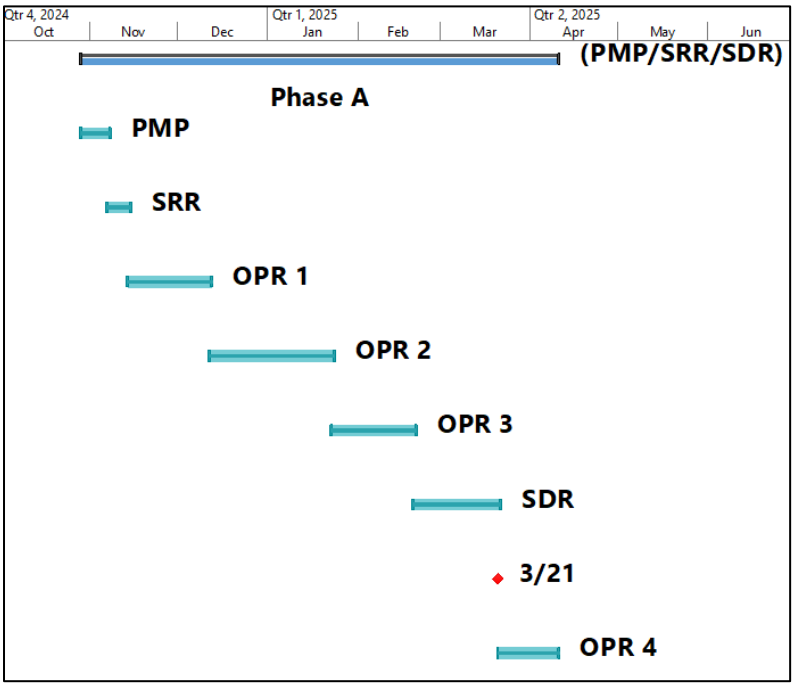

Figure 3.1-1: Design Review Schedule

In the team design phase, we were instructed to simultaneously design both conventional and creative approaches to the proposal. The orbiter/rover system was unable to meet the cost requirement, which left the team with multiple orbiter designs. A new design was introduced at the team design stage, which was the balloon/orbiter architecture. Two architectures were designed to the SDR level which are seen in Figure 3.1-2 and Figure 3.1-3.

The balloon/orbiter architecture, Duo, was selected as our creative design approach because of its potential to satisfy and exceed the high-level requirements with an unconventional method.

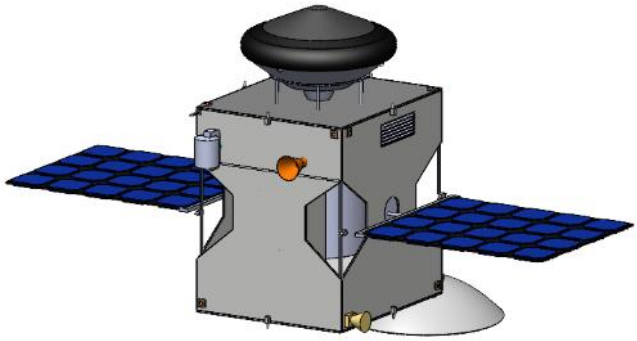

Figure 3.1-2: Duo at System Design Review Level

For the conventional design approach, the orbiter architecture, Solo, was selected because it meets all the high-level requirements with ease. Designs matured after each design review, and at the SDR, we were instructed to down-select architectures by the professor.

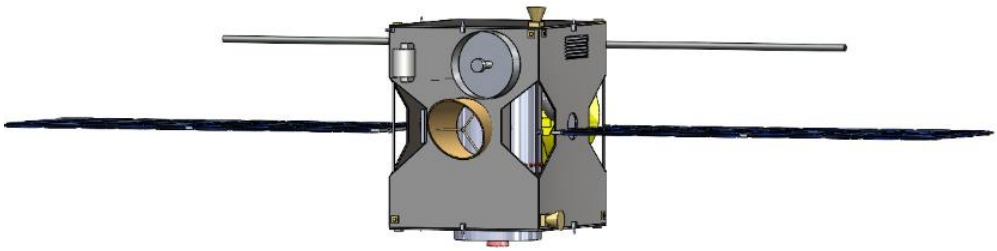

Figure 3.1-3: Solo at System Design Review Level

3.2 Architecture Down Selection

The down-selection process was a 3D orthogonal trade study where the operational Measure of Effectiveness was a product of the Key Performance Parameters and Key System Attributes of the architecture design. This method gave

us 3 different technical performance measurements to compare both architectures. Each technical performance measure was derived from the requirements of the mission or system itself, these can be seen in Table 3.2-1, Table 3.2-2, and Table 3.2-3.

Table 3.2-1: Operational Capabilities FOM

Operational Capabilities	Solo	Duo
Terrain/ Resources Coverage (%)	95	95
Time in Atmosphere (Days)	0	90
Operational Maturity (TRL)	8	7
RFP Timeline Margin (Months)	18.1	15.9

Table 3.2-2: Key Performance Parameter FOM

Key Performance Parameter	Solo	Duo
ΔV Required (km/s)	2.68	2.84
Desaturation Frequency (Days)	2.07	1.77
Min. FOV (deg)	1.14	4.3

Table 3.2-3: Operational Capabilities FOM

Key System Attributes	Solo	Duo
Payload Power (W)	110	52
Total Cost ($M)	807	951
OOWM (kg)	3,281	4,372

In the Operational Capabilities category, Terrain/Resources coverage, Time in Atmosphere, and Operational Maturity were selected as criteria to judge our spacecraft. In the Key Performance Parameter category, ΔV, desaturation frequency of the reaction wheels, and minimum FOV were selected as criteria to judge the performance of our spacecraft. In the Key System Attributes category, payload power, total cost, and on-orbit wet mass (OOWM) were selected as criteria to judge our spacecraft performance.

The face-off shows the design data at the SDR level for both designs. Highlighted in gold, we can see the key differences in the designs. Time in the atmosphere is significantly different for each architecture because Solo does not have any measurement time in the atmosphere, whereas Duo has 90 days in the atmosphere to take measurements. The minimum FOV affects the time that it takes to reach the high-level requirement of 75% coverage for Mars, but

also the ΔV required highly impacts our weight. The total cost for each design is significant because it is a high-level requirement, and Duo's cost nearly reaches the 1-billion-dollar program budget requirement.

A system trade study was conducted for Solo and Duo, with the baseline comparison being the MRO. The MRO was used to compare the performance of each architecture and was also included in the trade study. The MRO was selected as a baseline comparison because it is mission similar to that of the AIAA RFP. The MRO collected remote sensing data in orbit of the following categories: atmosphere data, terrain data, and resources on Mars. The goal of our system is then to meet and exceed the proposal requirements, while also expanding on the previous Mars missions like the MRO.

The figures of merit (FOM) in our system trade study are those listed on the previous page. The FOMs with the highest weights are the Time in Atmosphere, ΔV required, and OOWM of the system. The system trade study was conducted, and the results are shown in Table 3.2-4. Duo ranks higher than Solo in each category and meets/exceeds the system needs as seen in the legend. Duo was selected as the design architecture, which moves into the PDR.

Table 3.2-4: System Trade Study Summary

Trade Study Summary Sheet					
LEGEND	**Description**				
2.5	Extremely well-suited to system objectives	***System/ Technology***	***Operational Scores***	***Functional Scores***	***Physical Scores***
2	Meets/exceeds basic system needs	**Solo**	**1.75**	**1.85**	**2.15**
1	Potential value, but likely unacceptable	**Duo**	**2.25**	**2.3**	**2.35**
-1	Clearly unacceptable to meet system objectives	**MRO**	**1.3**	**1.6**	**1**

4.0 Mission Design

Bronco and Broncito's trajectory and orbit selection are discussed in section 4.0. The concept of operations displays the full mission of Duo.

4.1 Launch Date Selection

Historically, Mars missions typically take 5-6 years from winning the proposal to launch their mission. Therefore, launch dates before the latter half of 2030 were not considered for this mission. Table 4.1-1 below from NASA JPL's Interplanetary Mission Design Handbook [8] displays potential Earth-Mars launch opportunities available for this mission.

Table 4.1-1: Earth-Mars Mission Launch Opportunities

Earth Departure (m/d/yr)	Mars Arrival (m/d/yy)	C3 (km^2/s^2)	Mars Arrival Excess Speed (km/s)
1/28/31	8/6/31	9.00	5.541
2/23/31	1/9/32	8.237	5.53
3/1/31	9/27/31	17.89	3.777
12/13/30	**9/25/31**	**12.48**	**3.445**

During selection for launch opportunities, a lower Mars arrival excess speed was prioritized, due to less fuel being required for MOI. The golden row in Table 4.1-1 was selected as the ideal launch date for this mission due to it requiring the lowest Mars arrival excess speed. The green row in Table 4.1-1 is the backup launch date. NASA JPL also provides launch opportunities in 2033, but these were not considered as they require more fuel for MOI and are unlikely to meet the primary mission deadline of December 31, 2033.

4.2 Martian Trajectory Design

Duo's Martian trajectory requires three separate and unique orbits: the Mars capture orbit, primary mission Mars orbit, and a graveyard orbit.

4.2.1 Aerobraking Rationale

Between the 3 primary trajectories studied, an impulsive capture, a pump-down maneuver, or an aerobraking maneuver, the key differences are the fuel consumption of the spacecraft and the duration of each maneuver. An aerobraking maneuver was selected because the mission is not constrained by the additional 176 days required to perform the maneuver, and aerobraking uses the least amount of fuel compared to the alternative trajectories. For modeling the maneuver, the aerobraking profile used by the MRO was duplicated for use by the Duo spacecraft [9].

4.2.2 Orbit Selection

Next, to select an orbit for the primary mission, the driving requirements are the power consumption of the spacecraft, as well as the payload requirements. To minimize the amount of time required to complete the collection of data using the payloads, a SSO was proposed. Further studying this trajectory vs other low Martian orbits revealed it provides many benefits to the spacecraft and mission. Compared to other trajectories, the SSO, with careful selection of the mean local time of the ascending node, leads to the greatest amount of time in sunlight for the spacecraft. In fact, with the perfect selection of the location of the ascending node and the inclination of the orbit, the spacecraft will never enter Mars' shadow. This means the solar panels will always have access to sunlight, maximizing the power available to the spacecraft and reducing the size requirements for the spacecraft's battery and solar panels. Additionally, because the spacecraft won't be entering and exiting the planet's shadow, there won't be drastic changes in the thermal environment experienced by the spacecraft. Reducing these temperature oscillations will avoid putting extra strain on the structures and electronics on board the spacecraft. As a result of the studies performed, a 700 km altitude circular SSO was selected for the primary mission remote data collection orbit.

4.2.3 Mapping Simulation Method

To model the amount of time the spacecraft will require in its primary mission orbit to carry out its data collection objectives, a MATLAB orbit and mapping simulator was developed. This simulator models the orbit of the spacecraft around Mars. All orbital properties were checked against FreeFlyer version 7.9.1, and less than 1 second of deviation per orbital period was recorded between the two simulations. The MATLAB simulation tracks a nadir pointing FOV**;** in this case**,** the minimum FOV of Duo's remote sensing payloads is 4.3°. The simulation tracks which points along its orbital path this FOV has visited and analyzed on the oblate spheroid that is Mars' surface, accounting for the planet's rotational rate. This simulation records the amount of time required for the spacecraft to cover 75% and 96%

of Mars' surface (because the spacecraft is in a SSO rather than a polar orbit, it will never be able to see 100% of the planet's surface). For Duo, it was found that 15 days are required to complete 75% coverage, and 107 days are required to complete 96% coverage with a 4.3° FOV.

Based on the orbital mapping simulations and the end of primary mission requirement of January 1st, 2031, it was determined that in case of any issues with data collection during the primary mission, the primary mission orbit could be repeated up to 5 times. Once all data is collected by the remote sensing payloads on board Bronco, the spacecraft will deploy the balloon vehicle for entry into the Martian atmosphere. After doing so, it will continue its primary mission orbit until it is transferred into a projected disposal orbit.

At the end of Duo's mission, the spacecraft will be transferred into a disposal orbit that will allow for natural orbital decay and burn up in the Martian atmosphere. NASA required that all spacecraft of Duo's class must be completely deorbited within 300 years of the end of their mission. To ensure compliance with this requirement, another orbit simulation was conducted using the mass and area properties of the spacecraft, as well as Mars' gravitational and atmospheric properties. The simulations led to the selection of a 310 km altitude circular orbit with the same orbital inclination as the primary mission's orbit. This orbit will allow Bronco to burn up in the Martian atmosphere after 286 years.

4.3 Concept of Operations

4.3.1 Bronco Concept of Operations

Figure 4.3.1-1 shows the concept of operations for Bronco's portion of the mission.

Duo launches from Kennedy Space Center at Cape Canaveral, Florida, on 12/13/2030 and enters an interplanetary Hohmann transfer to Mars. Duo will coast on the route to Mars over the course of 286 days, performing in trajectory correction maneuvers (TCM) as needed, and arrive at Mars on 9/25/2031. Duo will perform a MOI burn to enter its aerobraking orbit, where, based on historic data from the MRO, Mars Global Surveyor, and Mars Odyssey missions [10], Duo will perform 26 precise burns over the course of 176 days to enter its 700 km altitude Mars SSO. At this point, Duo will spend three weeks performing system diagnostics to ensure all subsystems are functioning as intended and taking data samples to ensure payload functionality.

On 4/9/2032, Bronco will begin collecting atmospheric, topographic, and surface/subsurface resource data on Mars while transmitting its data back to Earth. After 15 days, Bronco will achieve 75% coverage of Mars' globe in all three data categories, completing the primary mission ~616 days before the RFP deadline. Bronco will achieve maximum coverage (~95.57%) of Mars' globe after an additional 92 days. Using the data collected by Bronco, mission planners on Earth will select a landing location of interest on Mars, and Broncito will be deployed to collect high-fidelity atmospheric and topographic data on the selected landing location and surrounding travel paths.

While Broncito conducts its operations within Mars' atmosphere (which is discussed in Section 4.3.2), Bronco will continue to collect additional atmospheric, topographic, surface/subsurface resource data on Mars while transmitting both its and Broncito's data back to Earth. By 4/4/2037, Bronco will have transmitted all Broncito's data back to Earth. From there, Bronco will continue to collect and transmit its environmental data on Mars' globe until 1/1/2040, at which point Bronco will cease data collection and enter a 310 km circular disposal orbit around Mars where its orbit will gradually decay over the course of 283 years.

Accounting for all maneuvers, orbital maintenance [11], propellant consumption estimates, and European Space Agency (ESA) guidelines for ΔV margins on analytical and non-analytical maneuvers [12], Bronco will require 2.85 km/s of ΔV to complete the mission. These estimates result in Bronco having ~5.3% of residual ΔV, allowing mission planners to extend Duo's mission by ~649 days, if necessary.

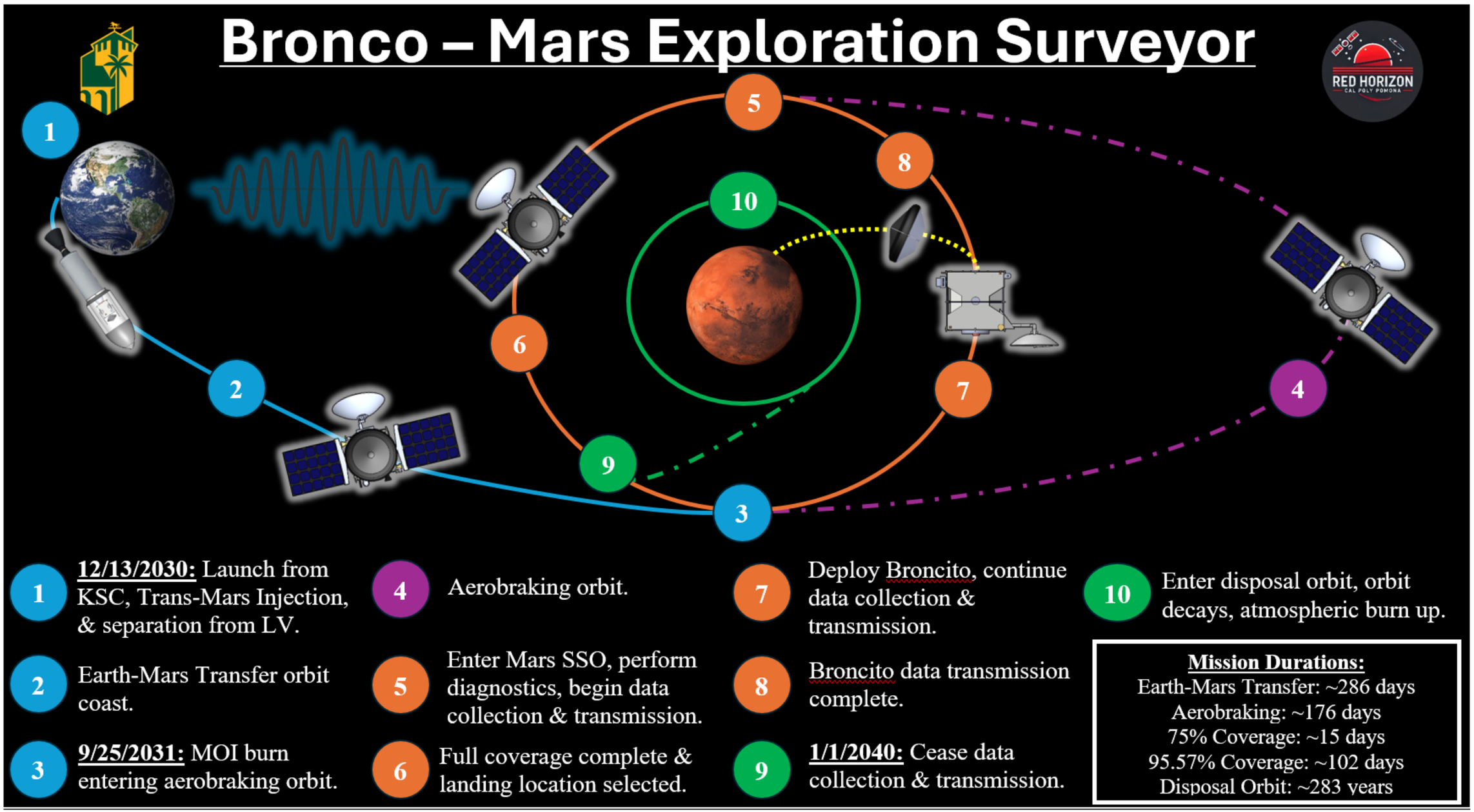

Figure 4.3.1-1: Bronco Concept of Operations

4.3.2 Broncito Concept of Operations

Figure 4.3.2-1 shows the concept of operations for Broncito's portion of the mission. Upon entering Mars' atmosphere, Broncito will decelerate using a combination of thrusters and drag from the heat shield. Once Broncito reaches an altitude of 11 km, approximately 2 hours after entry, Broncito will deploy its parachute, eject its heat shield, and drift down to the Martian surface using airbags to reduce the impact of the hard landing. After landing on Mars, Broncito will begin balloon inflation using its onboard hydrogen tank. Once fully inflated, Broncito separates from its hydrogen tank and begins its ascent. During this time, Broncito will collect atmospheric and topographic data using its direct sensing science instruments and transmit all its data to Bronco. After ~60 minutes, Broncito will reach its desired operational altitude of ~7 km, dropping ballast weight to counteract the loss of lift from hydrogen diffusion and maintain its altitude. After ~90 days of operation, Broncito will cease collecting data, descend to the Martian surface, disconnect from the balloon, and continue to transmit all its data to Bronco. Once all Broncito's data has been transmitted to Bronco, Broncito will retire from service.

Broncito – Mars' First Weather Balloon

1. **7/25/2032:** Atmospheric entry (150 km) using thrusters heat shield to decelerate.
2. Separation from parachute, inflating airbags to assist with hard landing.
3. Parachute deployment at 11 km altitude (~2 hours after entry).
4. Balloon inflation via LH_2 tank.
5. Ascent, separation from LH_2 tank, and start of data collection.
6. Target altitude met (7 km), periodically dropping ballast to maintain altitude (~90 days).
7. **10/23/2032:** Data cutoff, descent, and landing.
8. **4/4/2037:** Data transmission to Bronco until system is retired.

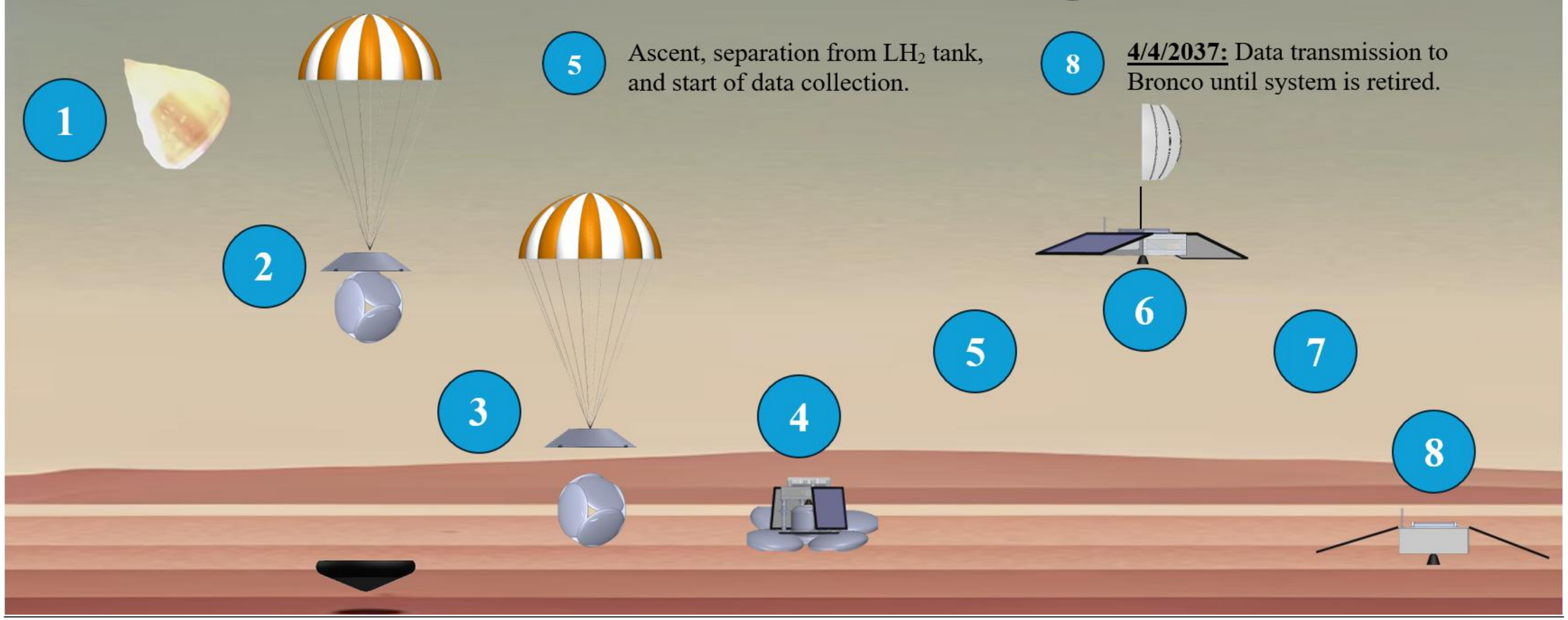

Figure 4.3.2-1: Broncito Concept of Operations

5.0 Science Instruments

To ensure Duo's science objectives were mapped and thought through; a science traceability matrix was developed to ensure each objective is addressed and met with the proper science instruments.

5.1 Science Traceability Matrix

For the selection of Duo's science instruments, a Science Traceability Matrix (STM) was constructed showing the relationship between the science objectives of the mission and the science instruments chosen to achieve those objectives. The STM is displayed on Table 5.1-1. On the STM, the light blue sections pertain to objectives and requirements of science instruments on Bronco, while the orange sections pertain to objectives and requirements of science instruments on Broncito.

Both the Bronco and Broncito systems must complete the three scientific objectives listed on the STM; however, due to their separate mission profiles, each vehicle has separate measurement objectives. Broncito's measurement objectives pertain to collecting high-fidelity atmospheric composition and density, terrain and topography, as well as surface and subsurface resource data on potential landing locations, while Bronco's measurement objectives pertain to collecting the same data at a lower level of fidelity on a global scale. Due to this separation, each vehicle has its own set of measurement requirements based on its separate measurement objectives. Each vehicle's individual measurement objectives and requirements, as well as the reasoning for their fidelity differences, are discussed in sections 5.1.1 to 5.1.3.

Based on the AIAA RFPs' preference for the use of technologies that have already been demonstrated on previous programs or are currently in NASA's technology portfolio, only scientific instruments satisfying this preference qualify for use on this mission.

Table 5.1-1: Duo Science Traceability Matrix

Program Goal: Support a Human Mars exploration campaign.						
Mission Objectives	**Science Objectives**	**Measurement Objectives**	**Measurement Requirements**	**Instruments**	**Instrument Requirements**	**Data Products**
1. Provide future mission planners with the data necessary to design entry, descent, and landing phases to support human exploration of Mars.	Characterize the atmospheric composition and create a detailed density profile of the Martian atmosphere.	Characterize the global composition and spatial distribution of the Martian atmosphere.	Spectral Resolution: 325 → 15000 nm Altitude Resolution:< 5 km	Mars Climate Sounder	Peak Power: 31 Watts, Ave Power: 15 Watts, Data Rate: 2.00 kbits/s, must be limb staring, nadir pointing, & off-nadir pointing for best results, Spectral Range: 0.3 to 45.0 µm, 9 spectral channels, Aperture: 4cm, Focal Ratio: f/1.7, FOV: 4.30° [2]	Atmospheric composition pie chart | Global atmospheric composition vertical profile
		Quantify the atmospheric density of Mars on a global scale.	Temperature Resolution: ≤ 2 K Altitude Range: < 80 km Vertical Resolution: < 5 km Horizontal Resolution: < 300 km			Global atmospheric temperature, pressure, & density profiles of Martian surface
			Pressure Resolution: ≤ 2% Altitude Range: < 80 km Vertical Resolution: < 5 km Horizontal Resolution <300 km			
		Quantify the atmospheric density of Mars at potential landing locations.	Temperature Resolution: ≤ 0.1 K	REMS Temp. Sensor	Range: 150 K - 300 K, Accuracy: 5 K, must be placed outside of adjacent object boundary layer [13]	High resolution atmospheric temperature, pressure, & density profiles of potential landing locations & travel paths
			Humidity Resolution ≤ 1%	REMS Humidity. Sensor	Accuracy: 10% (in 200-323 K range) [13]	
			Pressure Resolution: ≤ 1 Pa	REMS Press. Sensor	Range: 1 Pa - 1150 Pa, Accuracy: 3 Pa (BOL) & 20 Pa (EOL), HEPA filter needed to avoid contamination [13]	
2. Provide mission planners with the ability to pinpoint potential landing location and traverse paths to maximize the potential to achieve exploration objectives for Mars missions.	Conduct a detailed geographic survey of the Martian surface, including terrain and elevation profile.	Capture high-resolution imagery of Martian terrain on a global scale.	Horizontal Resolution: < 20 m Vertical Resolution: < 20 m	CTX	Peak power: 7 W, Idle power: 5 W, Focal length: 350 mm, Focal Ratio: f/3.25, FOV: 4.3° (2), Grayscale images [2]	Global Martian terrain imagery with identification of potential landing locations & travel paths
		Measure Martian surface topography on a global scale.	Ranging Resolution: ≤ 15 m In-track Resolution: < 1.8 km Cross-track Resolution: < 10.4 km	SHARAD	Power: 10 W, Data rate: 40 - 90 Gb/day, Freq: 15 - 25 MHz, Pulse duration: 85 µsec, Length: 10m, Vertical resolution: 7.5 m, Wavelength: 15m (free space) or better than 10 m (Martian subsurface) [2]	Global 3D topographic map of Martian surface
		Measure Martian surface topography of potential landing locations.	Ranging Resolution: ≤ 2 m Horizontal Resolution: ≤ 10 m Vertical Resolution: ≤ 10 m	Mini-SAR	Peak Power: 40 W, Ave Power: 11 W, Chirp Bandwidth: 75 MHz (average of typical mini-SAR system) [14]	High resolution 3D topographical map of potential landing locations & travel paths
		Capture high-resolution imagery of Martian terrain at potential landing locations.	Horizontal Resolution: ≤ 10 m Vertical Resolution: ≤ 10 m	MARDI	Power: 3.5 W (when imaging), FOV: 65.9°, Focal Ratio: f/5.6, Focal Length: 7.01mm, Data Return: up to 30 (four 256x256 heatshield jettison, sixteen 1024x1024 circularly edited, ten 800x800 on descent), Spectral Range: 500nm - 800nm, Max Imaging throughput: 667 ns/pixel (0.75 sec for full frame image) [15]	High resolution imagery of potential landing locations & travel paths
3. Enable mission planners to determine the potential of utilizing surface and subsurface resources in support of human exploration activities.	Investigate, identify, and quantify the potential surface and subsurface resources on Mars.	Characterize Martian surface and subsurface resources of a global scale.	Detect water deposits, regolith, nickel, iron, other metal deposits	SHARAD	Power: 10 W, Data rate: 40 - 90 Gb/day, Freq: 15 - 25 MHz, Pulse duration: 85 µsec, Length: 10m, Vertical resolution: 7.5 m, Wavelength: 15m (free space), 10 m (Martian subsurface) [2]	Global color-coded subsurface radargrams | Global color-coded resource maps of Mars | High resolution subsurface radargrams of potential landing locations & travel paths
		Characterize the global distribution of resources on Mars.	Subsurface Resolution: < 10 m			

5.2 Science Instrument Selection

5.2.1 Atmospheric Composition and Density Profile

Bronco's atmospheric measurement objectives are to characterize the global composition and spatial distribution of the Martian atmosphere as well as quantify the atmospheric density on a global scale. To do this, Bronco will require a remote sensing payload capable of detecting CO_2, H_2O, NO, CO, N_2, Ar, CH_4, and O_2 (major gases present in the Martian atmosphere) [16] as well as the temperature and pressure of these gases to derive the density profile of the atmosphere.

Based on these capabilities, the MCS remote sensing spectrometer was selected [2]. The MCS was originally used to measure changes in Mars' atmospheric temperature, pressure, composition, and dust content with height. The MCS possesses a spectral bandwidth from 300 nm to 45,000 nm across 9 spectral channels, which allows the MCS to characterize CO_2, H_2O, NO, CO, N_2, Ar, CH_4, and O_2 (major gases present in the Martian atmosphere). Additionally, 8 of its 9 spectral channels cover the thermal infrared range and possess the capability to measure the temperature and pressure of the Martian atmosphere. The MCS's heritage on the MRO gives it a TRL of 9. The data it collects will be used to generate 3D atmospheric composition distribution and density profiles over the entirety of the Mars globe to assist future mission planners.

As for Broncito, its atmospheric measurement objective is to quantify the atmospheric density of Mars at the selected landing location and surrounding travel paths. This objective can be met via the air temperature, humidity, and pressure sensors from the REMS [3]. The entire REMS is not necessary for this mission, and only the air temperature, humidity, and pressure will be required. These sensors were originally used to measure the ambient air temperature, humidity, and pressure of the Martian atmosphere. These sensors possess resolutions of ≤ 0.1 K, $\leq 1\%$, and ≤ 1 Pa for temperature, humidity, and pressure, respectively. Their use on the Mars Curiosity Rover provides them with a TRL of 9. The data they collect will be used to generate high-resolution atmospheric density profiles of the selected landing locations and surrounding travel paths to assist future mission planners.

5.2.2 Geographical Survey

Bronco's geographical measurement objectives are to capture imagery of the Martian terrain and measure Martian surface topography on a global scale. The resolution requirements for the imagery were driven by the size of small craters on the Martian surface, which are typically ≤ 20 m in diameter [16].

To collect imagery of the Martian terrain on a global scale, the CTX [2] was selected. The CTX was originally used to collect greyscale imagery of the Martian terrain, providing context for the data collected by other higher-fidelity scientific instruments onboard the MRO. The CTX will operate within the visible light range from 500 nm to 800 nm with an image resolution of ~10.5 m while in its Martian orbit. It will not be accompanied by other cameras in this mission, but its use on the MRO gives it a TRL of 9. The images collected by the CTX will be compiled into a Martian terrain map with identification of potential land locations and travel paths for Broncito's mission and future Mars missions.

To measure Martian surface topology on a global scale, the SHARAD [2] was selected. The SHARAD was selected to meet this objective because it is already being used for the surface and subsurface resource science objectives for this mission (this is discussed in Section 5.2.3 below). Although the SHARAD's primary purpose was to detect resources present in the Martian surface and subsurface, the data it collects can be utilized for altimetry. Studies from the Consortium for Research on Advanced Remote Sensing Systems [17] also support the use of the SHARAD for altimetry. While in its Martian orbit, the SHARAD's theoretical ranging resolution is ~15 m when operating between 15 MHz and 25 MHz, the in-track resolution is ~1.8 km, and the cross-track resolution is ~10.4 km. The SHARAD's heritage from the MRO gives it a TRL of 9. The data it collects will be used to support the generation of 3D topographic maps of the Martian surface to assist future mission planners.

Broncito's geographical measurement objectives are to capture high-resolution imagery of the Martian terrain and measure the Martian surface topography of the selected landing location and surrounding travel paths. The resolution requirements for the imagery and altimetry data were driven by the diameter of the SpaceX Starship (≤ 10 m) [18].

To collect high-resolution imagery of the Martian terrain of the selected landing location and surrounding travel paths, the MARDI [3] was selected. The MARDI is known for its capture of high-resolution color images/video of the Mars Curiosity Rover's landing location during descent. While the MARDI was originally designed to operate for ~2 minutes, it will instead operate over the course of the balloon vehicle's mission duration (~90 days) with an image

resolution of ~12 cm while at Broncito's apex altitude of ~7 km. The MARDI's heritage from the Curiosity Rover gives it a TRL of 9. The imagery captured by the MARDI will be compiled into a high-resolution terrain map of the selected landing location and surrounding travel paths to assist future mission planners.

To measure the surface topography of the selected landing location and surrounding travel paths, the Mini-SAR [4] was selected for use on the balloon vehicle. The Mini-SAR was designed to map dark, shadowed lunar craters and search for signs of water and ice on the moon; however, it will be used for radar altimetry for this mission. Studies from IEEE Transactions on Geoscience and Remote Sensing [19] support the use of the Mini-SARs for altimetry. While at the balloon's apex altitude, the Mini-SAR's theoretical range resolution is ~2.0 m when operating at a frequency of 75 MHz with a ground resolution of ~9.9 m. The Mini-SAR's heritage from India's Chandrayaan-1 gives it a TRL of 9. The data it collects will be used to support the generation of high-resolution 3D topographic maps of the selected landing location and surrounding travel paths to assist future mission planners.

5.2.3 Surface and Subsurface Resources

Bronco's surface and subsurface resource measurement objectives are to characterize Martian surface and subsurface resources as well as their distribution on a global scale. To do this, the orbiter will require a remote sensing payload capable of detecting water deposits, regolith, and metal deposits (which are resources potentially useful to Human-Mars missions) present on the Martian surface and subsurface [20].

To characterize Martian surface and subsurface resources as well as their distribution on a global scale, the SHARAD was selected. As previously mentioned in Section 5.2.2, the SHARAD was designed to detect resources present in the Martian surface and subsurface, making it a perfect instrument to meet this measurement objective. While in its Martian orbit, the SHARAD's in-track and cross-track resolutions remain ~1.8 km and 10.4 km, as stated in Section 5.2.2; however, its ranging resolution drops to ~10 m when analyzing the Martian subsurface. SHARAD's heritage on the MRO gives it a TRL of 9. The data collected from the SHARAD will be utilized to create 3D color-coded surface and subsurface radargrams of the Martian surface on a global scale to assist future mission planners.

6.0 Subsystem Design - Bronco

Bronco has several main subsystems, including telecommunications, command and data handling, propulsion, attitude control system, structure, thermal, and power. Each of these subsystems will be covered in the following sections, detailing the requirements and how each subsystem meets the requirements.

6.1 Telecommunications

6.1.1 Requirements

The Telecommunication Requirements in Table 6.1.1-1 were created according to the Program and Mission-Level Requirements from Table 2.0-1 and are to be used to design the telecommunication system.

Table 6.1.1-1: Telecommunication Requirements (Bronco)

Req. #	Telecommunication Requirements
9.0-1	The telecom system shall send back the primary mission data no later than January 1st, 2040.
9.0-2	The telecom system shall be capable of receiving no less than 100 bits/second at any given time.
9.0-3	The telecom system shall be compliant with the accepted DSN communication bands.
9.0-4	The telecom system shall operate reliably until January 1st, 2040.

Requirement 9.0-1 states that the telecommunication system shall transmit all primary mission data back to Earth no later than January 1st, 2040. This requirement drove the antenna diameter and transmitter power. For emergency communication scenarios, the minimum data rate of 100 bits/second (bps) from requirement 9.0-2 was used to ensure that Bronco can reliably receive command data in emergency scenarios to prevent mission failure. Requirement 9.0-3 mandates that the telecommunications system utilize a communication band compatible with the DSN because the DSN is essential for deep-space communication beyond $2x10^6$ km from Earth [21]. Lastly, the telecommunications system was designed for reliable operation through at least January 1st, 2040, fulfilling mission longevity requirements.

6.1.2 Mission Phases

The telecommunication system on Bronco ensures continuous and reliable communication with Earth throughout all mission phases, which include interplanetary coast, science data collection, and emergency case scenarios.

6.1.2.1 Interplanetary Coast

During the interplanetary coast phase, as Duo travels from Earth to Mars, stable communication with Earth is maintained via the MG horn antenna on Bronco. Bronco will downlink engineering/telemetry data or the status and health of the subsystems on the spacecraft [22] at a medium data rate.

Bronco will uplink command and telemetry data at a very low data rate using the same MG horn antenna as the downlinked telemetry data. Command data from ground stations on Earth controls the attitude and actions at specific times during mission phases. Accuracy is vital for command data because a single bit error can lead to mission failure [22]. Therefore, data is coded using BCH coding, and command data will be designed with a set bit error rate of 10^{-5}.

6.1.2.2 Bronco Science

While Bronco is collecting science data upon arrival at Mars, the data rate required will be much higher due to instruments like the SHARAD, which collects data at 2 Mbps. We compressed each science instrument's data rate by a factor of 10 [23] to lower the data rate significantly. Considering all other instruments, command, and engineering data, the total data rate is about 206 kbps. We will apply Reed-Solomon (255, 223) coding for science data with a BER of 10^{-4}. Data overhead was also considered and added with an overhead of 10%, which accounts for the instrument name, date, time, etc. [22]. All analyses for the science data collection phase, which lasts 105 days, allow the orbiter to collect and store about 2.7 TB of data to be sent back. We designed an HG parabolic antenna with a diameter of 3 meters and a transmitter power of 34 W. We designed the HGA to operate at an X-band frequency of 8.45 GHz with a contact time of 10 hours/day with the 34 m BWG DSN receiver, similar to the MRO's capabilities [24]. We also considered the time we would be in solar conjunction throughout the mission into the late 2030s. We found four solar conjunction events starting on May 1, 2032, with a periodicity of about 26 months. Solar conjunction occurs when the Sun is between Earth and the satellite at about 3° [22]. Designing the data rate based on all of this, as well as assuming the average distance from Earth to Mars of 2.25×10^8 km, we are capable of a data rate of 359 ksps, allowing us to easily send back data collected from Bronco as we are collecting it.

6.1.2.3 Emergency Scenarios

We also considered emergencies when we might lose contact with the DSN receiver due to pointing errors or after a solar conjunction. To regain contact, we designed two MG horn antennas that point in opposite directions to point

down to Earth. They operate at a low data rate of 100 symbols/s, which is just necessary for command data. The antennas weigh about 1.5 kg and have a transmitter power of 10 W.

6.2 Command and Data Handling

6.2.1 Bronco Requirements

The Bronco C&DH subsystem is responsible for managing high-bandwidth data collection, real-time subsystem control, and communication with Earth through the DSN. It takes on the key role by serving as the data relay to Broncito while autonomously carrying out its operations. Its requirements, shown in Table 6.2.1-1, highlight high processed data output, radiation-tolerant products, and long-term data reliability for transmission.

Table 6.2.1-1: Command and Data Handling Requirements

Req. #	Requirement
8.0-1	The C&DH system shall be able to store data at a rate of no less than 30 Msps.
8.0-2	The C&DH system shall operate reliably until January 1st, 2040.
8.1-2	The C&DH system shall be compliant with the accepted DSN communication bands.
8.0-3	The C&DH system shall possess a minimum data storage capacity of 512 GB to support science data buffering and Broncito data relay without loss.
8.0-4	The C&DH system shall process, prioritize, and packetize incoming data streams with onboard fault detection and autonomous correction to ensure safe relay of critical and science data.

These requirements are derived from deep space mission profiles from prior missions and the performance needed to support both Bronco and Broncito during their tandem operation.

6.2.2 Bronco C&DH Products

Comparison between various flight-tested processors: LEON3-FT, RTG4, and RAD750 of BAE Systems; the RAD750 [25, 26, 27] was chosen because it had the highest flight heritage, demonstrated radiation shielding, and software compatibility with the NASA DSN equipment. In data storage, the RH304T Solid State Data Recorder (SSDR) represented the best overall choice, considering radiation hardness, storage capacity, and system modularity. Communication architecture trades, for supporting infrastructure for this storage, established that the high throughput and flexible topology of SpaceWire outperformed CAN and MIL-STD-1553 [28, 29] for both inter-subsystem communication and Broncito interfaces. The Small Deep Space Transponder (SDST) was selected because of its

ruggedness, dual redundancy, and heritage, as it was developed to operate within the NASA-DSN for interplanetary missions.

Table 6.2.2-2: Main Storage Trade Study

Parameters			MS RH304T				MS 3440				Curtis-Wright CFDR			
Category	**FOM**	**Weight**	**Value**	**U%**	**U**	**W**	**Value**	**U%**	**U**	**W**	**Value**	**U%**	**U**	**W**
M (kg)	0.8	3	0.75	6%	5	15	0.62	33%	9	27	4	-20%	1	3
V (cm^3)	415	2	407	2%	3	6	406	2%	3	6	7590	-1760%	0	0
Storage (TB)	4	3	4.5	125%	9	27	0.44	-89%	0	0	2	-50%	0	0
Tolerance	3	2	3	0%	0	3	3	0%	0	3	2	-33%	0	0
Totals			**51**				**36**				**3**			

6.2.3 Bronco C&DH Methods

Development was accomplished by top-down systems engineering. With the use of functional flow diagrams, the subsystems were driven by command/control paths and anticipated data quantities, which enabled the implementation of a dual-string architecture where each processor string is the mirror image of the other in terms of function and coverage. Key software activities like packet verification, telemetry priority, and watchdog interrupt routines were built up in a hierarchical structure in layers, separating mission operations from contingency handlers. Timing synchronization was imposed by using internal pulse-per-second signals and time-tag propagation.

6.2.4 Bronco C&DH Assumptions

The C&DH subsystem assumes that Bronco will experience 10-hour DSN contact each day, which is sufficient to downlink approximately 1.6 TB of data in 60 days at the 359 ksps downlink rate that was established via the X-band through the SDST. Onboard payload science data is anticipated and assumed to be produced at an average of 2.7 TB, and Broncito will produce approximately 2.4 TB over its 90-day mission timeline, both via Bronco for storage and relay to Earth downlink. The C&DH system will consist of dual RH304T SSDRs, which will provide 9 TB of redundant total capacity. In addition, both units will be operating in a scheduled buffer mode to ensure quality storage even in the event of downlink delays, blackout periods, or extended data acquisition runs. Bronco will also be operating

under deep space environmental conditions, and thus, the required C&DH hardware must be able to operate in the -40°C to +85°C operating temperature range.

6.2.5 Bronco C&DH Input

The C&DH subsystem accepts input data from a number of spacecraft sources. They include time-tagged command sequences from DSN uplink, health and engineering telemetry from all spacecraft subsystems (thermal, power, propulsion, ACS), and science data from Bronco's onboard payloads (MCS, CTX, SHARAD). All received data is handled by the RAD750 processor, where it is categorized, authenticated, and queued by the system's bandwidth-prioritized queuing algorithm to label critical data with high priority for downlink or buffer protection immediately. Additionally, Broncito's science data stream, which should generate approximately 2.4 TB of high-fidelity atmospheric and geographic survey data over its 90-day mission, is received through the dedicated SpaceWire interface.

This data is then combined into the same priority queue as Bronco's own science data. All of the input data is compressed (assumed 10:1 ratio from past missions) and written into the dual RH304T SSDR array, each offering 4.5 TB of radiation-hardened storage capacity, in a cross-strapped configuration [23]. This configuration allows for writing all input data to the current SSDR, and the second SSDR is continuously verifying data integrity by cross-verifying and ECC checking so that there is no single-point loss or corruption of data throughout the mission.

6.2.6 Bronco C&DH Output

The Bronco C&DH subsystem manages data processing and transmission of all acquired science and telemetry data, doing high-quality, lossless processing and safe Earth downlink. The subsystem handles onboard-payload science data like MCS, CTX, and SHARAD radar science, along with spacecraft engineering telemetry, within the BAE Systems RAD750 processor, providing ≥200 MIPS processing capability. Furthermore, Broncito's science data stream of about 2.4 TB over its 90-day mission is received via the SpaceWire interface and processed by the C&DH system to be included in the data relay queue. The entire data is buffered in the C&DH storage array composed of two cross-strapped RH304T SSDRs, with a capacity of 4.5 TB for each. This configuration not only allows for an aggregate usable capacity of over 9 TB but also full system redundancy, without downtime during switchover in the event of drive failure, corruption, or hardware degradation. With the topic average mission data volume of ~5.1 TB, this dual-

SSDR design offers sufficient capacity for all science and relay data with over 75% margin, as well as active redundancy, and keeps the system always within safe operation storage limits. Additionally, the output management system uses a bandwidth-priority queuing algorithm and CCSDS-conformant telemetry formatting, which dynamically assigns priority flags based on mission phase, communication status, and data significance.

During nominal mission durations, the SDST transponder at X-band (8.45 GHz) provides a 359 ksps downlink rate for 10-hour DSN daily contacts such that the spacecraft can transfer approximately 1.6 TB of data for each 60 days. At this rate, the C&DH system is able to continue to clear the buffered data at acquisition rates without ever experiencing any interruptions in science collection and data relay. In degraded mode or solar conjunction blackout periods, the system will automatically give precedence to mission-critical health telemetry and fault reports over all science data for the purpose of spacecraft safety and to enable prompt ground response. Autonomous fault management scripts, which were created by the C&DH software, may be executed directly to spacecraft actuators and to critical subsystems without traversing regular command chains to minimize response latency. Both RH304T SSDRs also operate under error correction coding (ECC), parity checks, and self-scrubbing algorithms to ensure the integrity of data even in extremely high-radiation deep space conditions. Coupled with the double-string processor redundancy, cross-strapped storage of data, and sequenced prioritized outputting, the Bronco C&DH subsystem demonstrates its capability to provide safe support to mission activities, science data relaying, and spacecraft safety until January 1st, 2040, fulfilling and exceeding the subsystem throughput, storage, and mission longevity requirements.

6.2.7 Bronco C&DH Redundancy

The Bronco C&DH subsystem uses a complete dual-string cold-redundant design with two RAD750 processors and two RH304T SSDRs comprising C&DH flow. The two processors are arranged in a way that, in the event of failure of the primary processor, the secondary processor can take over all the mission control and data handling tasks via the implemented automatic switchover, alerted by the onboard fault flag detection.

Similarly, the two RH304T SSDRs each have a 4.5 TB storage capacity and run in an active-passive configuration. This is done where the primary SSDR writes all data while the other SSDR cross-verifies data constantly through parity checking and self-scrubbing algorithms. If the active SSDR shows any indication of degradation, data corruption, or hardware failure, the system will promote the secondary SSDR to active status and jointly demote the degraded SSDR that was the primary.

This cross-strapped redundancy guarantees that any single failure in the processing or storage chain will have no effect, and be single-fault tolerant, on mission operations and data integrity. This setup ensures both Bronco and Broncito mission data are securely processed, even in unpredictable circumstances, for the mission continuity with its design life extending through January 1st, 2040.

6.3 Propulsion

6.3.1 Overview

The Requirements Definition and Mission Design in sections 2.0 and 4.0 were utilized to create the propulsion requirements, as illustrated in Table 6.3.1-1. These propulsion requirements were then applied in the design of the propulsion system discussed below.

Table 6.3.1-1: Propulsions Requirements

Req. #	Requirement
5.0-1	The propulsion system shall provide no less than 2.85 km/s of ΔV.
5.0-2	The propulsion system tanks shall possess a factor of safety no less than 2.
5.0-3	The propulsion system shall possess the ability to perform near-impulsive burns.
5.0-4	The propulsion system shall possess multiple restart capabilities.
5.0-5	The propulsion system shall operate reliably until January 1st, 2040.
5.0-6	The propulsion system shall possess a TRL of no less than 8

Requirement 5.0-1 specifies the ΔV necessary for mission maneuvers, including cruise course corrections, MOI, and station keeping. Considering this requirement, the necessary propellant and pressurant masses were calculated and subsequently used to size the propellant and pressurant tanks. Tanks were designed with a factor of safety of 2 to comply with requirement 5.0-2, ensuring protection against potential failures. Requirements 5.0-3 and 5.0-4 stipulate that the propulsion system must possess near-impulsive burns and multiple restart capabilities, guiding the selection of the main engine. Additionally, the choice of the main engine adheres to the reliability and maturity constraints defined in requirements 5.0-5 and 5.0-6, requiring operational reliability through at least January 1st, 2040, and a TRL greater than 8.

6.3.2 Methods

Several propulsion systems were initially considered, including electric, solid, nuclear, cold gas, and liquid propulsion.

Electric propulsion was quickly eliminated due to its large power requirements, insufficient impulsive burn capability, and low thrust, complicating MOI. Cold gas systems were similarly ruled out due to inadequate impulsive burn and thrust capabilities. Solid rocket motors do not possess multiple restart capabilities and lack thrust variability, which led to their being discarded. Nuclear propulsion was excluded due to insufficient heritage and current developmental design immaturity.

Excluding each of these alternatives, liquid propulsion emerged as the only viable choice. Two types of liquid propulsion systems, monopropellant and bipropellant, were considered. Both propulsion systems provide pulsing capability and steady-state thrust and exhibit superior impulsive burn and thrust potential compared to the previously mentioned propulsion systems. Each system has advantages and limitations; both possess operational heritage on Mars missions.

6.3.3 Propulsion System Selection

Monopropellant propulsion systems only require fuel to operate, and they offer a simplified design due to their use of blowdown pressurization, where the propellant tank is pre-pressurized at a high initial pressure. This approach reduces system complexity, requiring fewer valves and transducers. The propellant tank needs to have a large wall thickness because of the high initial pressure, which increases the propulsion system mass. The pressure decays over time as more propellant is used, leading to the variable flow rate resulting in reduced thrust and specific impulse (I_{sp}) [30]. Additionally, monopropellant systems demand higher power due to the necessity of heaters to heat the catalyst beds, which decompose the hydrazine into hot gases to be expelled through the nozzle, producing thrust.

In contrast, bipropellant systems utilize a fuel and oxidizer that mix in the nozzle to produce thrust upon ignition. Bipropellant systems provide superior performance in terms of I_{sp} and thrust and a higher impulsive burn ability, making them exceptional for MOI. Bipropellant systems use a separate tank to pressurize the system, allowing for constant pressure throughout the mission. The drawbacks to bipropellant systems are their added complexity due to the mixture ratio requirements for designed performance and the need for multiple tanks, each with temperature requirements. Bipropellant attitude control is less capable of pulsing and has a greater minimum total impulsive capability than monopropellant, making it less ideal for fine control.

Duo employs a dual-mode system, combining a bipropellant main engine and monopropellant ACS to leverage the advantages of both propulsion systems. This enables Duo to possess superior I_{sp}, thrust, and impulsive burn capability

for the main engine used during MOI while having finer maneuverability and simplicity during station keeping and course correction. To simplify design further, hydrazine was selected as the fuel to utilize a standard tank between the main engine and the. NTO was chosen as the oxidizer to be paired with hydrazine because they possess simpler temperature requirements and are hypergolic, ignoring the need for a separate ignition source.

6.3.4 Main Engine Selection

Following the dual mode system selection, a trade study was conducted to compare three candidate main engines: the Ariane Group 200 N, Ariane Group 400 N, and R-4D-15 HiPAT Dual Mode engines [31, 32]. The evaluation is detailed in Table 6.3.4-1, which assesses the characteristics of each engine according to its I_{sp}, thrust, and TRL. The engines were scored according to weighted FOM, which reflect each engine's ability to meet or exceed the previously outlined propulsion requirements.

Table 6.3.4-1: Main Engine Trade Study

Parameters			Ariane Group 200N Bipropellant Thruster				Ariane Group 400N Bipropellant Thruster				R-4D-15 HiPAT Dual Mode High Performance Rocket Engine			
Category	**FOM**	**Weight**	**Value**	**U%**	**U**	**W**	**Value**	**U%**	**U**	**W**	**Value**	**U%**	**U**	**W**
I_{sp} (s)	307	3	270	-12%	1	3	321	5%	3	9	329	7%	5	15
Thrust (N)	348	2	200	-43%	0	0	400	15%	5	10	445	28%	9	18
TRL (1-9)	8	3	9	13%	5	15	9	13%	5	15	8	0%	3	9
Totals			**18**				**34**				**42**			

The R-4D-15 HiPAT engine achieved the highest weighted score of 42, outperforming the Araine Group main engines across most evaluated categories, leading to its selection.

The mixture ratio (MR) range required by the R-4D-15 HiPAT engine was used in the design of the propellant tanks discussed in Section 6.3.5 at an oxidizer to fuel ratio of 1.33, making the tanks as similarly sized as possible. The engine's mass was also accounted for in the total propulsion system mass covered in Section 6.3.6.

6.3.5 Propellant and Pressurant Tanks

The rocket equation was utilized with the required ΔV to determine the necessary usable propellant mass, calculated as 2,430 kg. To account for trapped propellant (3%), outage (1%), and loading uncertainty (0.5%), the total loaded propellant mass was calculated to about 2,500 kg [30].

Tank volumes were determined using the ideal gas law, including an additional 10% ullage for initial pressurization [30]. Structural reinforcements, including safety factors of 2, were incorporated into the tank design to ensure tank robustness.

Gas ingestion mitigation is an essential part of propulsion system design. In zero gravity conditions, the location of gas bubbles is unknown, and too much gas ingestion in the combustion chamber could lead to system failure. To prevent gas ingestion into the main engine, various methods were evaluated, including capillary devices, diaphragms, and bellows.

Although capillary devices offer high effectiveness, they introduce complexity and cannot be ground tested on Earth due to gravity. The below, while reliable, adds excessive mass due to its being made of metal. Consequently, various methods were evaluated to prevent gas ingestion into the main engine. Round testing was conducted. Elastomer diaphragms were chosen for the hydrazine tank, and Teflon diaphragms were specified for NTO tanks due to the incompatibility of elastomer with NTO [30].

A regulated pressurant-based system was employed rather than a blowdown system to ensure consistent propellant flow and proper mixture ratios throughout mission operations, which are necessary for bipropellant systems. Helium and nitrogen are the two typical pressurants used for bipropellant propulsion. Helium was chosen as the pressurant due to its significantly lower mass than nitrogen, despite potential minor leakage considerations.

Spherical tank designs were chosen for simplicity and efficiency. Two reinforcing bands were added at the girth welds to address reduced material strength near weld joints. Mass contributions from structural attachment, girth lands, penetrations, and membranes were calculated and incorporated into the total tank mass estimations according to Brown’s guidance [30].

6.3.6 Propulsion System Schematic

Figure 6.3.6-1 provides a schematic of Duo's propulsion system, detailing critical components such as valves, transducers, filters, heaters, lines, and fittings with corresponding identification of component quantities and masses in Table 6.3.6-1 [11,30, 33, 34].

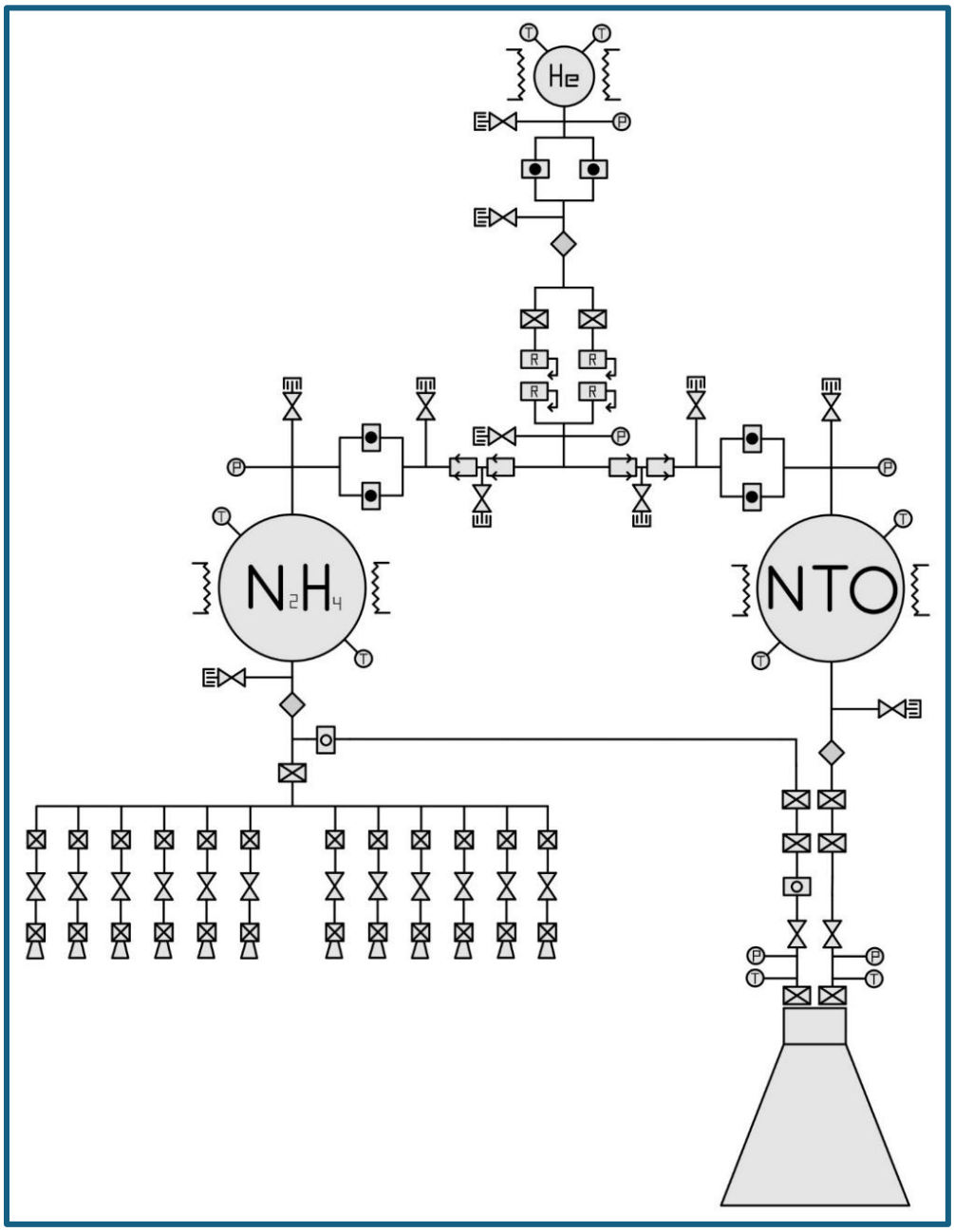

Figure 6.3.6-1: Propulsion Schematic

Table 6.3-4 is a legend that identifies each component depicted in Figure 6.3.6-2 along with its quantities and mass estimates.

Table 6.3.6-1: Propulsion Schematic Legend

Propulsion Mechanisms				
Item	**Symbol**	**Mass (kg)**	**Quantity**	**Total Mass (kg)**
Temperature Transducer		0.10	8	0.80
Pressure Transducer		0.22	6	1.32
Fill and Drain/Service Valve		0.11	11	1.21
Pyro/Squib Valve (Normally Closed)		0.50	6	3.00
Pyro/Squib Valve (Normally Open)		0.50	2	1.00
Isolation/Latch Valve		0.50	7	3.50
Solenoid Isolation Valve		0.50	12	6.00
Parallel Check Valve		0.30	4	1.20
Filter		0.03	3	0.09
Regulator-Series Pair	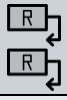	0.15	2	0.30
Cavitating Venturi/Orifice		0.22	14	3.08
Line Heaters		0.90	6	5.40
Lines and Fittings	N/A	26.7	N/A	26.7
Total Mechanism Mass (kg)				**53.6**
Fuel Tank Mass (kg)		94.3	1	94.3
Oxidizer Tank Mass (kg)		94.8	1	94.8
Pressurant Tank Mass (kg)		20.5	1	20.5
Main Engine Mass (kg)		5.4	1	5.4
Thruster Mass (kg)		N/A	12	N/A
Propulsion System Mass (kg)				**269**

The schematic illustrates the dual-mode propulsion system, highlighting the selected R-4D-15 HiPAT main engine, pressurant, and propellant tanks, and attitude control thrusters (discussed further in a subsequent section).

Each tank has heaters and temperature sensors to maintain optimal operational temperatures. Pressure transducers at critical junctions provide redundancy and system performance monitoring. They facilitate the detection of failures and enable assessments of thrust, I_{sp}, and propellant consumption. There are also redundant filters positioned downstream of each tank to ensure a particulate-free flow that may cause valve leakage or blockage, which could jeopardize the mission [11].

The design includes numerous redundant and parallel valves to mitigate the risk of individual valve failure, which could lead to critical mission failures. Fill and drain valves facilitate pre-launch propellant loading and ground testing to ensure immediate operational readiness and prevent gas ingestion. Pyrotechnic valves (pyro valves) are either normally open or normally closed and provide reliable isolation for single-use applications to isolate the main engine when not required [11].

Cavitating venturi valves are incorporated to mitigate sudden pressure spikes that occur during rapid valve operations. Additionally, parallel check valves and regulator pairs are strategically placed to manage propellant mixture ratios and prevent reverse flow. Regulators specifically manage pressure surges when valves rapidly change states. Check valves prevent unintended mixing of fuel and oxidizer vapors, avoiding potential catastrophic reactions. Solenoid isolation valves are employed for thrusters to provide rapid and precise control capability [11].

6.4 Attitude Control System

6.4.1 ACS Requirements

The ACS on Bronco is designed around 3 key requirements shown in Table 6.4.1-1.

Table 6.4.1-1: Bronco's ACS Requirements

Req. #	ACS Requirement
7.0-1	The ACS must be able to slew the spacecraft 90 degrees around any axis in no more than 300 seconds
7.0-2	The ACS must be able to account for all disturbance torques experienced by the spacecraft, be able to determine the required attitude at any time during the mission, and provide the required torque to maintain that attitude to less than 0.1° of deviation
7.0-3	The ACS must be able to operate reliably until January 1st, 2040

6.4.2 ACS Methods

To ensure compliance with the first requirement, the mass moment of inertia matrix for the spacecraft, along with the locations for each of the ACS thrusters, was plugged into a rotational kinetics model to determine the required thrust capability of each thruster. Based on this model, the maximum required thrust per thruster was determined to be 1.81 Newtons shown in Table 6.4.2-1.

Table 6.4.2-1: Rotational Kinematics Results

	X-axis	Y-axis	Z-axis	Total
Rotation Angle [°]	180	180	180	540
Maximum Torque [N-m]	0.4068	3.1728	3.4485	**3.4485**
Maximum Thrust [N]	0.2034	1.8130	1.1495	**1.8130**
Propellant Mass [kg]	0.0352	0.2790	0.1741	0.4883

Based on this thrust requirement, a trade study based on thrust capability, dry mass, and required power was performed to select a thruster. The trade study led to choosing the Aerojet Rocketdyne MR111-C 4 Newton thruster. To provide symmetric thrust about each of the spacecraft's axes, 12 ACS thrusters are required.

To ensure the ACS is compliant with its second key requirement, the system will need a way of precisely determining its attitude at any moment. This is achieved by using sun sensors, star sensors, and inertial measurement units. Each of these components for the ACS was also selected using a trade study shown in Table 6.4.2-2. Trade studies were performed based on accuracy, mass, power, and FOV; the Coarse Sun Sensor by Bradford Space, Leonardo Aerospace Star Sensor, and Northrop Grumman SIRU were selected.

Table 6.4.2-2: ACS Thruster Study

Thruster Trade Study														
Parameters			**MR-103G 1N**				**MR-111C 4N**				**MR-106L 22N**			
Category	**FOM**	**Weight**	**Value**	**U%**	**U**	**W**	**Value**	**U%**	**U**	**W**	**Value**	**U%**	**U**	**W**
Thrust (N)	1.81	3	1	-81	0	0	4	54.75	9	27	22	91	9	27
Mass (kg)	.35	1	.33	5.7	5	5	.33	5.7	3	3	.52	-48	0	0
Power (W)	8.3	2	8.25	.6	3	6	8.25	.6	3	6	13.2	-58	0	0
Totals			**11**				**36**				**27**			

Next, a 3-axis reaction wheel system is needed to allow the spacecraft to make small adjustments to its attitude. In selecting the reaction control wheels for the ACS, the disturbance torques the spacecraft will encounter during its primary mission also need to be modeled. The maximum and total disturbance torque the spacecraft encounters will determine the momentum capacity required by the reaction wheels.

In order to determine the disturbance torques using the properties of the trajectory, the spacecraft's physical properties and properties of Mars were required. The maximum disturbance torques were calculated and displayed in Table 6.4.2-3. Reaction wheel desaturation frequency as a function of the reaction wheel maximum momentum capacity was calculated.

Table 6.4.2-3: Disturbance Torques

Disturbance Torques in LEO		**Disturbance Torques in Martian Orbit**	
Solar Torque (N-m)	3.671×10^{-4}	Solar Torque (N-m)	2.447×10^{-4}
Drag Torque (N-m)	5.514×10^{-13}	Drag Torque (N-m)	1.767×10^{-14}
Magnetic Torque (N-m)	2.603×10^{-5}	Magnetic Torque (N-m)	2.673×10^{-8}
Gravity Gradient Torque (N-m)	9.031×10^{-13}	Gravity Gradient Torque (N-m)	2.447×10^{-4}

This number along with the minimum impulse bit was used to conduct another trade study shown in Table 6.4.2-4 to select the reaction wheel assembly, which led to the selection of the Bradford Space W45E. Based on the calculated disturbance torques and maximum momentum capacity of the reaction wheel, the desaturation frequency of the reaction wheels was calculated to be 2.25 days.

Table 6.4.2-4: Reaction Wheel Trade Study

Parameters			RW 4				RW-10NMS				RW Unit W45E			
Category	**FOM**	**Weight**	**Value**	**U%**	**U**	**W**	**Value**	**U%**	**U**	**W**	**Value**	**U%**	**U**	**W**
Max Torque (N-m)	3.671 x10^{-4}	3	0.25	99	9	27	0.19	99	9	27	0.2	99.81	9	27
Momentum (N-m-s)	8	2	4	-100	0	0	10	20	5	10	12	33.3	9	18
Mass (kg)	4	1	3.2	20	5	5	5	-25	1	1	5	-25	1	1
MAX Power Consumption (W)	100	1	10	90	9	9	110	-10	3	3	170	-70	0	0
Totals			**41**				**41**				**46**			

Finally, a computer and software are required to manage the data coming in from the sensors, model the spacecraft's dynamics, and send command signals to the reaction wheels and thrusters. For this purpose, the spacecraft's main command and data handling computer will be used. Figure 6.4.2-1 is a block diagram that shows how all the components of the ACS are connected and allowed to control the spacecraft's attitude.

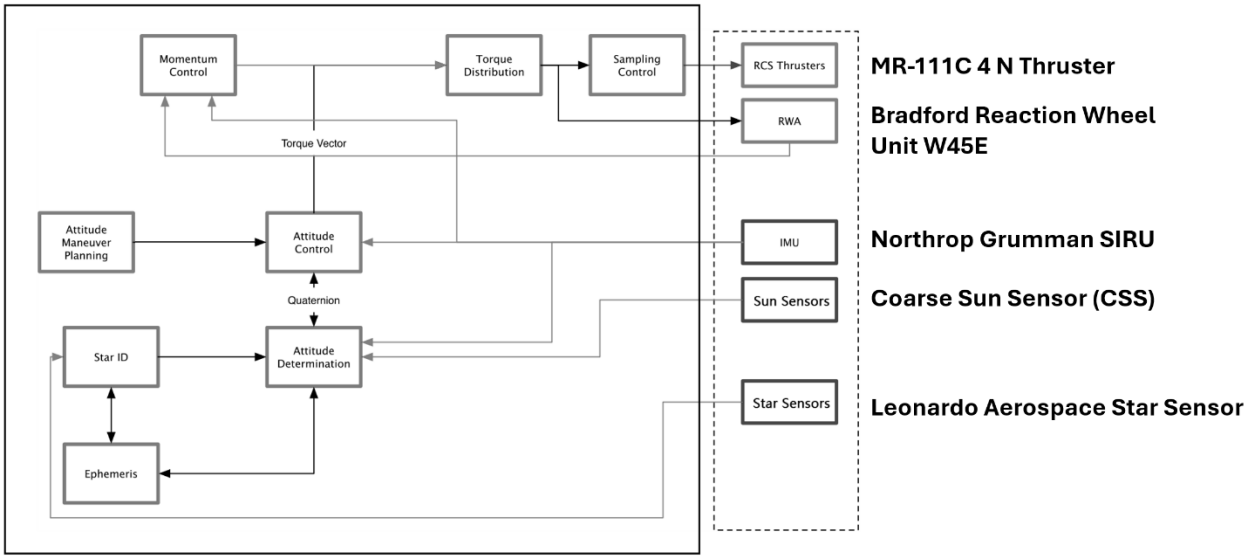

Figure 6.4.2-1: ADCS Block Diagram

6.4.3 ACS Redundancy

To reduce the risk of single-point mission-critical failures of the ACS, double redundancy is used on all sensors and thrusters. The reaction control wheel assembly has a 4th reaction wheel that is not orthogonal to any of the 3 main wheels, so if any one of the 3 fails, the 4th one can take its place. However, the reaction wheel desaturation frequency

will increase. Based on these redundant components, the total subsystem mass and power requirements were calculated and tabulated in Table 6.4.3-1.

Table 6.4.3-1: ADCS Mass and Power Statement

Equipment	Quantity	Mass (kg)	Power (W)
MR-111C 4 N Thruster	12	0.33	8.25
Bradford Aerospace Reaction Wheel W45E	4	7.45	29
Coarse Sun Sensor (CSS)	12	0.18	0.4
Leonardo Aerospace Star Sensor	2	3.5	13.5
Northrop Grumman SIRU	1	7.1	43
Bae Systems RAD750 Computer	1	2	10
Totals		**54.0**	**254**

6.5 Structures

6.5.1 Structural Requirements

Table 6.5.1-1 below shows the requirements for Bronco's structures subsystem.

Table 6.5.1-1: Structure Requirements (Bronco)

Req. #	Structural System Requirements
10.1-1	The system shall integrate with the Falcon Heavy Payload Fairing.
10.1-2	The system shall conform to standards of the standard Falcon Heavy Payload Attachment Fitting.
10.1-3	The structure shall withstand all launch loads including quasi-static, acoustic, and dynamic environments associated with the Falcon Heavy.
10.1-4	The structural design of the spacecraft shall maintain an ultimate factor of safety of 1.5 on all load-bearing structural elements.
10.1-5	All structural components and fasteners shall survive the shock load generated by stage separation.
10.1-6	Structural materials and bonds shall fail no earlier than January 1st, 2040.
10.1-7	The structure shall support all onboard payloads and subsystems without introducing excessive misalignments or displacements.
10.1-8	The structure shall not obstruct the FOV of any scientific instrument or sensor while the system is in its mission configuration.

6.5.2 Material Selection

For a Mars science mission such as Duo's, the selection of materials is critical to enable mission success under strict mass, structural, and thermal limitations. Sandwich composites of carbon fiber and aluminum honeycomb offer a highly optimized solution that satisfies these requirements. The sandwich composite construction combines carbon fiber's high strength-to-weight ratio and directional stiffness with an aluminum honeycomb core that has high shear strength, rigidity, and thermal damping to create a material that is significantly lighter and stiffer in bending than a solid material of the same thickness. This also makes it well suited for survivability under intense launch vehicle loads, where dynamic pressure, acoustic, vibrational, and g-loads impose severe risks to payload integrity.

Carbon fiber-aluminum honeycomb structures also offer advantages in manufacturability and system integration. The inherent vibrational damping of the sandwich composite reduces the need for additional damping hardware and the flat panel construction simplifies the integration of subsystem hardware such as instrument mounts, electronic bays, and antenna booms.

In contrast, traditional materials such as solid aluminum or titanium present several limitations. Aluminum, while lightweight and low-cost, lacks the stiffness and stability needed to protect high-precision instruments from deformation under launch loads or thermal cycling. Aluminum is also more susceptible to fatigue over time and damage from micrometeoroids. Titanium, while stronger and more stable, comes with a higher mass penalty and is more expensive and difficult to machine and integrate, especially for larger spacecraft. For a spacecraft constrained in both mass and volume, these limitations translate into a reduced payload capacity, more complex thermal control systems, and higher structural margins, which can impact mission performance or increase cost.

6.5.3 Configurations

The Bronco orbiter construction was based around a cylindrical structure that acts as both the primary load path and housing for propulsion fuel tanks. Each end of the cylinder has attached upper and lower decks for housing the payload. Figure 6.5.3-1 shows the overall configuration of Bronco as well as general dimensions.

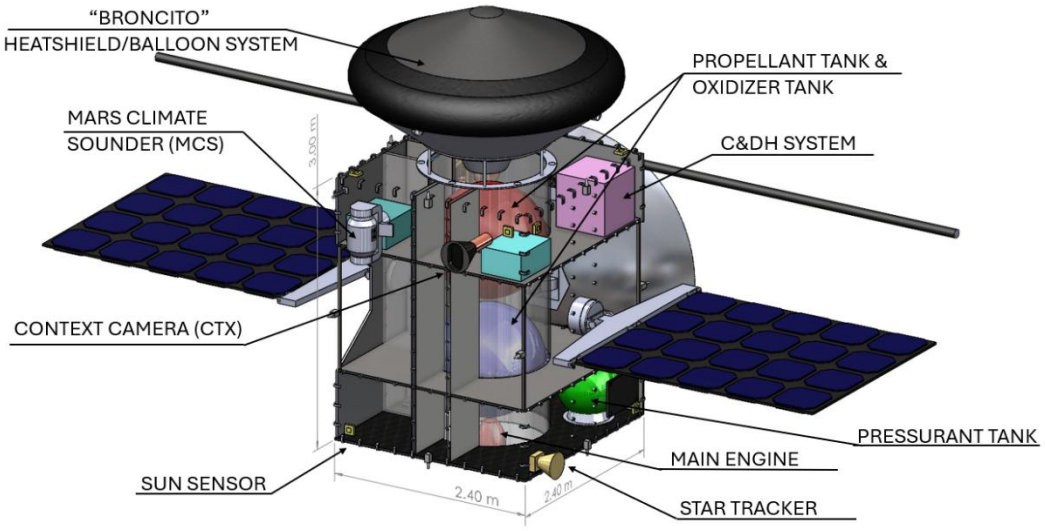

Figure 6.5.3-1: Internal Bronco Configuration

The Duo system is designed to fit well within the 4.6-meter diameter and 7-meter payload fairing of the Falcon Heavy as shown in Figure 6.5.3-2. The spacecraft is mounted vertically in the 1,575 mm payload adapter that is the default for the Falcon payload fairing. The spacecraft will be secured at the end of the central cylinder with a spring-loaded release payload adapter ring. In this configuration, the solar arrays, high-gain antenna, and SHARAD are put in a stowed configuration to meet the size constraints and secure them for launch.

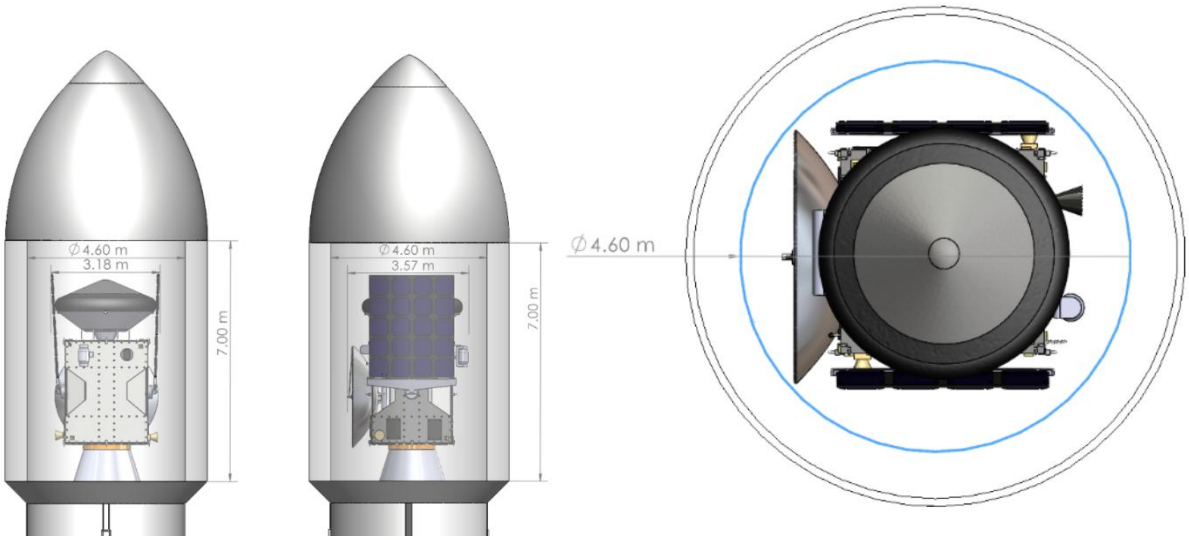

Figure 6.5.3-2: Duo system inside the Falcon Payload Fairing

After a successful launch, the Duo spacecraft will separate from the Falcon payload fairing using the spring-loaded mechanism and initiate deployment phase as shown in Figure 6.5.3-3. In the deployment configuration, the solar panels are released and lowered into a perpendicular position to the spacecraft, SHARAD is released, and the antenna arm deploys outward and points back toward Earth to begin communications.

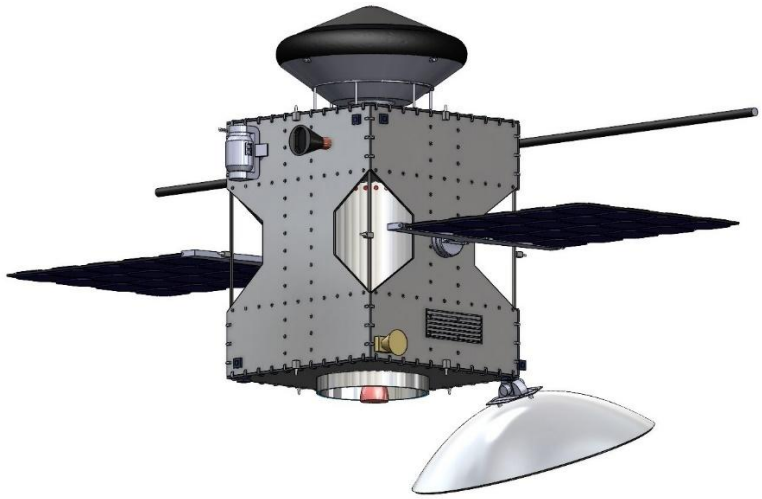

Figure 6.5.3-3: Deployed Configuration of the Bronco Orbiter

6.5.4 Design Loads

The time when Duo will see its largest structural loads is during launch from Earth into Low Earth Orbit. From Figure 6.5.4-1 provided by the Space X Falcon User Guide [5], the maximum launch loads are 6g axial and 2g lateral. While these loads do not happen together during launch, these combined loads are what the spacecraft structure will be simulated at for FEA analysis. The primary load path that will endure these loads is the central cylinder which also houses the propulsion tanks which will help support the structure even more.

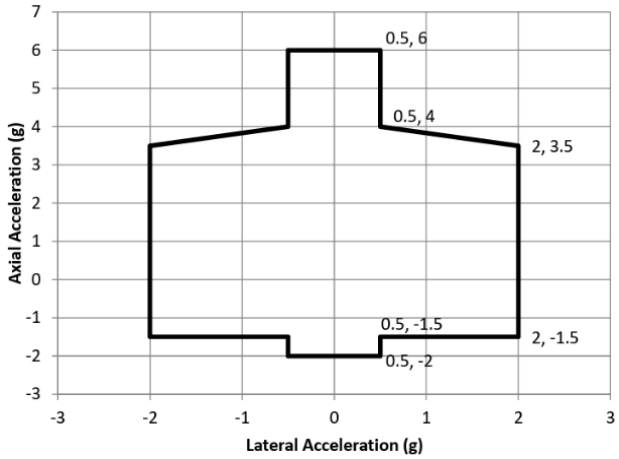

Figure 6.5.4-1: Falcon 9 and Heavy launch loads for <4000kg payloads

6.5.5 Discussion of Solid Works Structural Analysis

The primary load-bearing element of Bronco is a cylindrical structure, constructed from the same carbon fiber-aluminum honeycomb mentioned in Section 6.5.2. It was sized to carry the maximum axial and lateral loads of the Falcon Heavy launch, keeping high stiffness and minimal mass in mind.

The sizing process began with preliminary hand calculations based on the properties of IM7 carbon fiber, Cyanate 996 Epoxy, and Aluminum 5052 Honeycomb, the properties of both were taken from manufacturer HexCel's datasheets [35]. Using Bruhn's Analysis and Design of Flight Vehicle Structure [36] an iterative method process was used by calculating a Bending Stiffness parameter, D, and using it to calculate a Critical Buckling Load, N_{cr}. These equations can be found below.

(Eq.6.5.5-1) $$D = \frac{E_f t_f h^2}{2(1-v_f)}$$

(Eq.6.5.5-2) $$N_{cr} = \frac{K\pi^2 D}{L^2}$$

Then by using the maximum axial launch loads, the maximum applied running load along the circumference of the cylinder is calculated and used to calculate the Margin of Safety. By iterating different size variations of face sheets and core, the optimum values for facesheet thickness of 0.85 mm and 25.4 mm core thickness were found. This results in a factor of safety of ~1.8, which puts us in a realistic range to go into further analysis.

Using SolidWorks, a model of the cylinder was created as shown in Figure 6.5.5-1 and was simulated under the 6g axial compression from launch to test for buckling. The results show very minimal deformation of the cylinder, only having 0.274 mm deflection at the base of the cylinder.

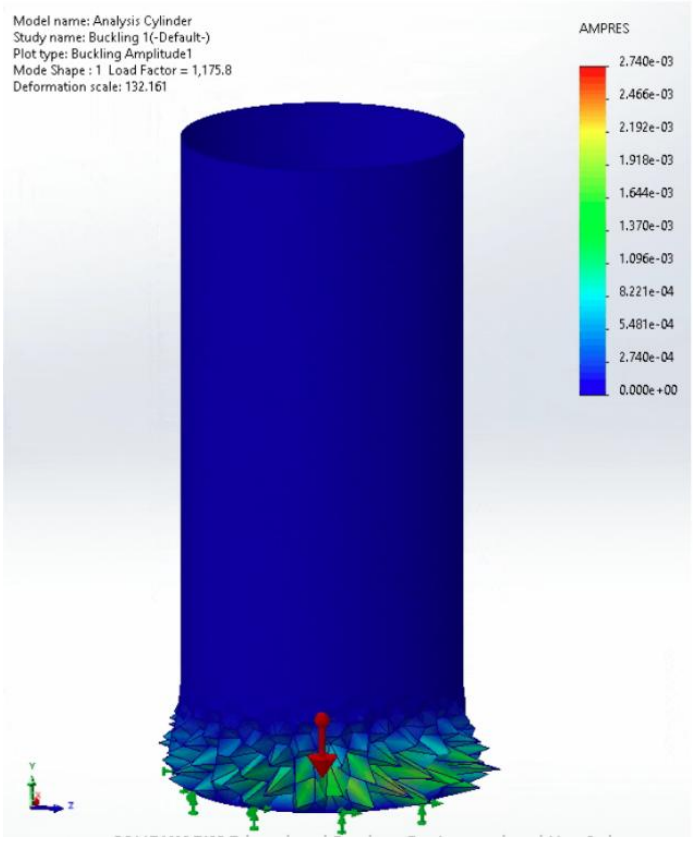

Figure 6.5.5-1: Cylinder Structure Analysis

With the cylinder indicating positive results that it can survive, a simulation of the entire primary structure is run. This simulation includes the cylinder, the top and bottom decks, the support panels, and the titanium rods used for mounting and extra structural stiffness. The result shows minimal deformations, with only a 2.77 mm maximum deflection in the cylinder. We also see some notable deformation in the bottom shelf panel, which is expected due to the lack of support structure for the aft side of the spacecraft that was left out to have room for the High Gain Antenna.

Figure 6.5.5-2 displays the primary structural deflections of Bronco when under launch loads through analysis in SolidWorks.

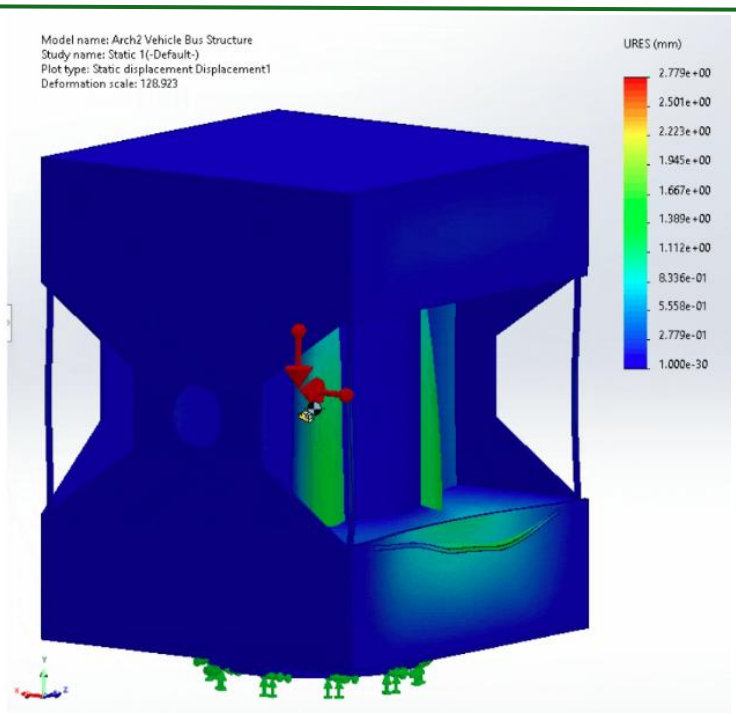

Figure 6.5.5-2: Primary Structure Deflections Under Launch Loads

To verify that the primary structure meets the launch dynamic requirement, a modal analysis was conducted in SolidWorks as shown in Figure 6.5.5-3 simulation to assess the natural frequency of the primary structure. The requirement to be met is a natural frequency of 50 Hz to be within margin to survive the Falcon Heavy vibrational loads. The analysis results show a natural frequency of ~100 Hz for the first five vibrational modes, double the required threshold. This indicates a highly stiff structure with a substantial margin.

While the results of the SolidWorks simulations show positive results, it is noted that there are limitations to these simulations and that in the future a higher fidelity model will be created in industry standard software such as FEMAP/NASTRAN.

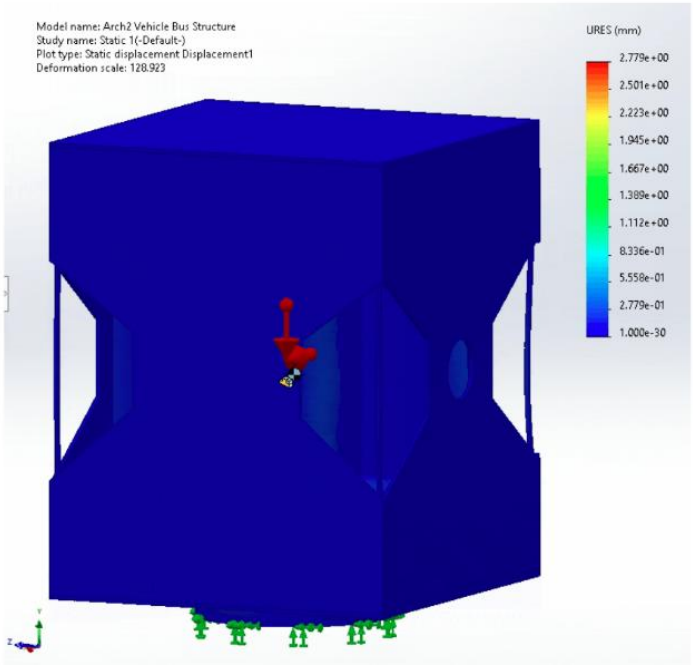

Figure 6.5.5-3: Primary Structure Vibration Modal Analysis

6.6 Thermal

6.6.1 Thermal Overview

The requirements for Bronco's thermal control system are shown in Table 6.6.1-1 below.

Table 6.6.1-1: Thermal Requirements (Bronco)

Req. #	Requirement
6.0-1	The thermal control system shall ensure all components remain within their operational temperature limits.
6.0-2	The thermal control system shall operate reliably until January 1st, 2040.
6.0-3	The thermal control system shall possess a 5°C thermal buffer.

The thermal design in this section addresses Bronco's Martian orbit, where it spends most of its life cycle. Due to Bronco's SSO, one half of the orbiter is always exposed to direct sunlight while the other half receives no direct sunlight. Additionally, Bronco is nadir-pointing, thus the external nadir side of the orbiter receives heat from Mars' thermal emission as well as sunlight reflected off Mars, while the other sides of Bronco do not.

The thermal control strategy implemented into the design of Bronco was to iteratively select thermal paints/coatings for Bronco's exterior to minimize net heat flux while keeping all critical components onboard Bronco within their operational temperature limits with a 5°C margin. From there, radiators were designed to reject the excess heat out through the sides of Bronco not exposed to any form of sunlight or Mars thermal emission. This strategy sought to reduce the use of active thermal control via heaters and avoid increasing the mass and power draw required for Bronco's thermal control system. However, redundant Kapton heaters were included in the design for the components with the most critical low temperature limits to mitigate the risk of these components dropping below their lowest thermal limits.

6.6.2 Component Temperature Ranges

The operational, non-operational, and failure temperature ranges for each critical component onboard Bronco are shown in Figure 6.6.2-1 below.

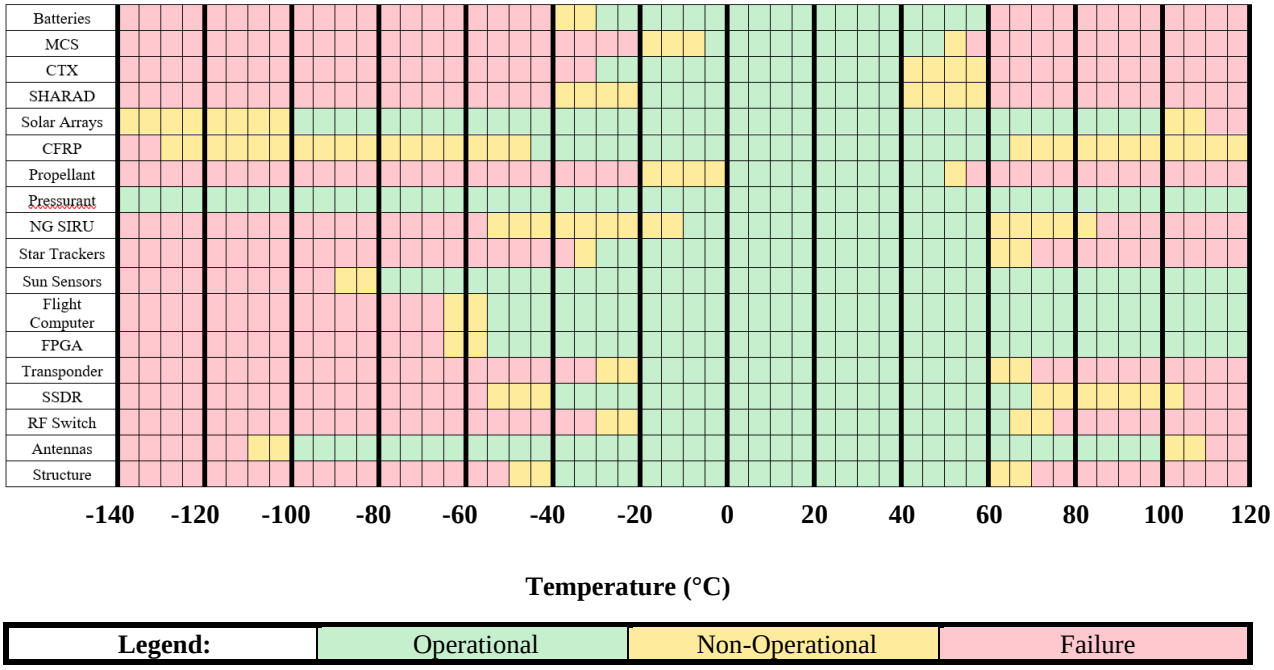

Figure 6.6.2-1: Critical Component Temperature Ranges (Bronco)

6.6.3 Thermal Design Approach

The thermal control methodology and design approach for Bronco are similar to the method outlined in Brown [37]. First, the mechanisms of heat transfer to and away from Bronco were determined. While orbiting Mars, the Bronco will experience heating from direct solar heating, indirect solar heating via Mars' albedo, Mars' thermal emission, and

heat generated from the power consumed by onboard electronics. Bronco's sole mechanism for ejecting heat is via radiation into space. These mechanisms of heat transfer are shown in Figure 6.6.3-1 below.

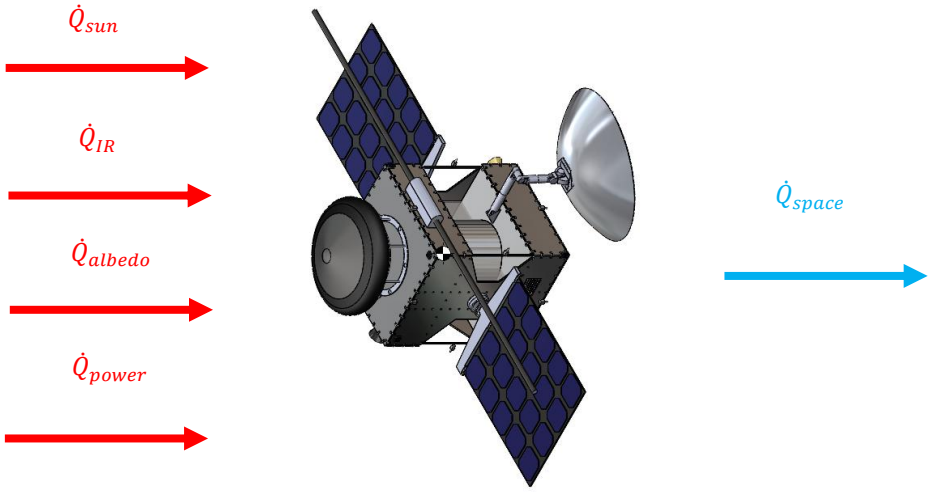

Figure 6.6.3-1: Bronco Heat Transfer Diagram

The generalized steady-state heat transfer for Bronco is shown in Equation 6.6.3-1 below.

(Eq. 6.6.3-1) $$\dot{Q}_{sun} + \dot{Q}_{IR} + \dot{Q}_{albedo} + \dot{Q}_{power} = \dot{Q}_{space}$$

The individual radiative heat terms for Equation 6.6.3-1 are defined in Equations 6.6.3-2 through 6.6.3-6 below.

(Eq. 6.6.3-2) $$\dot{Q}_{sun} = G_s \alpha_{surf} A_{surf} F_{sun}$$

(Eq. 6.6.3-3) $$\dot{Q}_{IR} = q_{IR} A_{proj} \varepsilon_{surf} F_{mars}$$

(Eq. 6.6.3-4) $$\dot{Q}_{albedo} = a G_s \alpha_{surf} A_{surf} K_a F_{mars}$$

(Eq. 6.6.3-5) $$\dot{Q}_{power} = \frac{P}{SA}$$

(Eq. 6.6.3-6) $$\dot{Q}_{space} = \sigma \varepsilon_{surf} A_{surf} T_{surf}^4 F_{space}$$

Where G_s is the solar energy from the sun (~589.2 W/m^2 at Mars), α_{surf} is the absorptivity of the Bronco's external surface, ε_{surf} is the emissivity of the Bronco's external surface, A_{surf} is the external surface area of Bronco, F is the view factor between the external surface and the mechanism of heat transfer, *a* is the albedo of Mars (~25%), K_a is the light reflection collimation term (~97% for a 700 km altitude orbit above Mars), P is the power generated by the

power consumed by Bronco's onboard electronics, σ is the Stefan-Boltzmann constant ($5.67 \times 10^{-8} \frac{W}{m^2 \cdot K^4}$), and T_{surf} is the temperature of Bronco's external surface. To simplify the use of these equations, the absolute temperature of space was 0 K rather than 2.7 K.

It is important to note that not every external surface will experience each of the heat transfer mechanisms previously discussed. For instance, the anti-nadir, anti-sunward, and external panels that connect to the solar panels connect to Bronco's primary structure do not receive heating from direct sunlight, reflected sunlight, or Mars' thermal emission since they have no view factor with the sun or Mars.

Heat then transfers from the exterior of the orbiter into the internal components of the orbiter. This heat transfer was assumed to be purely conductive since none of the internal components would be exposed to significant mechanisms of radiative heat transfer, like the sun or Mars.

6.6.4 Thermal Analysis

Equations 6.6.3-1 through 6.6.3-6 were used to determine the steady-state temperature of each external surface, iterating through several paints/coatings from reports by Henninger [38] and Red Rock Energy [39] to minimize the heat flux without exceeding any external surfaces' operational temperature range. The selected paints/coatings for each external component, as well as their α/ε ratios, are shown in Table 6.6.4-1 below.

Table 6.6.4-1: Bronco Paint/Coating Selection

External Component	Paint/Coating	α/ε
Payload Plate (+X)	Zinc Oxide with Sodium Silicate	0.163
Back Plates (-X)	Molybdenum	2.667
Left Plate (+Y)	Molybdenum	2.667
Right Plate (-Y)	Molybdenum	2.667
Top Plate (+Z)	OSO-H White Paint 63W	0.325
Bottom Plate (-Z)	Molybdenum	2.667
SHARAD	Barium Sulphate with Polyvinyl Alcohol	0.068
Telecomm Antenna	Barium Sulphate with Polyvinyl Alcohol	0.068
Radiators	Martin Black Velvet Paint	0.968

A simplified FEMAP thermal model was then constructed to model the external temperatures and the resulting conductive heat transfer through Bronco's internal structure and components. This preliminary model determined the

steady-state temperatures of Bronco's internal components. Images of the model are displayed in Figure 6.6.4-1 and Figure 6.6.4-2 below.

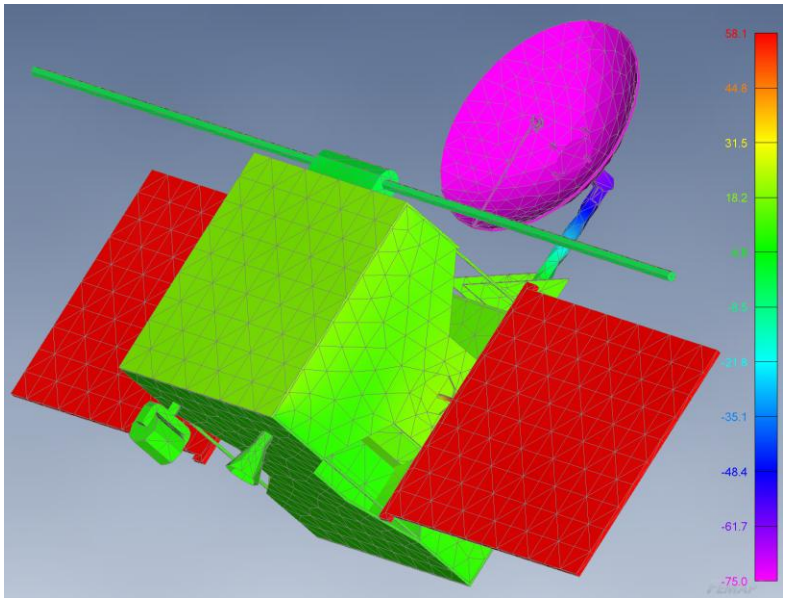

Figure 6.6.4-1: Bronco Thermal Model (Externals)

The coating for the telecommunications antenna shown in pink in Figure 6.6.4-1 was selected to keep its steady-state temperature close to its minimum operating temperature without exceeding it to achieve the antenna's best performance possible.

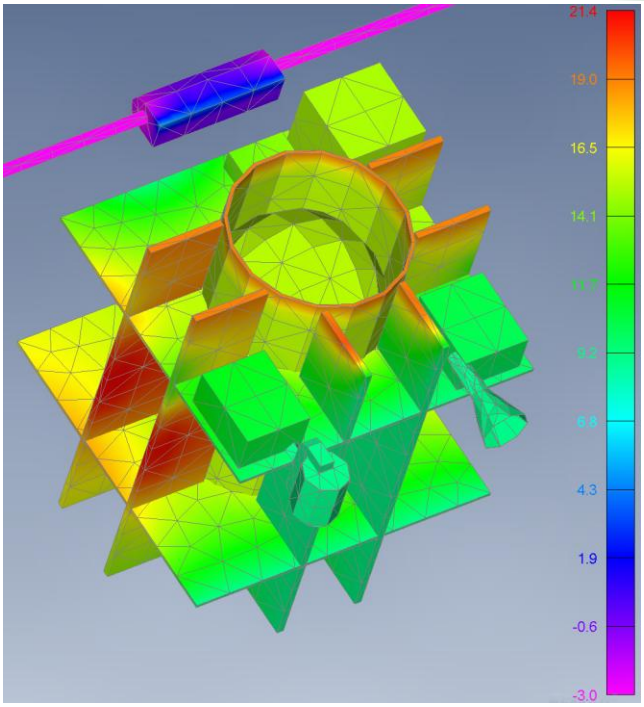

Figure 6.6.4-2: Bronco Thermal Model (Internals)

This model reported that all components were within their operational temperature ranges; however, the model does not account for internal heat generation from the power consumed by electronic components. To account for this, the heat flux required to raise each electrical component to its maximum operating temperature was subtracted from the heat flux generated by these components, assuming each component operated at its average operating power. This determined the excess heat flux experienced by the electrical components that must be radiated away to keep the components within their operational temperature ranges.

Table 6.6.4-2 displays heat flux going into and out of each component as well as the excess heat flux experienced by Bronco that must be radiated away to keep all Bronco's components operational.

Table 6.6.4-2: Bronco Component Heat Flux Summary

Component	$\dot{Q}_{in}$ (W/m^2)	$\dot{Q}_{out}$ (W/m^2)	$\dot{Q}_{net}$ (W/m^2)
Payload Plate (+X)	88	-88	0
Back Plates (-X)	0	-80	-80
Left Plate (+Y)	0	-82	-82
Right Plate (-Y)	0	-82	-82
Top Plate (+Z)	109	-109	0
Bottom Plate (-Z)	0	-79	-79
SA Wide Face (+Y)	268	-268	0
SA Wide Face (-Y)	268	-268	0
MCS	10	-5	6
CTX	7	-5	2
SHARAD	83	-83	0
Telecomm Antenna	24	-24	0
Batteries	2471	-1430	1041
ACS	1556	-1430	126
C&DS	70	0	70
$\Sigma\dot{Q}_{net}$			**922**

The required surface area of the radiator to reject the excess heat flux experienced by Bronco, assuming the radiator operated at the steady-state temperature of the face it is mounted on, was determined using Equation 6.6.4-1 below.

(Eq. 6.6.4-1) $$\frac{\dot{Q}_W}{A_R} = \sigma \varepsilon_R {T_R}^4$$

Where $\dot{Q}_W$ is the heat the radiator must reject, and A_R, ε_R, and T_R are the area, emissivity, and temperature of the radiator, respectively. Using Equation 6.6.4-1, Bronco will require ~2.6 m^2 of radiator surface area to reject the ~922 W/m^2 of excess heat flux experienced by Bronco. Using historic data from the design of the Space Shuttle's radiators [40], Bronco's radiators will be ~3 cm thick.

While Bronco does not require the use of electric heaters to remain operational, redundant Kapton heaters were designed to increase the temperature of the most critical components, including all the science instruments, propellant tanks, batteries, as well as and C&DH electronics by 5°C over the course of a minute to mitigate the risk of these components becoming non-operational. If necessary, these Kapton heaters will require ~87W of power to operate.

In addition to radiators, heaters, and thermal paints/coatings, the design includes estimates for the mass of Multi-Layer Insulation (MLI) and foam insulation required to reduce the heat flux affecting the science instruments and propellant.

The mass of heat pipes to transfer heat away from the electrical components and towards the radiators was also estimated, and four parallel thermostats, two required and two redundant [41], were included to measure the temperature of critical components. The total thermal system mass is ~13.7 kg using the estimation methods for thermal devices outlined in Brown [37].

6.7 Power

6.7.1 Power Requirements

Table 6.7.1-1 below displays the requirements for Bronco's electrical power subsystem (EPS).

Table 6.7.1-1: Power Requirements (Bronco)

Req. #	Bronco Power Requirements
4.0-1	The EPS shall support no less than 35 W for the payload.
4.0-2	The EPS shall operate reliably until January 1st, 2040.
4.1-5	The battery shall support an On-Orbit power of no less than 1150 W.
4.2.1	The solar array shall support an On Orbit power of no less than 1150 W.

The power system for Bronco was driven by the need for sustained, efficient power generation and storage in the Martian Environment. Based on design heritage from successful missions such as the MRO and Mars Odyssey, solar power was selected as the primary energy source. This choice was reinforced by our mission constraints, cost limit of under $1 billion, and the extensive flight heritage and reliability of solar-based systems in Mars orbit.

A detailed review of subsystem power allocations and margins were performed using industry-standard guidelines from Brown [42]. Power sizing was driven by on-orbit power requirements using subsystem-level power allocations and design margins, ensuring sufficient energy availability across all mission phases. These power margins also assure our system remains fully operational considering a 15% Solar Array degradation typical of Mars missions, as noted in Brown [42].

6.7.2 Battery System Design

Battery selection and configuration centered around providing reliable energy during possible eclipse periods and high-power draw phases, especially for the orbiter and balloon platforms. The design assumed a perfect fully SSO

with a 30-minute eclipse period margin, achievable through a precise Right Ascencion of the Ascending Node (RAAN) selection.

After consideration of various battery chemistries including nickel-hydrogen, nickel-cadmium, and silver-zinc, lithium-ion (Li-Ion) batteries were identified as the clear choice for both the orbiter and the balloon platforms due to their high specific energy, low mass, and extensive flight heritage. As such, a focused trade study was conducted exclusively among different types of Li-Ion battery technologies to optimize our design. This study examined parameters such as specific energy, mass per cell, nominal voltage, and cell capacity, with the highest weighting placed on energy density and mass efficiency to minimize the mass of the spacecraft as shown in Table 6.7.2-1.

Table 6.7.2-1: Duo Battery Trade Study

Parameters			**LP 33037**			**LiFeP04**			**LP32770**		
Category	**FOM**	**Weight**	**Value**	**U**	**W**	**Value**	**U**	**W**	**Value**	**U**	**W**
Specific Energy (Wh/kg)	MAX	2	160	1	2	135.5	.06	.12	134	0	0
Normalized			1			.06			0		
Nominal Voltage (V)	MAX	2	3.6	1	2	3.075	0	0	3.6	1	2
Normalized			1			0			1		
Mass Per Cell (kg)	MIN	3	1.6	1	3	1.89	0	0	1.68	.72	2.17
Normalized			1			0			.72		
Cell Capacity (Ah)	MAX	2	60	.11	.22	100	1	2	55	.06	.12
Normalized			.11			1.0			.06		
Totals			7.22			2.12			4.28		

For the orbiter, the selected battery configuration consists of 16 Li-Ion cells arranged into 8 cells per string with 2 strings in parallel, resulting in a total battery mass of 26 kg sized using methods and recommendations outlined in Brown [42].

6.7.3 Solar Array System Design

Deployable solar arrays were selected for Bronco, designed to maintain a compact stowed configuration during launch. Upon fairing separation, these arrays are deployed and can be oriented using a two-axis gimbal system, allowing precise alignment for optimal sun exposure throughout the mission.

The solar array trade study considered a range of advanced photovoltaic technologies. As shown in Table 6.7.3-1 based on efficiency, mass, and proven performance in the Martian environment. Triple-junction GaAs solar cells were selected for both the orbiter and balloon platforms. These cells offered the best balance of energy density, resilience, and flight heritage, ensuring mission success over a 10-year duration

Table 6.7.3-1: Duo Solar Cell Trade Study

Parameters			EXA Triple Junction				CAVU Triple Junction GaAS				CTJ30			
Category	**FOM**	**Weight**	**Value**	**U%**	**U**	**Weighted**	**Value**	**U%**	**U**	**Weighted**	**Value**	**U%**	**U**	**Weighted**
Max Area (m^2)	40.2	3	64	59%	9	27	30.2	-25%	0	0	26.5	-34%	0	0
EOL Ppmp (W/cell)	1.06	3	2.1	97%	9	27	1.05	-1%	3	9	4.36E-02	-96%	0	0
EOL Efficiency (%)	26.7	2	25.7	-4%	3	6	25.4	-5%	3	6	29	9%	5	10
Mass Per Cell (g)	4.65	1	7.68	-65%	0	0	3.6	23%	5	5	2.68	42%	9	9
Totals			**60**				**20**				**19**			

Bronco's solar array spans were sized using methods outlined in Brown [42]. They span an area of 14.39 m² using a two-wing configuration comprising 4232 cells arranged in 14 series-connected cells per string and 303 strings. These designs were modeled to support power generation with a 15% degradation rate and margin over the full mission duration, from launch in 2030 through the extended mission's conclusion around 2040.

6.7.4 Mission Power Phase Profiles

Mission-specific power draw modeling was completed for both the orbiter and balloon systems. For Bronco, power consumption was modeled across launch, post-separation, cruise, MOI, aerobraking, primary mission operations, and extended science operations. During nominal science mode, the orbiter requires an average of 798 W, with a peak power draw of 820 W during intensive peak payload power draw as shown in Table 6.7.4-1.

Table 6.7.4-1: Bronco Power Phase Profile

Phase	Launch	Postseparation	Cruise	Aerobraking	Mars Orbit Insertion	Primary Mission	Secondary Mission	Peak Power Draw
Power Draw (W)	275	667	769	769	769	798	798	820

7.0 Subsystem Design - Broncito

7.1 Entry Vehicle Design Summary

The Mars descent module is designed to allow for a safe and gentle landing on the Martian surface. The descent capsule performs its control descent through a sequence of thrusters to reduce its ΔV of 0.68 km/s to enter Mars' atmosphere, drag is then produced from its heat shield, which is followed by a parachute further lowering its velocity to a reasonable speed where the payload is then cushioned by an airbag system to ensure a Broncito lands undamaged.

7.2 Entry Vehicle Sizing

7.2.1 Heat Shield Sizing

Considering an entry velocity of 3500 km/s at an altitude of 150 km, the heat shield was sized accordingly. Before sizing the heat shield, we ran a MATLAB simulation (Figure 7.2.1-1) to find what our most optimal entry angle and ballistic coefficient would be, considering our max heating rate and total heat load. Running this simulation, the team found that our best-case scenario would be found at a flight path angle of 3 degrees and a ballistic coefficient of 26, which means that at these parameters, the descent module would experience its least max heating rate and total heat load without compromising the mission with instabilities in its trajectory.

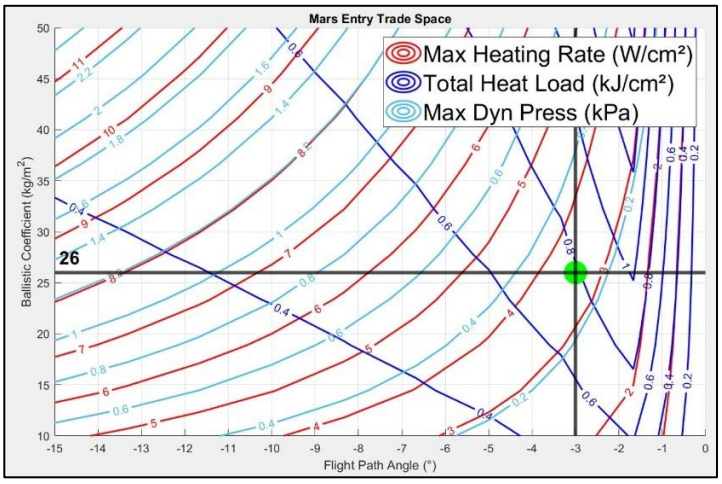

Figure 7.2.1-1: Mars Entry Trade Space

There are two main materials for entry capsules, ablative and non-ablative. An ablative material is typically lighter, can withstand extreme temperatures of up to 3000ºC, and is generally designed to remove or burn off once it has

absorbed enough heat. On the other hand, non-ablative material like Reinforced Carbon-Carbon or Silica Tiles found on the Space Shuttle is designed to withstand temperatures reaching roughly 2000ºC but is significantly heavier. To reduce the total mass of the system and for its high thermal resistance, the ablative material was chosen. There are three common ablative materials, each of which have flown on previous missions proving their reliability: Phenolic Impregnated Carbon Ablator (PICA), Avcoat, and SLA-561V. Each possesses relatively low conductivity with PICA at 0.16 $\frac{W}{m-K}$ Avcoat at 0.24 $\frac{W}{m-K}$ and SLA-561V at 0.05 $\frac{W}{m-K}$ which is crucial for the mission profile. The goal is to slow down the heat transfer from the surface to the interior, this is typically achieved using a material with low conductivity. Another key factor to consider is their density as it is directly related to the mass of the material; PICA – 0.26 $\frac{g}{cm^3}$, Avcoat - 0.51 $\frac{g}{cm^3}$, and SLA-561V – 0.28 $\frac{g}{cm^3}$. With these material characteristics in mind, it may seem as if Lockheed Martin's SLA-561V should be selected, however, due to PICA's higher heat load tolerance of up to 3000ºC and due to the extensive experimenting and data collection done on PICA and its derivatives, it is a safer technology to choose from, the ablative pattern is also far easier to predict. The back shield of the descent module is composed of Aluminum 6061 panels due to its flight history and reliability.

The heat shield was designed referencing the NASA Ames Research Center [43] . The team began by defining a radius capable of housing the 1.2 x 1.0 x 1.5 m payload. With a heat shield base radius of 1.78 m, the nose radius was sized using the ratio listed in Equation 7.2-1, with R_n defining the nose radius and R_b defining the base radius, resulting in a calculated nose radius of 0.89 m, to fit the Broncito it was increased to 0.91 m which ultimately keeps the same aerodynamic properties without having a major considerable change. The shoulder radius was designed following a similar ratio as seen in Equation 7.2-2, with R_s being defined as the shoulder radius, resulting in a calculated shoulder radius of 0.089 m. Considering that the max allowable tapered angle is 70°, the tapered angle resulted in 31°, which was ultimately sized again to accommodate the payload dimensions.

(Eq. 7.2.1-1) $$\frac{R_n}{R_b} = 0.5$$

(Eq. 7.2.1-2) $$\frac{R_s}{R_n} = 0.1$$

The PICA layer was coupled with a Thermal Protection System (TPS) underlayer to further provide a higher temperature rating, ensuring no internals would be affected by the resulting heat. This TPS structure is composed of FRCI-12, which is an alumina-borosilicate and silica composite, as its support beams separate the PICA from its Aluminum Base Plate. The TPS structure is molded into a honeycomb structure to ensure loads and heat loads are accounted for.

Once the ballistic coefficient and general sizing of the system were determined, using a drag coefficient for blunt bodies of 1.6. Iterative calculations suggested that the heat shield would experience a max temperature of roughly 916 K. This was done through a sequence of defining the heat transfer coefficient of 35900 $\frac{W}{Km^3}$, an emissivity of 0.9. A cross-section of the PICA material was defined as 1 m^2 to further simplify the equation. From here, Equation 7.2.1-3 was used to solve for max temperature. With this max temperature, max heat load, and max heating rate, a thickness of 0.02 m for both the PICA and a thickness of 0.05 m for its TPS underlayer. Using a similar principle, its aluminum back shield's thickness results in 0.02 m, and its I-beam is also composed of the same aluminum with a thickness of 0.02 m, all dispersed along the back shield to provide mounting points for these panels.

(Eq. 7.2.1-3) $$T_{max} = (\frac{q}{\epsilon\sigma})^{\frac{1}{4}}$$

The designed heat shield has a total mass of 213 kg, with a total volume of 0.582 m^3, Figure 7.2.1-2 calls out important heat shield characteristics.

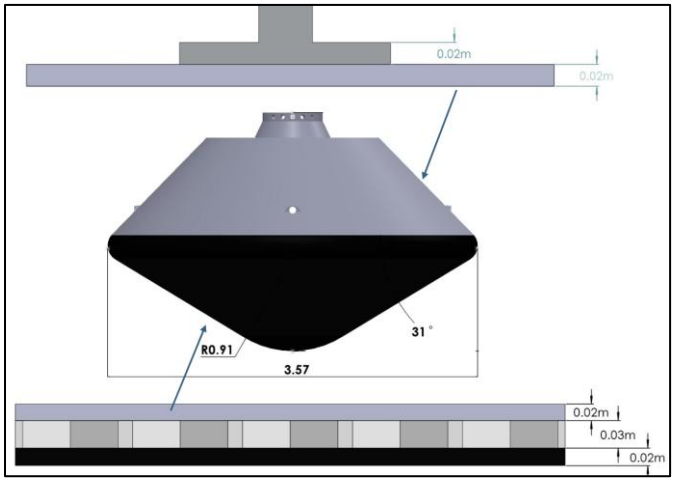

Figure 7.2.1-2: Fully Sized Entry Capsule

7.2.2 Parachute Sizing

When designing the heat shield parachute, the maximum force it would be experiencing was a driving variable. Iterative calculations suggested that it would be experiencing a max force of roughly 14000 N. This was calculated through an iterative series of kinematic equations, first solving for its updated velocity and using the Drag equation to solve for its resulting drag.

The down selection for the parachute's appropriate material was based on the material's density, its tensile strength, and its flight heritage. Some of the materials considered were Zylon (PBO Fiber) and Nylon Type 6,6, each of which has shown their in-flight capabilities previously with successful missions. These materials were selected due to their density profile and tensile strength rating as well, with a density of 1140 $kg.m^3$ for Nylon and 1549 $kg.m^3$ for nylon. They also contain a high tensile strength when grouped together, each with 5.8 GPa for Zylon and 117 MPa for Nylon. Both materials were selected due to their integration capabilities with one another, allowing for higher stress capabilities and a lighter canopy. They were then covered with Polyurethane coating to decrease their permeability and increase their thermal protection. The suspension lines were selected with the same design considerations, with a Kevlar Aramid Fiber being selected due to its relatively low density of 1440 $kg.m^3$ and its tensile strength of 3.62 GPa. These lines are coated with a silicone coating to improve its ductile performance.

Sizing the canopy was relatively straightforward; using its expected force and tensile strength, the area of the canopy was calculated, with a total radius of roughly 5.64 m. The canopy thickness was determined following the same principle, with a variation of the tensile stress formula being rearranged to solve for the thickness. The suspension lines were done following the same tensile stress formula. In this case, the load was distributed along six different lines to reduce the thickness of the material and ensure proper deployment. The canopy thickness resulted in 1.3 mm and the suspension lines came out to 4 mm, with a total mass of 89 kg.

7.2.3 Airbag System Design

The airbag system is designed to withstand roughly 1607 N per airbag, with the design consisting of six airbags. Each airbag covers a plane of the payload system, this is done to ensure that the system lands relatively unharmed, as it is expected to land at a velocity of 6 m/s. Using the Kinetic energy equation, the airbags are expected to experience roughly 3185 J of energy.

Similar to the descent vehicle parachute, the material was selected based on its density and tensile strength. The airbag system can be simplified to perform similarly to the parachute system, based on the fact that it will be experiencing high loads. Therefore, Kevlar is being used in its tethers to reinforce the airbag upon impact, again due to its high tensile strength and density, like the parachute previously mentioned. For its main fabric, Zylon and Dacron were considered alongside the Vectran, which was ultimately chosen due to its high tensile strength of 2.9 GPa and density of 1.41 $\frac{g}{cm^3}$ which is ideal for the mission profile. Vectran serves as a balanced middle ground as Zylon beats it in strength but possesses higher density and Dacron beats it in density but lacks strength. The airbags have been sized to conform to the Vectran outer layer. As for the bladder, a basic silicone-coated bladder suffices as its main purpose is to ensure the inflated chambers retain the gas at low Martian pressures. Small solid propellant gas generators are then ignited to produce Nitrogen gas to inflate the system. Other concepts were considered, from a CO_2 pump extracted from Martian air and a compressed gas tank, but these systems rely on an extensive amount of power and mass, which is not ideal.

Using the thinned-walled pressure vessel theory, an internal pressure of 1 psi, the minimum thickness considering the Kevlar and bladder as well as an increase of 0.1 mm for manufacturing feasibility, the total thickness results in 0.2 mm, which is consistent when compared to different missions. The overall mass of the airbag system results in 14 kg with the radius of each airbag being 0.83 m.

7.3 Lifting Gas & Tank Sizing

The Martian atmosphere is extremely thin, with very few gases capable of serving as a lifting gas for any payload, no matter the mass. Hydrogen, helium, and methane are widely considered due to their low molecular mass. Iterative calculations suggested that hydrogen would be the best lifting gas, as less is required to lift our 211 kg payload. Selecting Hydrogen reduces the volume and mass of the tanks used to store the lifting gas and reduces the overall mass of the balloon as well. The Archimedes Principle and the ideal gas law were used to find the amount of hydrogen required to lift Broncito, with a total mass of 5.7 kg. Considering the Hydrogen used, a MATLAB simulation was conducted to simulate an altitude profile of 180 minutes with a total ascent time of 60 minutes to reach a max altitude of 7 km, with a maximum velocity of 3.5 km/s. The flight profile is seen in Figure 7.3-1.

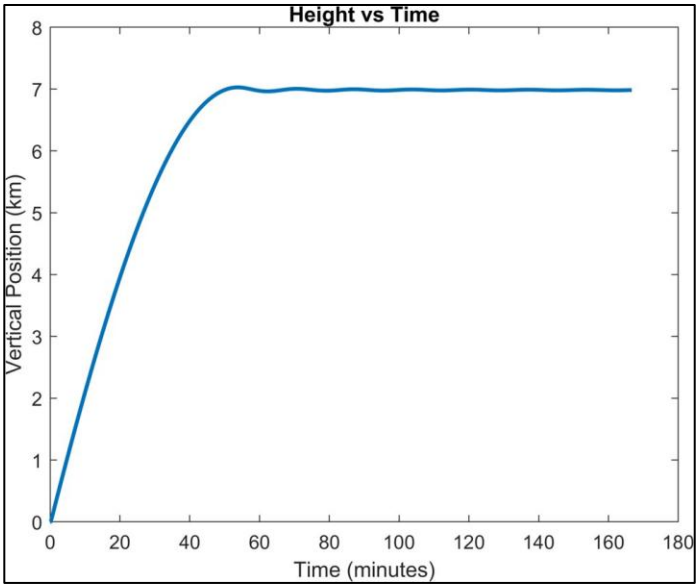

Figure 7.3-1: Inflation Profile

Hydrogen will be stored under 30 MPa, which is done to reduce the tank size drastically as it's required to store a total volume of 26881 m3. This pressure is well above the 1.29 MPa of critical pressure that hydrogen has, meaning it will be stored as supercritical liquid hydrogen. Finding a tank with low mass while being strong enough to withstand such pressure was critical when selecting the material of the tank. For simplicity, the tank will be a pre-pressurized system, similar to that of a propane tank. This reduces the need for excess valves, piping, and other electronics needed to run, ultimately reducing the system mass as well. Two of the tank materials considered were Titanium and Carbon Fiber Reinforced Plastic (CFRP). Both materials are high in tensile strength and capable of withstanding the designed pressure, however, CFRP has a tensile strength of 965 MPa, significantly higher than Titanium's 220 MPa. With density also playing a major role in this decision, Titanium has a density of 4.51 $\frac{g}{cm^3}$ while CFRP has one of 1.2 $\frac{g}{cm^3}$, making a CFRP tank the obvious choice. The reinforced plastic ensures there is no leakage, as the name suggests, in case of any unforeseen manufacturing weaknesses within the tank [44]. Tank sizing was performed through an iterative process, considering the internal pressure of the tank and CFRP's material process. Using Brown's [30] design recommendations for a pressurized tank, the ideal gas law, and hoop stress analysis for pressurized tanks, the tank thickness came out to be roughly 0.01 m. The spherical tank measures 17.4 kg with a diameter of 0.53 m, which is also considered a factor of safety of 2. The tank is also composed of a vacuum shell, serving as an insulating space to mitigate heat transfer into the tank by keeping the tank cold, this shell weighs 5.6 kg. The following sizing also allows for an allowed burn-off of 100% as the thickness difference is minimal.

7.4 Balloon Selection and Sizing

Finding the material adequate to contain the hydrogen in flight requires a material with low diffusivity when coupled with hydrogen to determine the mission duration and a low-density profile. The materials compared were 25-gauge Polyethylene, Natural Latex, and Neoprene. When comparing their Hydrogen diffusivity, Polyethylene has the lowest permeability with a diffusivity of 10^{-10} $\frac{cm^2}{s}$, Natural Latex has a diffusivity of 10^{-6} $\frac{cm^2}{s}$, and 10^{-8} $\frac{cm^2}{s}$ for Neoprene. This in turn ensures a longer mission duration, which is calculated later. Polyethylene is tied for the lowest density with Natural Latex at 940 $\frac{kg}{m^3}$, ensuring a lightweight balloon. Like the heat shield parachute material, Kevlar Aramid Fiber was chosen due to its material properties and reliability. Which is also implemented into the 20 gores spreading from the top to the bottom of the balloon.

When sizing the polyethylene balloon, the balloon was designed to run at 6894 Pa, which is slightly higher than that of Mars' atmosphere. This was done to ensure a minimal pressure differential between the balloon and the atmosphere to reduce the structural stress on the balloon material. The balloon was once again sized according to the amount of hydrogen we needed, giving us a balloon volume of 16138 m^3. After performing a hoop stress analysis on the balloon, the overall thickness of the balloon is roughly 15 µm, which is in line with most experimental polyethylene balloons [45]. Each tendon experiences 22 MPa of stress and is also sized accordingly. The overall balloon mass results in 42 kg with a balloon diameter of 30.7 m.

7.5 Telecommunications

7.5.1 Broncito Science

During Broncito's deployment and data collection which occurs after the 105-day collection phase of Bronco, Broncito is deployed and begins its data collection using the instruments described in Section 5.5.1. Broncito's mission is for about 90 days and during that time it collects data at a significantly higher rate due to its higher fidelity with a total data rate of about 2.55 Msps. We also applied an overhead of 10% with a BER of 10^{-4} using Reed-Solomon coding to protect the data. The total data collected during that time is about 2.4 TB and with a contact time of 0.85 hours per day we are capable of sending back all data in about 0.59 years from Broncito to Bronco using a LG helix antenna that both have with a weight of 0.4 kg and transmitter power of 4.7 W. Overall considering both orbiter and balloon,

"Duo" is capable of sending back all science data in about 5 years which is well before the end of the mission and can allow for further data collection during that time.

7.6 Command and Data Handling

7.6.1 Broncito C&DH Requirements

Broncito's C&DH subsystem supports localized scientific payload operations, real-time housekeeping functions, and high-frequency data uplink to the Bronco. As a secondary operator in its joint operation with Bronco for data downlink to Earth, its design must balance functional autonomy with power and mass constraints, while operating in a dynamic Martian atmospheric environment. The requirements for Broncito C&DH are shown in Table 7.6.1-1.

Table 7.6.1-1: Broncito Command and Data Handling Requirements

Req. #	Requirement
8.2-1	Max-Data Throughput: The system shall support a data throughput of ≥ 5 Mbps to enable fast transfer of high-resolution atmospheric data to Bronco.
8.2-2	Operating Temperature Range: The system shall operate within -40°C to +85°C to survive diurnal thermal swings in the Martian atmosphere.
8.2-3	Processor Speed: The processor shall operate at ≥ 100 MIPS to support real-time payload management, fault detection, and data staging.
8.2-4	Storage: The system shall include ≥ 128 GB of storage to temporarily hold science data before scheduled relay to Bronco.
8.2-5	Fault Tolerance: The system shall implement dual-string redundancy to provide resilience against temporary resets and transient faults.
8.2-6	Communication Interface: The system shall use SpaceWire interfaces to match Bronco's standards for seamless packet handoff.

7.6.2 Broncito C&DH Products

Due to software reuse and hardware consistency, Broncito shares the same RAD750 architecture as Bronco but with reduced performance demands. RH304T is selected again for Broncito due to its lower volume and the reliability of materials to withstand thermal radiation. Lower-level alternatives like CubeSat-rated C&DH boards were not an option because there was not sufficient radiation mitigation for this mission. SpaceWire was chosen instead of wireless RF for this mission due to drivers such as security, noise immunity, and compatibility with integration into Bronco hardware.

7.6.3 Broncito C&DH Methods

The Broncito C&DH uses a lightweight version of the Bronco software stack. A simplified flowchart-driven control scheme governs sensor polling, data logging, and buffer transmission. Local decision trees allow the system to operate semi-autonomously during blackouts or signal gaps with the Bronco. Watchdog-based resets and onboard memory scanning routines ensure short-term continuity. The software is modular, enabling hot-swaps or firmware upgrades via the Bronco link.

7.6.4 Broncito C&DH Assumptions

The Broncito operates in a lower-radiation environment but still includes SEU-protection. A typical sol yields 2–5 GB of scientific output, which is temporarily stored and batch-sent to the Bronco every orbit or during dedicated comm passes. The Broncito assumes thermal control is passive with radiative cooling. It also assumes stable power input from a small onboard solar array with buffer batteries.

7.6.5 Broncito C&DH Input

Incoming data includes sensor feedback (wind, temp, pressure), health telemetry, and command signals from the Bronco or mission control. Inputs are polled on a loop and stored in memory stacks until relay confirmation is received. Fault condition inputs trigger local safety scripts (e.g., data freeze, orientation adjust).

7.6.6 Broncito C&DH Output

Broncito outputs raw telemetry data to the Bronco by directing control signals for the onboard instruments. Broncito additionally provides status feedback for subsystem health. When fault flags arise, pre-scripted responses execute and generate diagnostic data for the Bronco. Scientific data is sent in compressed batches tagged by priority level and time.

7.6.7 Broncito C&DH Redundancy

While Broncito is scaled down in relation to its counterpart Bronco, it still uses cold-redundant RAD750 processors. Cross-strapped I/O channels and watchdog-controlled reboot protocols allow recovery from crashes. Memory scrubbers and parity checkers maintain data integrity. While less sophisticated than the Bronco, redundancy is sufficient to allow continued operation even with single-point failures.

7.7 Propulsion

The team evaluated various propulsion systems with a focus on reliability, simplicity, and mass efficiency to meet the mission's ΔV requirement of 0.68 km/s. Solid motors were dismissed early due to their inability to shut off and restart which is an essential feature for fine-tuning the Martian entry angle of 3º. Electric propulsion was ruled out due to its low thrust and high power demands which would also increase system mass, despite its great efficiency. This led to a final comparison between monopropellant and bipropellant systems. A monopropellant system was selected for its lower mass, reduced complexity, and sufficient thrust for the short-duration maneuvering required. Due to the minimal propellant needed, the potential pressure loss within the system made this a manageable tradeoff. Hydrazine (N_2H_4) was chosen over hydrogen peroxide due to its superior performance and proven use in previous space missions.

Trade studies suggest that the Aerojet Rocketdyne MR-106E Thruster was the best for the mission. The Aerojet Rocketdyne MR-106E was compared against the 20M Monopropellant Hydrazine Thruster and Aerojet Rocketdyne MR-103G Thruster. They were graded based on their specific impulse (Isp), Thrust, TRL, and the calculated propellant mass that would be needed to run it. The propellant mass was calculated following a series of iterative calculations and a similar trade matrix as in Section 6.3.4 proved that the Aerojet Rocketdyne MR106-E Thruster was the best fit, where five will be used to satisfy its required ΔV, one on top of the descent vehicle, and four around the diameter of the heat shield 90 degrees apart.

When sizing the amount of propellant being used, using the rocket equation with our desired ΔV of 0.68 km/s, the system would need roughly 45 kg of Hydrazine. Using the ideal gas equations the tanks were then sized appropriately with a total mass of roughly 4 kg for the propellant and a pressurant mass of 1 kg. The total amount of pressurant used came out to roughly 0.3 kg, which was sized to fit the needs of the total Hydrazine and velocity change of the mission.

Considering Section 6.1.1, the system accounts for outage, trapped, and loading errors. With the same ullage of 10% and a factor of safety of 2, the tanks were designed to fit well within their operating range. For the same reasons, a diaphragm tank was also chosen as well as a spherical tank. Further sizing of the system was performed by referencing Brown's book [30]. The total propulsion system mass is 23 kg (dry), Figure 7.7-1 depicts a piping and instrumentation diagram of the following system with the same nomenclature described in Table 6.3-4.

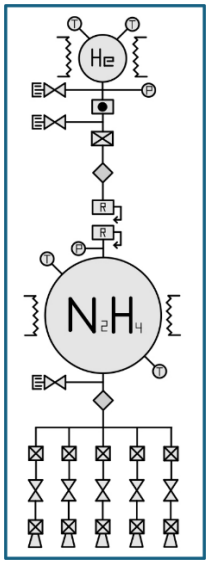

Figure 7.7-1: Heat Shield Thruster Schematic

7.8 Thermal

7.8.1 Thermal Overview

The thermal requirements for Broncito are shown below in Table 7.8.1-1.

Table 7.8.1-1: Thermal Requirements (Broncito)

Req. #	Requirement
6.0-1	The thermal control system shall ensure all components remain within their operational temperature limits.
6.0-2	The thermal control system shall operate reliably until October 23rd, 2032.
6.0-3	The thermal control system shall possess a 5°C thermal buffer.

The thermal design in this section addresses the thermal conditions Broncito experiences on Mars both during the day and night. The fundamental challenge when designing Broncito's thermal control system is that it must adapt to the wide temperature range it will experience on Mars (-70°C to 20°C), depending on the time of day [16]. Additionally, special thermal analysis needed to be conducted for the liquid hydrogen tank during entry to ensure the tank would not rupture due to hydrogen vaporization.

The thermal control strategy implemented into the design of Broncito was similar to the strategy discussed in Section 6.6.1. Thermal paints/coatings for the exterior of Broncito were iteratively selected to minimize net heat flux in both

day and night cases while keeping all critical components onboard Broncito within their operational temperature limits with a 5°C margin. This strategy prioritized minimizing the net heat flux at night to reduce the use of active heaters, which require additional power to operate. Radiators were designed to reject the excess heat through the upper external panel of Broncito during the day, and redundant Kapton heaters were designed to heat the critical components of Broncito by 5°C during the night.

7.8.2 Component Temperature Ranges

The operational, non-operational, and failure temperature ranges for each critical component onboard the orbiter are shown in Figure 7.8.2-1 below.

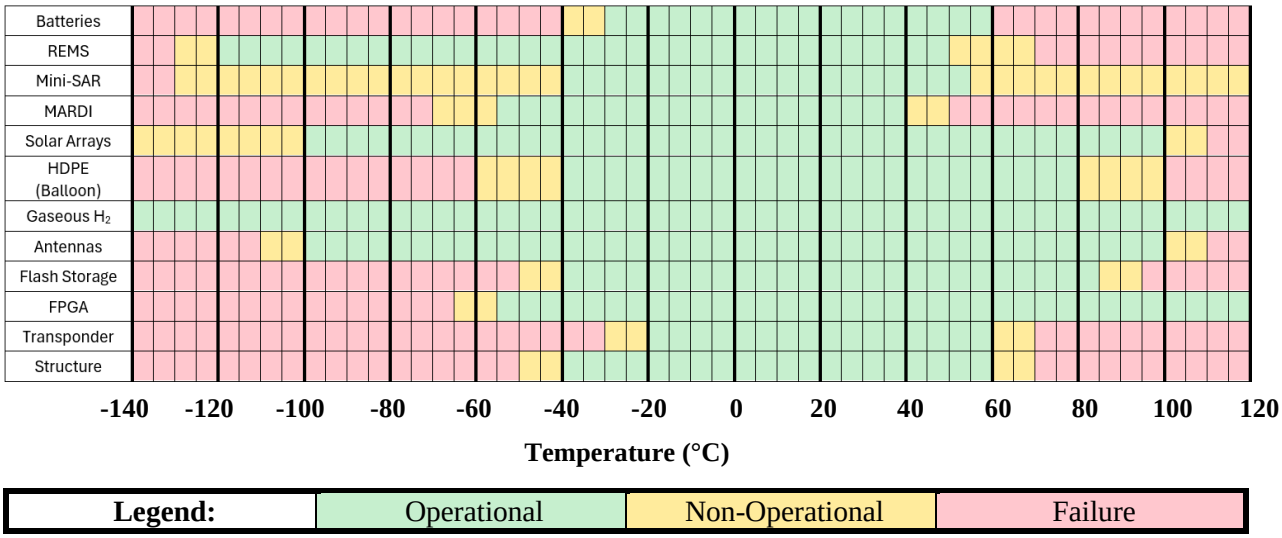

Figure 7.8.2-1: Broncito Component Temperature Ranges

7.8.3 Thermal Design Approach

For entry, the liquid hydrogen tank must remain at -255°C to keep the hydrogen in a liquid state. To achieve this, an aluminum 6061-T6 vacuum jacket was designed to prevent heat from conducting into the tank [46]. Then, MLI was sized to further reduce the radiative heat transfer into the tank. The thermal network for the liquid hydrogen tank is shown in Figure 7.8.3-1 below.

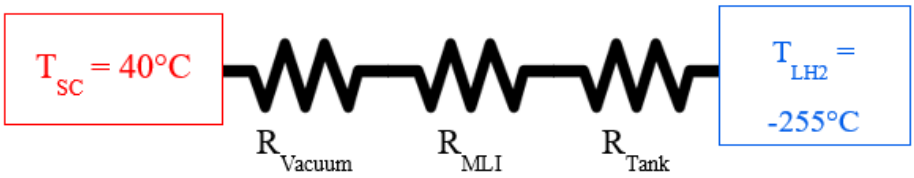

Figure 7.8.3-1: Liquid Hydrogen Tank Thermal Network

Using MLI thermal property estimates from Moeini [47], this analysis determined that ~34 layers of MLI will be required to keep the hydrogen in its liquid state during entry.

The thermal control methodology and design approach for Broncito while in flight are similar to the method outlined in Section 6.6.3. First, the mechanisms of heat transfer to and away from Bronco were determined. Since Broncito will operate within Mars' atmosphere, Equation 7.8.3-1 was utilized to determine the impact of convective heat transfer on Broncito's thermal analysis.

(Eq. 7.8.3-1) $$\frac{p}{p_0} = e^{-\frac{h}{H}}$$

Where h is the altitude of Broncito, H is the scale height of Mars (~11 km), and $\frac{p}{p_0}$ represents the percentage of Mars' atmosphere underneath Broncito's altitude. This analysis estimated that ~50% of Mar's atmosphere was underneath Broncito during operation. This, coupled with the fact that Mars' atmospheric density is ~1% that of Earth's, justified the exclusion of convective heat transfer in the thermal analysis of Broncito.

Ignoring convection, Broncito will experience heating from direct solar heating, indirect solar heating via Mars' albedo, Mars' thermal emission, and heat generated from the power consumed by onboard electronics during the day. At night, Broncito will only experience heating from Mars' thermal emission and heat generated from the power consumed by onboard electronics. Broncito's sole mechanism for ejecting heat in both cases is via radiation into Mars' upper atmosphere, which was treated as space with a temperature of 0 K due to Mars' extremely thin atmosphere and Broncito's high altitude. These mechanisms of heat transfer for both day and night are shown in Figure 7.8.3-2 below.

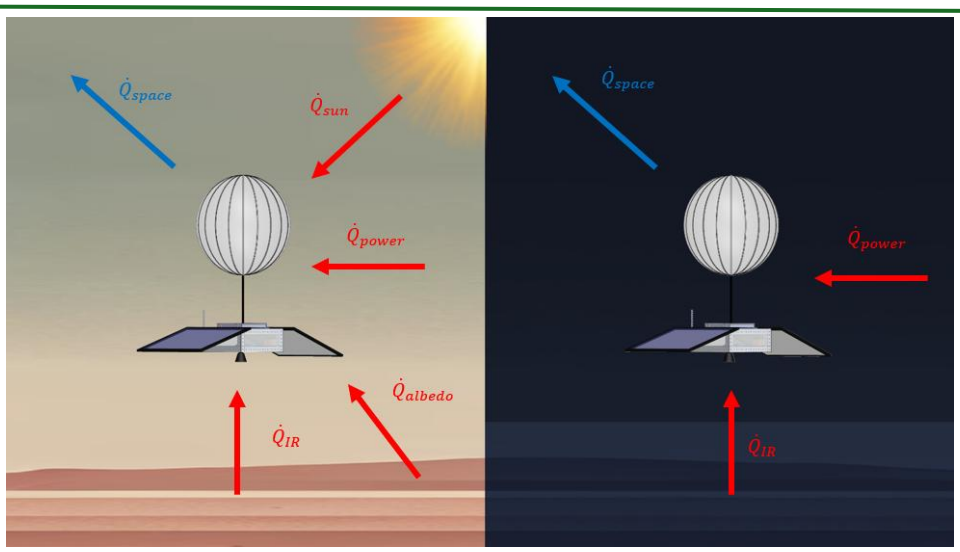

Figure 7.8.3-2: Broncito Heat Transfer Diagram (Day vs. Night)

The generalized steady-state heat transfer for Broncito during the day is identical to Equation 6.6.3-1, and the individual radiative heat terms are shown in Equations 6.6.3-2 through 6.6.3-6. The generalized steady-state heat transfer for Broncito during the night is shown in Equation 7.8.3-2 below.

(Eq. 7.8.3-2) $$\dot{Q}_{IR} + \dot{Q}_{power} = \dot{Q}_{space}$$

In this case, K_a is ~100% while drifting at a 7 km altitude above Mars, and, like Bronco, not every external surface of Broncito will experience each of the heating mechanisms discussed above due to its nadir orientation.

7.8.4 Thermal Analysis

Equations 6.6.3-1 through 6.6.3-6 were used to determine the steady-state temperature of each external surface, iterating through several paints/coatings from reports by Henninger [38] and Red Rock Energy [39] to minimize the heat flux without exceeding any external surfaces' operational temperature range. The selected paints/coatings for each external component, as well as their α/ε ratios, are shown in Table 7.8.4-1 below.

Table 7.8.4-1: Broncito Paint/Coating Selection

External Component	Paint/Coating	α/ε
Ext Front Panel (+X)	Potassium Fluorotitanate White Paint	0.170
Ext Back Panel (-X)	Potassium Fluorotitanate White Paint	0.170
Ext Left Panel (+Y)	Potassium Fluorotitanate White Paint	0.170
Ext Right Panel (-Y)	Potassium Fluorotitanate White Paint	0.170
Ext Top Panel (+Z)	Solec LO/MIT selective surface paint	1.105
Ext Bottom Panel (-Z)	Brilliant Aluminum Paint	0.968
Helix Antenna	Dupont Silver Paint 4817	0.878
Radiators	Martin Black Velvet Paint	0.968

Using these paints/coatings, as well as accounting for heat generated from power consumption, the steady-state temperatures of Broncito's critical components for the day and night conditions are shown in Table 7.8.4-2 and Table 7.8.4-3 below.

Table 7.8.4-2: Broncito Component Steady-state Temperature (Day)

Critical Component	T (°C)
Ext Front Panel (+X)	4
Ext Back Panel (-X)	4
Ext Left Panel (+Y)	4
Ext Right Panel (-Y)	4
Ext Top Panel (+Z)	54
Ext Bottom Panel (-Z)	-15
SA Wide Face (+Y)	87
SA Wide Face (-Y)	87
Batteries	-15
Helix Antenna	36
REMS Temp.	-15
REMS Humidity	-15
REMS Pressure	-15
MARDI	-15
Mini-SAR	-15

Table 7.8.4-3: Broncito Component Steady-state Temperature (Night)

Component	T (°C)
Ext Front Panel (+X)	-34
Ext Back Panel (-X)	-34
Ext Left Panel (+Y)	-34
Ext Right Panel (-Y)	-34
Ext Top Panel (+Z)	-38
Ext Bottom Panel (-Z)	-24
SA Wide Face (+Y)	-63
SA Wide Face (-Y)	-63
Batteries	-24
Helix Antenna	-87
REMS Temp.	-24
REMS Humidity	-24
REMS Pressure	-24
MARDI	-24
Mini-SAR	-24

Table 7.8.4-4 and Table 7.8.4-5 display the heat flux going into and out of each component for both day and night conditions. The tables also display the heat flux experienced by Broncito that must be radiated away to keep all Bronco's components operational for both day and night conditions.

Table 7.8.4-4: Broncito Component Heat Flux Summary (Day)

Component	$\dot{Q}_{in}$ (W/m^2)	$\dot{Q}_{out}$ (W/m^2)	$\dot{Q}_{net}$ (W/m^2)
Ext Front Panel (+X)	148	-148	0
Ext Back Panel (-X)	148	-148	0
Ext Left Panel (+Y)	148	-148	0
Ext Right Panel (-Y)	148	-148	0
Ext Top Panel (+Z)	124	-124	0
Ext Bottom Panel (-Z)	34	-78	-44
SA Wide Face (+Y)	756	-756	0
SA Wide Face (-Y)	756	-756	0
Batteries	33	0	33
REMS Temp.	27	0	27
REMS Humidity.	27	0	27
REMS Pressure.	22	0	22
MARDI	69	0	69
Mini-SAR	32	0	32
$\Sigma\dot{Q}_{net}$			**165**

Table 7.8.4-5: Broncito Component Heat Flux Summary (Night)

Component	$\dot{Q}_{in}$ (W/m^2)	$\dot{Q}_{out}$ (W/m^2)	$\dot{Q}_{net}$ (W/m^2)
Ext Front Panel (+X)	82	-82	0
Ext Back Panel (-X)	82	-82	0
Ext Left Panel (+Y)	82	-82	0
Ext Right Panel (-Y)	82	-82	0
Ext Top Panel (+Z)	33	-33	0
Ext Bottom Panel (-Z)	67	-67	0
SA Wide Face (+Y)	87	-87	0
SA Wide Face (-Y)	87	-87	0
Batteries	33	0	33
REMS Temp.	27	0	27
REMS Humidity.	27	0	27
REMS Pressure.	22	0	22
MARDI	0	0	0
Mini-SAR	32	0	32
$\Sigma\dot{Q}_{net}$			**140**

The required surface area of the radiator to reject the excess heat flux experienced by Broncito, assuming the radiator operated at the steady-state temperature of the face it is mounted on, was determined using Equation 6.6.4-1.

Since the heat flux that must be rejected for Broncito to remain operational is greatest during the daytime condition, the radiator for Broncito was designed with ~0.27 m^2 of radiator surface area to reject the ~165 W/m^2 of excess heat flux. Using historic data from the design of the Space Shuttle's radiators [40], Bronco's radiators will be ~3 cm thick.

While Broncito does not require the use of electric heaters to remain operational, redundant Kapton heaters were designed to increase the temperature of the most critical components, including all the science instruments and the batteries, by 5°C over the course of a minute to mitigate the risk of these components becoming operational. If necessary, these Kapton heaters will require ~4.7W of power to operate.

In addition to radiators, heaters, and thermal paints/coatings, the design includes estimates for the mass of Multi-Layer Insulation (MLI) and foam insulation required to reduce the heat flux affecting the science instruments. Four parallel thermostats, two required and two redundant [41], were included to measure the temperature of critical components. Heat pipes were not included in this design due to Broncito's small scale and sensitivity to mass increases. The total thermal system mass is ~3.7 kg using the estimation methods for thermal devices outlined in Brown [37].

7.9 Broncito Power

7.9.1 Broncito Power Overview

The requirements for Broncito Power Requirements are shown in Table 7.9.1-1 below

Table 7.9.1-1: Power Requirement (Broncito)

Req. #	Power Requirements
11.2-1	The EPS shall support no less than 17 W for the payload.
11.2-2	The EPS Shall operate reliably until October 23rd, 2032
11.2.1-4	The battery shall support a flight power no less than 287 W
11.2.2-1	The solar Array shall support a flight power of no less than 287 W.

Unlike the orbiter, which operates continuously in a SSO, the Broncito balloon vehicle must sustain operations through a 90-day mission with alternating 12-hour day and night Martian cycles. This unique operational profile demands a EPS capable of maintaining consistent power availability even during extended nighttime periods.

To achieve this, Broncito utilizes the same high-efficiency triple-junction GaAs solar cells and Li-Ion batteries as the orbiter, ensuring energy efficiency while minimizing mass. Solar arrays with a total area of 5.20 m^2 were sized using guidelines outlined in Brown [42], ensuring sufficient energy generation to power all systems during the day while recharging the batteries. The 24-cell Li-Ion battery pack, arranged in a 3P4S configuration, was also sized based on guidelines outlined in Brown [42] to maintain continuous nighttime operations without exceeding the battery's discharge capacity.

During the daytime, solar arrays directly power Broncito's systems while simultaneously recharging the batteries. At night, the system seamlessly transitions to battery power, with high-power sensors, including the camera, powered down to conserve energy. By maintaining consistency in solar cell and battery technology across both platforms, the mission maximizes power efficiency and mass optimization without introducing unnecessary complexity. This approach ensures reliable power availability for the Broncito balloon throughout its 90-day mission timeline. This careful balance between solar generation and battery storage ensures continuous, reliable operation

7.9.2 Broncito Power Profile

The Broncito balloon operates in two primary power modes: daytime and nighttime. During the day, solar arrays generate sufficient energy to power all systems and fully recharge the batteries. At night, the balloon transitions to battery power, with high-power sensors like the camera deactivated to conserve energy, maintaining an average draw of 208 W as shown below in Table 7.9.2-1 below.

Table 7.9.2-1: Broncito Power Phase Profile

Phase	Daytime	Nighttime
Power Draw (W)	212	208

7.10 Structure

7.10.1 Material Selection and Design

Considering that Broncito is a relatively small vehicle with only four small data collection instruments, the structure needed to be sized to fit its respective batteries and solar arrays. The main structure is composed of Aluminum 6061-T6 which is industry standard for most space vehicles in production today. This material was chosen due to its light profile, ultimate strength, different material properties, and manufacturability. The structure is composed of eight 1m long and four 0.5m long squared beams to allow for seamless mounting of the plates used for payload mounting. A mounting frame was designed for the tank to ensure a secure connection to Broncito prior to separating, the material chosen is the same as Broncito's primary structure. When mounting instruments and mounting systems into the structure, a corrugated structure was considered but immediately ruled out due to its heavy profile and complexity in manufacturing. When considering mass and ease of integration into the current structure, a general honeycomb structure was an obvious choice. The honeycomb structure is composed of Aluminum 6061-T6 for its affordability, durability, and light mass profile with a density of 2700 $\frac{kg}{m^3}$. One of these honeycomb structures is at the bottom of the general structure which is where the MARDI, Mini SAR, and REMS sensors are located for the best data collection. Another is located within the side of the general structure to allow for further mounting of other harnesses, cabling, and more. The final honeycomb panel is located on the top of the structure where the mounting points for the spring separation mechanisms are located alongside the packaged balloon housing, the helix antenna, and the eyebolts

suspending the balloon. The total structure mass comes out to roughly 35 kg with overall dimensions of 1.1 x 1.1 x 0.5 m.

7.10.2 Mechanisms

There are five different separation planes: between the descent module and Bronco, parachute deployment and heat shield separation from the backplate, airbag separation, balloon unpacking, and tank separation. When looking into the separation between the descent module and Bronco, a cable-cutting mechanism, pyrotechnic separation devices, and non-pyrotechnic systems were considered. Due to the overall risk of pyro shock, pyrotechnic devices were ruled out completely as they propose a risk of flying other systems that are crucial to the mission's performance. In this case, a cable-cutting mechanism became too unstable despite it proving to be a reliable source in previous missions. A non-pyrotechnic system was chosen with a clamp band spring loaded mechanism being the selected choice. This was due to the availability of reliable manufacturers for these systems and their flight history. It works like a pyrotechnic clamp system but rather than using pyrotechnics, an actuator actuates this mechanism opening a ring band clamped within the top of the heat shield. A spring-loaded mechanism then separates the descent module from Bronco. A similar mechanism for the heat shield separation is used upon ablation. However, this separation requires a latch-based separation without the separation springs. It works in a similar electrical manner but in this case, there are four large clamps under their respective thrusters detaching the heat shield from the back shield. These clamps are expanded and chosen over the smaller burn wire or frangible bolts due to their reliability under extreme loads and conditions. Figure 7.10.2-1 depicts the clamps used to separate the heat shield from its back shield.

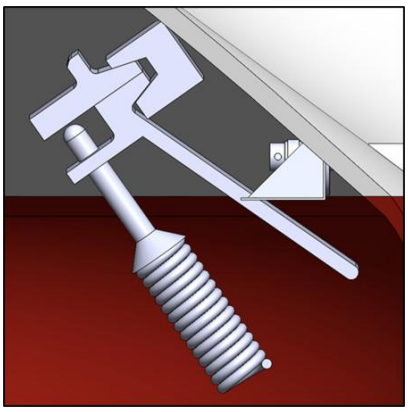

Figure 7.10.2-1: Heat Shield Separation Clamp

The following planes are composed of the same separation mechanism again due to their simplistic nature, compactness, mounting ability, mass, and reliability. Burn wire separation springs were used for the parachute separation, airbag separation, balloon separation, and tank separation because of their lack of exposure to high loads during actuation. The burn wire separation spring is composed of a top and a bottom housing coupled together by an exposed wire capable of receiving enough current through it to burn off ejecting the compressed spring between both housings coupled. There are four burn wire separation springs at each of the packaged corners for both the parachute and balloon. The wire burns once the balloon has reached an altitude of 11 km, unlatching the parachute from its packaging. A similar principle is followed by the balloon as once it has reached a reached its position, the burn wires actuate freeing the balloon from its housing allowing it to inflate. Since there are six airbags in total, there are a total of 4 separation springs in each of the respective airbag corners. In total there are twenty-four total separation springs for the airbag system. They actuate once the airbags have fulfilled their mission in ensuring the payload system has come to a complete rest. These are again chosen due to their compactness and mass. Finally, these same springs are found in the mounting system of the hydrogen tank under the balloon structure. In this case, these four are burned once the balloon has completed its inflation process, allowing the Broncito to leave behind the unnecessary mass of the tank, these can be seen in Figure 7.10.2-2. The final separation mechanism is in the end-of-life stage where the balloon separates from the Broncito structure. This is done through a separation bolt that fractures at a pre-determined separation point through a pyrotechnic input, in this case pyrotechnics are considered as the mission has been completed, and the risk of pyro shock is minimal.

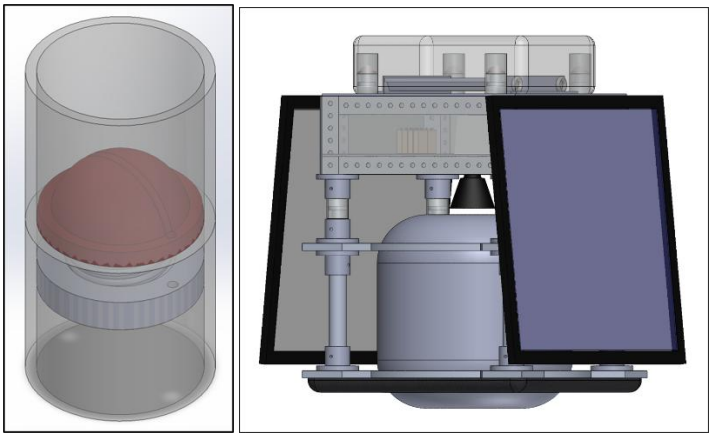

Figure 7.10.2-2: Burn Wire Separation Spring and Mounted Locations

8.0 Architecture Overview

The architecture overview includes the mass and power statements of Bronco and Broncito. The mass of Duo is crucial in the selection of a launch vehicle.

8.1 Mass & Power Breakdown

The initial mass estimation for Duo was determined using the guidelines outlined by AIAA in Elements of Spacecraft Design [48], focusing on the On-Orbit Dry Mass (OODM) estimations for planetary missions based on the selected payload mass. Historical data from analogous planetary missions guided the allocation of mass percentages to each subsystem. Following AIAA recommendations appropriate for a PDR level, a mass margin of 20% was applied to the spacecraft. When combined with the previously calculated propellant mass from the propulsion analysis, the OOWM for Bronco totals 3,862 kg.

The same methodology was applied to Broncito, with an increased mass margin of 25%, reflecting its design stage. The heat shield mass was also included, resulting in an OOWM of 549 kg for Broncito. Integrating these individual mass statements, the total combined launch mass for the Duo system is 4,690 kg, with an additional launch vehicle margin of 110 kg.

Power budgeting followed a similar structured approach, employing AIAA guidelines for power margin recommendations based on the PDR design stage and on-orbit power requirements. This process yielded power margins of 40% for Bronco and 45% for Broncito. Consequently, the calculated on-orbit power requirement is 704 W for Bronco and 287 W for Broncito.

Table 8.1-1: Bronco Mass and Power Statement

Bronco- Mass and Power Statement			
Subsystem	Current, kg	Current, W	Status
Structure	276	87	C
Thermal	14	164	C
Attitude Control	43	62	C
Power	203	41	C
Cabling	79	126	C
Propulsion	264	3	C
Telecom	86	3	C
C&DS	13	461	C
Budget Total	978	207	C
Margin	163	35	C
Payload	23	704	R
ON-ORBIT DRY	1164	N/A	C
Propellant	2506	N/A	C
Pressurant	13	N/A	C
ON-ORBIT WET	3682	N/A	C

Table 8.1-2: Broncito Mass and Power Statement

Subsystem	Current, kg	Current, W	Status
Structure	10	5	C
Thermal	2	10	C
Attitude Control	5	38	C
Power	43	16	C
Cabling	11	40	C
Propulsion	6	40	C
Telecom	7	38	C
C&DS	4	187	C
Budget Total	88	84	C
Margin	20	17	C
Balloon	43	287	C
Payload	8	N/A	R
ON-ORBIT DRY	160	N/A	C
Propellant	75	N/A	C
Pressurant	0.4	N/A	C
ON-ORBIT WET	235	N/A	C
Heat Shield	314	N/A	C

Table 8.1-3: Duo Combined Mass Statement

Subsystem	Current, kg	Status
BV OOWM	549	C
Balloon Adapter	82	C
Orbiter OOWM	3765	C
TOTAL OOWM	4314	C
LV Adapter	376	C
Launch Mass	**4690**	**C**
LV Launch Mass Margin	**110**	**C**

8.2 Launch Vehicle Selection

The requirements for Duos Launch Vehicle Selection are shown in Table 8.2.1 below

Table 8.2-1: Launch Vehicle Requirements

Req. #	Requirement
2.2-1	The Launch Vehicle shall provide a C3 no less than 12.48 $\frac{kg^2}{m^2}$.
2.2-2	The Launch Vehicle shall support a launch mass to Mars of no less than 4690 kg.

Our mission required a Launch Vehicle capable of delivering at least 4690 kg to a Mars transfer trajectory with a minimum C3 of 12.48 km²/s². Additionally, the vehicle had to meet these performance thresholds while keeping the total mission cost under $1B. These constraints, alongside the retirement of legacy NASA vehicles such as the Atlas V and Delta IV, significantly limited our viable launch vehicle options. As a result, commercially available launch systems with demonstrated performance and lower cost were prioritized.

To identify the optimal vehicle, we conducted a trade study comparing Falcon Heavy in both expendable and recoverable configurations and the Vulcan Centaur VC4S. FOM included C3 margin, cost, and reliability, weighted at 1, 3, and 2 respectively, and evaluated using min-max normalization to reflect mission priorities.

Table 8.2-2: Launch Vehicle Trade Study

Launch Vehicle Trade Study											
Parameters			**Falcon Heavy (Recoverable)**			**Vulcan Centaur (VC4S)**			**Falcon Heavy (expendable)**		
Category	**FOM**	**Weight**	**Value**	**U**	**W**	**Value**	**U**	**W**	**Value**	**U**	**W**
C3 Margin (km^2/s^2)	Max	1	0.52	0	0	17.5	0.52	0.52	33.2	1	1
Normalized			0			0.52			1		
Cost ($M)	Min	3	97	1	3	124	0.49	1.47	150	0	0
Normalized			1			0.49			0		
Reliability	Max	2	1	1	2	0.17	0.17	0.34	1	1	2
Normalized			1			0.17			1		
Totals			**5**			**2.33**			**3**		

Falcon Heavy (Recoverable) emerged as the top performer with a normalized score of 5. This vehicle configuration provided a C3 of 13 km^2/s^2—exceeding the requirement by 0.52 km^2/s^2—while maintaining a relatively low cost of approximately $97 million. The vehicle's capability was validated against both the SpaceX Payload User Guide [5] and NASA's High-Performance Query (HPQ) tool [49]. The final launch mass of our system was 4690 kg, which remains within the performance bounds of the Falcon Heavy with margin included.

We selected Kennedy Space Center (LC-39A) as the launch site. This facility is the only operational pad for Falcon Heavy offering established infrastructure, operational readiness, and exclusive compatibility with the Falcon Heavy.

In conclusion, Falcon Heavy (Recoverable) was selected as the optimal launch vehicle due to its combination of low cost, sufficient C3 performance, and schedule-ready infrastructure. It satisfies all performance requirements while maximizing cost-efficiency and minimizing risk for launch to Mars.

9.0 Scheduling & Risk Management

The following sections will discuss the design phase and mission schedule. Follow risk management and how system risks were accounted for in our design to prevent failures.

9.1 Scheduling

NASA systems engineering terminology was used to divide our mission into several phases. Phase A is the concept and technology development phase where the Systems Requirements Review, series of Oral Progress Reviews, and SDR took place. Phase B is the Preliminary design and tech completion phase where we conducted our PDR and will submit our proposal as well. Phase C is the Final Design and fabrication phase, and Phase D is the System Assembly, Integration, Test, Launch and Checkout phase. Phase E is the mission Phase, and Phase F is the Disposal Phase. The proposal winner will be announced in August 2025, and the selected launch date is 12/13/2030.

Phase A lasted 118 days, many major design reviews took place in this phase. Cal Poly Pomona has an industry collaboration with Lockheed Martin and Northrup Grumman to allow engineers to give feedback to senior student's designs. The SDR was conducted virtually to Lockheed Martin Engineers on 3/21/2025, and the PDR was in person at Northrup Grumman to tech fellows on 4/17/2025.

Phase B is typically the shortest phase in Mars missions, and Phase D is typically the longest. From submitting the proposal to launch, there is a total of 5.5 years (May 2025 – Dec 2025), the reason for the launch date is discussed in the trajectory section of the report. Phase B was allocated 1.2 years, Phase C was allocated 1.6 years, and Phase D was allocated 2.7 years. Phase E begins at interplanetary cruising and ends at the disposal orbit maneuvers. The interplanetary maneuver's duration is 286 days. Aerobraking maneuvers take 176 days from arrival to completion. The orbit is circularized on March 19, 2032; a diagnostic phase takes place for 21 days. Concluding the system diagnostics, the instruments start taking data on Mars. The 75% requirement takes 36 days, and max coverage takes 107 days. Following the max coverage, the balloon vehicle is deployed into the Martian atmosphere to complete its science mission (90 days). Bronco is left in orbit for its secondary mission until the disposal period (Phase F). The conceptual design started in 2024, and the end phase out of the mission is in 2040, a total of 16 years.

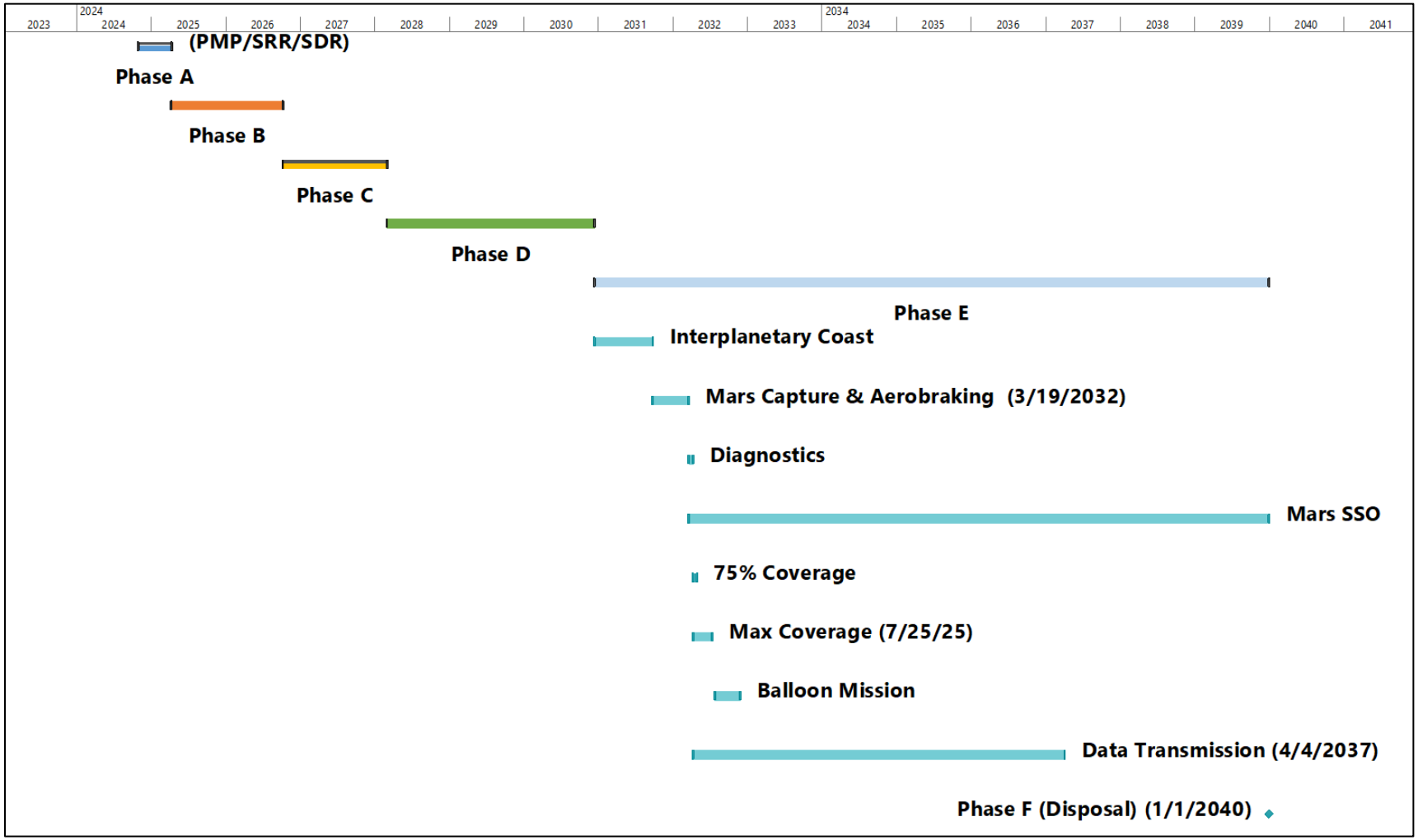

Figure 9.1-1: Duo Scheduling (Phase E Expanded)

9.2 Risk Management

Risk mitigation in space missions is critical because of the high cost and inability to fix problems after launch. Programmatic risks can hinder the development of space missions, governmental budget cuts today threaten NASA missions such as the Mars Sample Return mission. Technical risks and environmental risks must also be identified early into mission development to avoid potential failures due to issues discovered down the line. Single point failures have the highest consequences to Duo. Mitigation strategies must be planned to avoid the likelihood of failures that may be catastrophic to Duo's mission.

Table 9.2-1 shows identified programmatic, environmental, and technical risks that pose a high consequence to DUO. Risk PR 1.1 is particularly relevant because instruments like the MCS and HiRISE were either developed or funded by NASA. Given the political climate, back-up instruments must be selected from non-governmental entities. Environmental risks pose a threat to Bronco and Broncito. Solar storms, micrometeorites, and high-speed winds on Mars pose a threat to the mission, and mitigation strategies have been developed to reduce the consequences of the risks. Balloon inflation will be conducted quickly, as Mars wind speeds may be unpredictable and can cause catastrophic damage to our balloon system Broncito (ER 1.0). High accuracy pointing requirements on the spacecraft have driven our design to have a redundant reaction wheel, as losing control over one axis will hinder our ability to collect data (TR 1.0). These are risks that could be identified in Phase B of our design, as the design matures, early identification and assessment is critical to ensure mission success.

9.2.1 Planetary Protection Risk Management

In alignment with NASA Planetary Protections [50] and the Committee on Space Research (COSPAR) [51] planetary protection policies, our mission has implemented a comprehensive plan to prevent forward contamination of Mars. The inclusion of a lander component necessitates compliance with Category IV requirements, which are more stringent than those for orbiters alone. Consequently, we have adopted enhanced sterilization and bioburden control measures to meet these standards. All spacecraft assembly and integration activities are conducted within ISO Class 8 cleanroom facilities, ensuring controlled environments that limit particulate and microbial contamination. Sterilization protocols include the use of dry heat microbial reducing bioburden to acceptable levels. A thorough trajectory analysis has been performed to ensure compliance with planetary protection requirements, demonstrating that the probability of

inadvertent impact with Mars is less than 1×10^{-2} over 20 years and less than 5×10^{-2} over 50 years. To further mitigate contamination risks, the orbiter is planned to enter a disposal orbit with a lifetime of around 300 years, satisfying end-of-mission planetary protection criteria. An inventory of organic materials used in the spacecraft has been compiled to assess potential contamination sources. This documentation supports our commitment to preserving the Martian environment for future scientific exploration and aligns with international planetary protection standards.

Table 9.2-1: Risk Statements and Mitigation Strategies

Risk #	Risk Statement	Mitigation Strategy
PR 1.0	If the design, manufacturing, or integration and testing phase is not completed in time due to contractors not meeting deadlines, then Duo may face delays resulting in missed launch windows and potentially missing the 2033 deadline.	Back-up launch dates, identify reputable contractors, use standard guidelines and practices.
PR 1.1	If instruments produced by government entities cannot be acquired due to government budget cuts, then spacecraft operations may be reduced and instrument development costs may increase resulting in becoming overbudget.	Identify back-up instruments and prioritize system level requirements.
ER 1.0	If the balloon cannot deploy due to high wind speeds on the Mars surface, then the mission risks losing hydrogen resulting in reduced flight time and lower flight altitude.	Avoid windy season at landing location, avoid locations known for high winds on Mars, and use Bronco to predict weather.
ER 1.1	If intense solar storms damage instruments due to unexpected solar activity, then bit flips can corrupt data and unshielded electronics can suffer permanent damage.	Use shielding and radiation hardened electronic equipment.
ER 1.2	If the spacecraft becomes damaged due to micrometeorites, then the mission may fail.	Add redundant strings to solar array in the event of an impact.
TR 1.0	If a reaction wheel fails due to poor manufacturing from the supplier, then spacecraft operations will be affected and mission requirements may not be met.	Include redundant reaction wheel to prevent loss of control in 1 axis.
TR 1.1	If a heater becomes detached due to being improperly installed by the assembly team, then the propulsion system or payload systems may become inoperable resulting in mission failure.	Set standard installation procedures for heaters and include redundant heaters on critical areas.
TR 1.2	If the balloon suffers a tear during the packing process due to being the first mars balloon mission, then the entire balloon phase will be lost.	Conduct many tests to ensure proper packing procedures and conduct vibration tests to ensure balloon is flight ready.

10.0 Cost Estimation

Duo's budget was calculated with the NASA PCEC tool [6]. NASA PCEC is a tool used to estimate the cost of unmanned spacecraft, landers, launch vehicles, and other space systems. The software functions with various inputs from the spacecraft schedule, weights, and type of mission Duo is considered. Templates are available in the software, the robotic spacecraft template was chosen. Using the mass summary and power summary, subsystem weights can be input in the excel sheet.

Requirement C0-1 states that cost shall not exceed $1.0 Billion US Dollars (FY24) which includes development through the primary mission phase. Duo's cost estimations will cover two scenarios. Scenario 1 covers the system requirement which requires operations throughout the primary mission phase (75% Coverage), and scenario 2 covers full data transmission back to Earth. The addition of the full science data transmission adds 5 years into the schedule in spacecraft operations.

Table 10.0-1 includes the output of Duo's cost estimate, recurring, non-recurring, and operational costs are included. The total cost of acquiring and operating the spacecraft until the RFP requirements are met is $874 (FY24, $M). The acquisition cost of the spacecraft is $291 (FY24, $M). Operational costs are minimal ($37 M) but grow significantly if the estimate includes full data transmission ($149 M).

Table 10.0-1 shows the output of Scenario 1 (75% Coverage) which is the requirement from the AIAA RFP. The total cost to meet the RFP requirements is $874 (FY24, $M). The margin we have with our budget for this scenario is $125 (FY24, $M). Scenario 2 included the 5 years required for 100% data transmission from the orbiter and balloon mission. If Scenario 2 was used, our total cost would be $989 (FY24, $M). The margin in Scenario 2 would be $10.9 (FY24, $M). The schedule can be seen in Figure 9.1-1. The inclusion of the 5-year transmission period greatly increases the operational costs of the mission. Since the RFP explicitly states that costs should be accounted for throughout the primary mission phase, team Red Horizons can confidently say that Duo meets the budget requirements with a $125 (FY24, $M) margin.

Table 10.0-1: Duo NASA PCEC Cost Estimate (FY24, $M)

WBS #	Level	Line Item Name/Description	Non-Recurring	Design & Development	System Test Hardware	Flight Unit	Recurring Production	Non-Allocated	Operations	TOTAL
0	1	System Name	$ 213.3	$ -	$ -	$ -	$ 501.4	$ 121.7	$ 37.8	$ 874.2
1.0	2	Project Management	$ 30.9	$ -	$ -	$ -	$ 39.9	$ -	$ -	$ 70.8
2.0	2	Systems Engineering	$ 12.1	$ -	$ -	$ -	$ 26.4	$ -	$ -	$ 38.5
3.0	2	Safety and Mission Assurance	$ 16.7	$ -	$ -	$ -	$ 26.5	$ -	$ -	$ 43.2
4.0	2	Science/Technology	$ -	$ -	$ -	$ -	$ -	$ 18.7	$ -	$ 18.7
5.0	2	Payload(s)	$ 9.1	$ -	$ -	$ -	$ 15.9	$ -	$ -	$ 25.0
5.01	3	Payload Management	$ 4.1	$ -	$ -	$ -	$ 5.2	$ -	$ -	$ 9.3
5.02	3	Payload System Engineering	$ 0.9	$ -	$ -	$ -	$ 2.0	$ -	$ -	$ 2.9
5.03	3	Payload Product Assurance	$ 0.4	$ -	$ -	$ -	$ 0.6	$ -	$ -	$ 1.0
5.10	3	Instruments - EMPTY ROLLUP	$ -	$ -	$ -	$ -	$ -	$ -	$ -	$ -
5.x	3	Payload I&T	$ 3.8	$ -	$ -	$ -	$ 8.1	$ -	$ -	$ 11.8
6.0	2	Flight System \ Spacecraft	$ 96.8	$ -	$ -	$ -	$ 268.0	$ -	$ -	$ 364.8
6.01	3	Flight System Project Management	$ 1.6	$ -	$ -	$ -	$ 2.1	$ -	$ -	$ 3.7
6.02	3	Flight System Systems Engineering	$ 2.0	$ -	$ -	$ -	$ 4.5	$ -	$ -	$ 6.5
6.03	3	Flight System Product Assurance	$ 4.9	$ -	$ -	$ -	$ 7.8	$ -	$ -	$ 12.7
6.10	3	Spacecraft	$ 72.1	$ -	$ -	$ -	$ 219.3	$ -	$ -	$ 291.5
--	4	Structures & Mechanisms	$ 6.9	$ -	$ -	$ -	$ 50.8	$ -	$ -	$ 57.7
--	4	Thermal Control	$ 0.6	$ -	$ -	$ -	$ 3.3	$ -	$ -	$ 3.9
--	4	Electrical Power & Distribution	$ 4.6	$ -	$ -	$ -	$ 34.4	$ -	$ -	$ 39.0
--	4	GN&C	$ 5.6	$ -	$ -	$ -	$ 9.6	$ -	$ -	$ 15.2
--	4	Propulsion	$ 12.3	$ -	$ -	$ -	$ 64.2	$ -	$ -	$ 76.5
--	4	Communications	$ 13.3	$ -	$ -	$ -	$ 34.5	$ -	$ -	$ 47.9
--	4	C&DH	$ 19.0	$ -	$ -	$ -	$ 10.8	$ -	$ -	$ 29.8
--	4	Entry, Descent, and Landing	$ 9.8	$ -	$ -	$ -	$ 11.7	$ -	$ -	$ 21.6
--	5	Parachutes	$ 8.0	$ -	$ -	$ -	$ 6.4	$ -	$ -	$ 14.4
--	5	Thermal Protection System	$ 1.8	$ -	$ -	$ -	$ 5.3	$ -	$ -	$ 7.2
6.x	3	Flight System I&T	$ 16.1	$ -	$ -	$ -	$ 34.4	$ -	$ -	$ 50.4
7.0	2	Mission Operations System (MOS)	$ 16.7	$ -	$ -	$ -	$ 58.3	$ -	$ 37.8	$ 112.8
--	3	MOS/GDS Development (Phase B-D)	$ 16.7	$ -	$ -	$ -	$ 58.3	$ -	$ -	$ 75.0
--	3	Mission Ops & Data Analysis (Phase E)	$ -	$ -	$ -	$ -	$ -	$ -	$ 37.8	$ 37.8
8.0	2	Launch Vehicle/Services	$ -	$ -	$ -	$ -	$ -	$ 103.0	$ -	$ 103.0
9.0	2	Ground Data System (GDS)	$ -	$ -	$ -	$ -	$ -	$ -	$ -	$ -
10.0	2	System Integration, Assembly, Test & Check Out	$ 31.0	$ -	$ -	$ -	$ 66.4	$ -	$ -	$ 97.4
11.0	2	Education & Public Outreach	$ -	$ -	$ -	$ -	$ -	$ -	$ -	$ -

Budget	TOTAL	Margin
1,000.00	$ 874.2	$ 125.8

Appendix A: Compliance Matrix

Table A-1: Compliance Matrix

RFP Ref.	Req. #	Requirement	Compliant?	Rationale	Proposal Section #
4.2	0.0-1	The system shall support a human Mars exploration campaign.	YES	This requirement is driven by the RFP's primary program goal.	5.0
4.4 - 4.7	0.0-2	The mission shall cover no less than 75% of the Mars globe in at least one of the following areas: a) Atmospheric composition and density profile b) Geographic terrain and elevation survey c) Surface and subsurface resource investigation, identification, and quantification.	YES	This requirement is driven by the primary science requirements of the RFP to support Mars mission planners develop future Mars missions.	4.0
4.8	0.0-3	The system should use technologies already demonstrated on previous programs or currently in the NASA technology development portfolio.	YES	The RFP clearly states a preference for technology NASA is familiar with or has already been flight tested.	5.0
4.8	0.0-4	The system should utilize technologies with a Technology Readiness Level of no less than 7.	YES	Flight proven technology must meet the NASA TRL of 7.	5.0
4.12	0.0-5	The mission shall not exceed a total cost of $1.0 Billion USD (FY24), including development, hardware, launch, and operations through the primary mission phase.	YES	This requirement is driven by the RFP's constraints.	9.0
4.13	0.0-6	The system should complete deployment and primary data-gathering activities no later than December 31, 2033.	YES	This requirement is driven by the RFP's constraints.	4.0
4.13	0.0-7	The system shall be designed to operate into the late 2030s.	YES	This requirement is driven by the RFP's constraints.	4.0

References

[1] "2024–2025 AIAA Undergraduate Team Space Design Competition," *AIAA* Available: https://aiaa.org/wp-content/uploads/2024/12/2024-25-aiaa-undergraduate-team-space-design-competition.pdf.

[2] NASA, "Mars Reconnaissance Orbiter Science Instruments - NASA Science," *NASA Science Mission Directorate* Available: https://science.nasa.gov/mission/mars-reconnaissance-orbiter/science-instruments/.

[3] NASA, "Curiosity Science Instruments - NASA Science," *Curiosity Science Instruments: Mastcam* Available: https://science.nasa.gov/mission/msl-curiosity/science-instruments/#h-mastcam.

[4] NASA, "NASA - NSSDCA - experiment - details," *Miniature Synthetic Aperture Radar (Mini-SAR)* Available: https://nssdc.gsfc.nasa.gov/nmc/experiment/display.action?id=2008-052A-10.

[5] "Falcon's User Guide," *Spacex Falcons User Guide* Available: https://www.spacex.com/media/falcon-users-guide-2025-03-14.pdf.

[6] "PCEC – Project Cost Estimating Capability," NASA Available: https://www.nasa.gov/ocfo/ppc-corner/pcec-project-cost-estimating-capability/.

[7] "Mars Global Surveyor - NASA science," NASA Available: https://science.nasa.gov/mission/mars-global-surveyor/.

[8] Burke, L. M., Falck, R. D., and McGuire, N. L., "Interplanetary mission design handbook: Earth-to-mars mission opportunities 2026 to 2045 - NASA technical reports server (NTRS)," *NASA* Available: https://ntrs.nasa.gov/citations/20100037210.

[9] Long, S. M., You, T.-H., Halsell, C. A., Bhat, R. S., Demcak, S. W., Graat, E. J., Higa, E. S., Highsmith, D. E., Mottinger, N. A., and Jah, M. K., "Mars Reconnaissance Orbiter Aerobraking Daily Operations and Collision Avoidance," *Proceedings of the 20th International Symposium on Space Flight Dynamics*, Annapolis, MD, Sept. 24–28, 2007.

[10] Long, S. M., You, T.-H., Halsell, A., Bhat, R. S., Demack, S. W., Graat, E. J., Higa, E. S., Highsmith, D. E., Mottinger, N. A., and Jah, M. K., "Mars Reconnaissance Orbiter Aerobraking Daily Operations and Collision Avoidance," *NASA Technical Reports Server* Available: https://ntrs.nasa.gov/citations/20080012690.

[11] Leyva, I. A., "Spacecraft Subsystem I-Propulsion," *Space Mission Engineering: The New SMAD*, Torrance, CA: Microcosm Press, 2018, pp. 527–564.

[12] SRE-PA & D-TEC staff, *Margin philosophy for science assessment studies* Available: https://sci.esa.int/documents/34375/36249/1567260131067-Margin_philosophy_for_science_assessment_studies_1.3.pdf.

[13] Gómez-Elvira, J., Armiens, C., Castañer, L., Domínguez, M., Genzer, M., Gómez, F., Haberle, R., Harri, A.-M., Jiménez, V., Kahanpää, H., Kowalski, L., Lepinette, A., Martín, J., Martínez-Frías, J., McEwan, I., Mora, L., Moreno, J., Navarro, S., de Pablo, M. A., Peinado, V., Peña, A., Polkko, J., Ramos, M., Renno, N. O., Ricart, J., Richardson, M., Rodríguez-Manfredi, J., Romeral, J., Sebastián, E., Serrano, J., de la Torre Juárez, M., Torres, J., Torrero, F., Urquí, R., Vázquez, L., Velasco, T., Verdasca, J., Zorzano, M.-P., and Martín-Torres, J., "Rems: The Environmental Sensor Suite for the Mars Science Laboratory rover," *REMS: The Environmental Sensor Suite for the Mars Science Laboratory Rover*, vol. 170, Aug. 2012, pp. 583–640.

[14] Spudis, P., Nozette, S., Bussey, B., Raney, K., Winters, H., Lichtenberg, C. L., Marinelli, W., Crusan, J. C., and Gates, M. M., *Mini-SAR: An Imaging Radar for the Chandrayaan-1 Mission to the Moon - NASA technical reports server (NTRS)* Available: https://ntrs.nasa.gov/archive/nasa/casi.ntrs.nasa.gov/20050176014.pdf.

[15] Malin Space Science Systems, "Mars Polar Lander Mars Descent Imager (MARDI) Technical Details," *Malin Space Science Systems* Available: https://www.msss.com/mars_images/mardi_mpl/mardi_hardware/description/tech_details/index.html.

[16] NASA Goddard Space Flight Center, "Mars Fact Sheet," *NASA Space Science Data Coordinated Archive (NSSDC)* Available: https://nssdc.gsfc.nasa.gov/planetary/factsheet/marsfact.html.

[17] Alberti, G., Dinardo, S., Mattei, S., Papa, C., and Santovito, M. R., "Sharad Radar Signal Processing Technique," *2007 4th International Workshop on, Advanced Ground Penetrating Radar*, Jun. 2007, pp. 261–264.

[18] SpaceX, “Starship,” *SpaceX* Available: https://www.spacex.com/vehicles/starship/.

[19] Egido, A., and Smith, W. H., “Fully focused SAR altimetry: Theory and applications,” *IEEE Transactions on Geoscience and Remote Sensing*, vol. 55, Jan. 2017, pp. 392–406.

[20] Mars Exploration Program Analysis Group (MEPAG), “MEPAG Goals Document, 2020 / Supplemental Hierarchical Summary Table,” *Mars Science Goals, Objectives, Investig1ations, and Priorities: 2020 Summary* Available: https://www.lpi.usra.edu/planetary_news/2020/01/16/2020-mepag-goals-document-draft-is-now-available-for-community-comments-feedback-due-february-14/.

[21] Bokulic, R. S., and DeBoy, C. C., “Spacecraft Subsystems IV-Communications and Power,” *Space Mission Engineering: The New SMAD*, Torrance, CA: Microcosm Press, 2018, pp. 627–662.

[22] Brown, C. D., Green, C. H., “Telecommunication,” Elements of Spacecraft Design, Reston, VA: AIAA, 2002, pp. 447–501.

[23] *Space Data Compression Standards* Available: http://secwww.jhuapl.edu/techdigest/Content/techdigest/pdf/V15-N03/15-03-Beser.pdf.

[24] Taylor, J., Lee, D. K., and Shambayati, S., *Chapter 6 Mars Reconnaissance Orbiter* Available: https://descanso.jpl.nasa.gov/monograph/series13/DeepCommo_Chapter6--141029.pdf.

[25] 1“Leon3,” *Gaisler* Available: https://www.gaisler.com/products/leon3.

[26] 1*RTG4TM radiation-tolerant fpgas | microchip technology* Available: https://www.microchip.com/en-us/products/fpgas-and-plds/radiation-tolerant-fpgas/rtg4-radiation-tolerant-fpgas.

[27] 1*RAD750® family of radiation-hardened products* Available: https://www.baesystems.com/en-media/uploadFile/20210404044504/1434555689265.pdf.

[28] 1*Can specification* Available: http://esd.cs.ucr.edu/webres/can20.pdf.

[29] 1“Sital’s MIL-STD-1553 single and Multi I/O boards and Testers,” *Sital Technology* Available: https://sitaltech.com/mil-std-1553/mil-std-1553-boards-and-

testers/?https%3A%2F%2Fsitaltech.com%2F%3Futm_source=google&utm_medium=cpc&utm_campaign=big_spenders&gad_source=1&gad_campaignid=20677782238&gbraid=0AAAADE4W3Oe1mSFb_Nddxi2ZTo-d6NCF&gclid=Cj0KCQjwoZbBBhDCARIsAOqMEZXl3k9T_217getuawNhXeJb8ImENTC9Y4E1k7Sf9Tcnj_ejU4U1O4EaAs_oEALw_wcB.

[30] Brown, C. D., "Propulsion," Elements of Spacecraft Design, Reston, VA: AIAA, 2002, pp. 153–254.

[31] Strasse, R. K., "Space-propulsion," *10N, 200N, 400N chemical bi-prpellant thruster family* Available: https://www.space-propulsion.com/brochures/bipropellant-thrusters/bipropellant-thrusters.pdf.

[32] "R-4D-15 hipat 445N high performance (375-to-1)," *SatCatalog* Available: https://www.satcatalog.com/component/r-4d-15-hipat-445n-high-performance-375-to-1/.

[33] Sutton, G. P., and Biblarz, O., "Liquid Propellant Rocket Engine Fundamentals," *Rocket Propulsion Elements*, Hoboken, NJ: John Wiley & Sons, Inc., 2017, pp. 189–243.

[34] Edberg, D., "Propulsion," *Spacecraft Design, Development, & Operation*.

[35] "Material Data Sheets." *Hexcel*, 15 Apr. 2025, www.hexcel.com/Resources/DataSheets/.

[36] Bruhn, E. F. "C12 Sandwich Construction and Design." *Brunh's Analysis and Design of Flight Vehicle Structures*, Tri-State Offset Company, 1973.

[37] McMordie, R. K., "Thermal Control," Elements of Spacecraft Design, Reston, VA: AIAA, 2002, pp. 373–407.

[38] John, H. H., *Solar Absorptance and Thermal Emittance of Some Common Spacecraft Thermal-Control Coatings* Available: https://ntrs.nasa.gov/citations/19840015630.

[39] Red Rock Energy, "Heliostat Design Concepts," *Heliostat concepts* Available: http://www.redrok.com/concept.htm#emissivity.

[40] Williams, J. L., Oren, J. A., Modest, M. F., and Howell, H. R., *Challenges in the Development of the Orbiter Radiator System*.

[41] Nguyen, D. D., Owen, J. W., Smith, D. A., and Lewter, W. J., *A Programmable Heater Control Circuit for Spacecraft* Available: https://ntrs.nasa.gov/api/citations/19950004744/downloads/19950004744.pdf.

[42] Brown, C. D., “Power System,” Elements of Spacecraft Design, Reston, VA: AIAA, 2002, pp. 315–371.

[43] Dinesh K. Prabhu and David A. Saunders, *On Heatshield Shapes for Mars Entry Capsules* Available: https://ntrs.nasa.gov/api/citations/20120004297/downloads/20120004297.pdf

[44] *Rocket tanks of carbon fibre reinforced plastic proven possible,* Available: https://www.esa.int/Enabling_Support/Space_Transportation/Rocket_tanks_of_carbon_fibre_reinforced_plastic_proven_possible

[45] *Types of Scientific Balloons,* Available: https://www.nasa.gov/scientificballoons/types-of-balloons/

[46] Yanch, J. C., and Hallowell, S. F., *Design of a High-Power Vacuum-Jacketed Target System* Available: http://kirkmcd.princeton.edu/mumu/target/MIT/design/vacjack.pdf.

[47] Moeini, E., Karimian, S. M., Najafi, H. R., and Esfahani, A. G., *Thermal Performance Evaluation of a Fabricated Multilayer Insulation Blanket and Validity of Cunnington-Tien Correlation for this Mulitlayer Insulation*.

[48] Brown, C. D., “System Engineering,” Elements of Spacecraft Design, Reston, VA: AIAA, 2002, pp. 13–44.

[49] “NASA Launch Vehicle Performance Website,” *NASA* Available: https://elvperf.ksc.nasa.gov/Pages/Default.aspx.

[50] *NASA Planetary Protection Handbook* Available: https://ntrs.nasa.gov/api/citations/20240016475/downloads/PlanetaryProtection_Hdbk_2024_Final_For508ing_comp.pdf.

[51] “COSPAR policy on planetary protection,” *COSPAR Policy on Planetary Protection* Available: https://cosparhq.cnes.fr/assets/uploads/2020/07/PPPolicyJune-2020_Final_Web.pdf.